STUDIES AND DEVELOPMENT OF INTELLIGENT STREET -LIGHTING LUMINAIRE BASED ON LIGHT EMITTING DIODES AND DIGITAL TECHNOLOGY IN INDIAN SCENARIO

Thesis submitted by

Parthasarathi Satvaya

Doctor of Philosophy (Engineering)

Electrical Engineering Department

Faculty Council of Engineering and Technology

Jadavpur University

Kolkata, India

2022

PROFORMA -- 1

"Statement of Originality"

'I Parthasarathi Satvaya registered on 05th May, 2015 do hereby declare that this thesis entitled "**Studies and Development of Intelligent Street-lighting Luminaire based on Light Emitting Diodes and Digital Technology in Indian Scenario"** contains literature survey and original research work by the undersigned candidate, as part of my Doctoral studies.

All information in this thesis have been obtained and presented in accordance with existing academic rules and ethical conduct. I declare that, as required by these rules and conduct, I have fully cited and referred all material and results that are not original to this work.

I also declare that I have checked this thesis as per the "Policy on Anti Plagiarism, Jadavpur University, 2019", and the level of similarity as checked by iThenticate software is 08 %.'

Signature of Candidate: Parthasarathi Satvaya

Date: 28/12/22

Certified by Supervisors:

(Signature with date, seal)

1. Saswati Mazumdar 29/12/22
Professor
Electrical Engineering Department
JADAVPUR UNIVERSITY
Kolkata-700 032

2.

PROFORMA – 2

CERTIFICATE FROM THE SUPERVISORS

'This is to certify that the thesis entitled "Studies and Development of Intelligent Street-lighting Luminaire based on Light Emitting Diodes and Digital Technology in Indian Scenario" submitted by Shri Parthasarathi Satvaya, who got his name registered on 05th May, 2015 for the award of Ph.D. (Engineering) degree of Jadavpur University is absolutely based upon his own work under the supervision of Prof. (Dr.) Saswati Mazumdar and Dr. Rajat Subhra Mandal and that neither his thesis nor any part of the thesis has been submitted for any degree / diploma or any other academic award anywhere before.'

1. Saswati Mazumdar 29.12.22
Prof. (Dr.) Saswati Mazumdar

Professor
Electrical Engineering Department
JADAVPUR UNIVERSITY
Kolkata - 700 032

2. _____
Dr. Rajat Subhra Mandal

List of Publication:

- Satvaya P, Mazumdar S. "Performance analysis of a variable flux and CCT-based outdoor LED luminaire," accepted for publication in the Journal of Optics, (UGC Listed, Scopus indexed)

- Satvaya P., Supakar R. "Performance Assessment of Smart Dynamic Controller for Variable CCT White LED Light Source - A SVM Based Approach," publication in the Science and Technology Journal (UGC Listed), Vol. 10, Issue 2, July 2022, ISSN 2321-3388

- Satvaya P, Mondal I, Mazumdar S, "Development of an Intelligent Security lighting system using wireless Communication technology," published in the International Journal of Engineering, Technology, Science and Research (UGC Listed) , Volume 5, Issue 1, January 2018, ISSN 2394- 3386

- Satvaya, P; Anand, A; Mazumdar, S; "Design and Development of a LED based Outdoor Luminaire with Variable CCT and its Performance Analysis" published in AIP Conference Proceedings, volume 2640, Article number 020026, (Scopus Indexed) published dated September 30, 2022; doi.org/10.1063/5.0110940

- Satvaya P, Mondal I, Sur A, Mazumdar S; "Design and Development of an intelligent street lighting system using Zigbee protocol for communication" published in the 8th Lux Pacifica Life and Lighting Proceedings, pp 100-106, Tokio, Japan, March, 2018.

- Roy, S., Satvaya, P., Bhattacharya, S. et al. "An exposition of a road lighting model to facilitate simple estimation of road surface illuminance parameters for conventional system specifications and recommendations for retrofitting of luminaires." Journal of Optics; Volume 51, Issue 2, Pages 444 – 455, June 2022. https://doi.org/10.1007/s12596-021-00792-x

- Mukherjee, S; Satvaya, P; Mazumdar, S; "Development of A Microcontroller Based Emergency Lighting System with Smoke Detection and Mobile Communication Facilities." Light & Engineering Journal, Vol. 27 Issue 1, pp 46-50, 2019.

List of Presentations in National / International / Conferences / Workshops:

- Satvaya P, Mondal I, Mazumdar S; "Development of Wireless communication based outdoor lighting system using Light Emitting Diodes" Presented in the International Conference on "Sustainable Environmental Engineering & Science 2021 (SEES 2021)", Kolkata, India, December, 2021.

- Satvaya, P; Anand, A; Mazumdar, S; "Design and Development of a LED based Outdoor Luminaire with Variable CCT and its Performance Analysis" presented in 2nd International Conference on Industrial Electronics, Mechatronics, Electrical and Mechanical Power (IEMPOWER 2021) at Kolkata, India, 26th – 28th November, 2021.

- Satvaya P, Mondal I, Mazumdar S, “Development of an Intelligent Security lighting system using wireless Communication technology”, presented in International Conference on New Frontiers in Engineering, Sciences, Management and Humanities at Hissar, India on 4th February, 2018.

Other Papers published

- Ghosh, A., Satvaya, P., Kundu, P.K. et al. “Machine Learning Based Illuminance Estimation from RGB Sensor in a Wireless Network. Wireless Personal Communication,” Volume 125, Issue 2, Pages 1895 - 1911 July, 2022. https://doi.org/10.1007/s11277-022-09639-5
- Ghosh A, Satvaya P, et al. “Calibration of RGB sensor for estimation of real-time correlated color temperature using machine learning regression techniques,” Optik, Volume 258, May, 2022, Article Number 168954, ISSN 0030-4026, https://doi.org/10.1016/j.ijleo.2022.168954
- Ganguly P., Gupta V., Satvaya P. “Performance Study and Stability Analysis of an LED Driver.” Published in Advances in Control, Signal Processing and Energy Systems. Lecture Notes in Electrical Engineering book series, LNEE, vol 591, pp 147-158, Springer, Singapore, First online 15 September 2019 DOI: 10.1007/978-981-32-9346-5_12
- Satvaya, P; Mazumdar, S; “Studies on Road Lighting Luminaires with Advanced Features.” Light & Engineering, Vol. 22 Issue 2, p59-64, 2014

ACKNOWLEDGEMENT

Foremost I would like to express my sincere, deep sense of gratitude and indebtedness to my thesis supervisor Prof. (Dr.) Saswati Mazumdar, Professor of Electrical Engineering Department, Jadavpur University and Dr. Rajat Subhra Mandal, Lighting Expert & Consultant, President, Society of Integrated Technology School & Promotion (SITSP), General Secretary, Indian Society of Lighting Engineers for the continuous support of my thesis work, for their patience, motivation, enthusiasm, invaluable guidance and supervision.

I would like to acknowledge my sincere thanks to HOD, Electrical Engineering Department, and Lab In-Charge, Illumination Engineering Section, Electrical Engineering Department, for providing me the opportunity to carry out my project work in Illumination Engineering Laboratory of Jadavpur University.

I would like to acknowledge my sincere thanks to Prof. (Dr.) Biswanath Roy, Professor of Electrical Engineering Department, Dr. Suddhasatwa Chakraborty, Assistant Professor, Electrical Engineering Department for encouragement they provided me in carrying out this thesis work.,

I am also very much thankful to Mr. Gobinda Paul, Sr. Technical Attendant, Mr. Samir Mandi and Mr. Pradip Pal, Laboratory Instructors and staffs of Illumination Engineering Laboratory of Jadavpur University, for their indispensable co-operation during my thesis work especially in measurement and instrument handling.

Finally, this thesis would not have been possible without the confidence, endurance and support of my mother Gayatri Satvaya, father Sricharan Satvaya, wife Rinku and daughter Pratiti with whom I share tons of fond memories. They are always been a source of inspiration and encouragement.

Parthasarathi Satvaya

JADAVPUR UNIVERSITY

Kolkata-700032

Date: …….

Abstract

Outdoor lighting luminaires play an important role in lighting the night time environment. Adequate lighting on the streets serve and work as the identity of a city. Recently municipalities in India and throughout the world, are replacing the conventional street lights with LED street lights in order to improve lighting quality energy saving and other purposes.

Installation of new road lighting systems or retrofitting of the existing ones would require careful consideration of the design configurations that would maintain road surface average illuminance, uniformity and other parameters in accordance with regional, national, or international standards and guidelines. Moreover, a framework for LED luminaire power rating selection for retrofitting operations has been proposed to assist manufacturers, electrical contractors and utility operators entrusted with such work.

Integrating LED Street light with embedded system and communication module will add more functionality to the streetlight that has multiple advantages like monitoring the luminaire health status remotely, reduces maintenance and operational costs, provides better visual performance, provides automatic detection of pedestrian and finally serves citizens intelligently.

A detail design and development of intelligent street lighting luminaire and controller porotype has been done and described. Various properties have been implemented and integrated in this work like remote monitoring of the health and other parameters of the luminaire using wireless communication protocols and operated using a Smart Phone as a Hand Held Device (HHD). Suitable light control logic has been implemented and Pulse Width Modulation (PWM) approach has been incorporated in the system to modulate the light outputs of Warm White LED (WWLED) and Cool White LED (CWLED) arrays.

Light output, Illuminance values, Correlated Color Temperature (CCT), Color Rendering Index (CRI) Spectral power of the developed luminaire have been varied wirelessly. Performance parameters of the developed luminaire have been presented and analysed. Machine learning technique has been used to train and analyze various statistical parameters. The developed luminaires have been mounted on street lighting poles for photometric, electrical and environmental parameters measurement, recording and performance analysis at outdoor environment.

Keywords:

Intelligent Luminaire, LED, Warm White LED, Cool White LED, CCT, PWM, Wireless Communication,

Table of Contents

List of Figures

List of Tables

Nomenclature

LED	Light Emitting Diode
CW LED	Cool White Light Emitting Diode
WW LED	Warm White Light Emitting Diode
HPS Lamp	High Pressure Sodium Vapor Lamp
MH Lamp	Metal Halide Lamp
CCT (Tcp)	Co-related Color Temperature (K)
CRI (Ra)	Color Rendering Index (Average)
HHD	Hand Held Device
CIE	International Commission on Illumination
IES	Illuminating Engineering Society
IES R_g	Color Gamut Index
IES R_f	IES Color Fidelity Index
CES	Color Equivalent Samples
CVG	Color Vector Graphics
DIALux	Lighting Design Software
LAN	Local Area Network
WAN	Wide Area Network
WiFi	Wireless Fidelity
LoRa	Long Rang Radio
LPWAN	Low Power Wide Area Network
IP	Internet Protocol
IoE	Internet of Everything
IoT	Internet of Things
ANOVA	Analysis of Variance
SVM	Support Vector Machines
MLP	Multilayer Perceptron
RF	Random Forest
NB	Naïve Bayes
RT	Random Tree
RMSE	Root Mean Square Error

Preface

Outdoor lighting luminaires play an important role in lighting the night time environment. When it comes to transportation and communication at night, one of the most important aspects of night time activity is adequate lighting for the streets. They serve and work as the identity of a city. They are used to treat an area more globally. Since the invention of light sources in very early times, non-electrical lighting has been used to illuminate roads using oil, gas, sodium vapour, mercury vapour, and eventually LED. Since 2015 onwards countries all over the world have been transitioning from traditional lighting to LED lighting in order to improve their lighting situations.

Nowadays, advanced and connected luminaires are replacing the conventional luminaires as they are more advantageous in terms of efficiency, high initial performance & sustained throughout the lifetime of the luminaire and easy maintenance. Energy savings, aesthetics and wellbeing provision in the night time environment are the most important features of modern luminaires. The use of intelligent and smart LED-based lighting, which includes street lighting as well, has entered a new age in recent years. In the field of lighting, the introduction of internet of things (IoT) or internet of everything (IoE) further makes street lighting and environmental lighting a very entertaining, challenging, and environmentally friendly exercise. IoT-based lighting has recently come to the forefront of discussion among members of the lighting community and a significant amount of work, including both theoretical and practical implementation is currently being done in this area to make lighting more beneficial, in particular to human beings and the natural environment. Saving energy is no longer a concern thanks to the widespread adoption of LED lighting. In both indoor and outdoor lighting applications, the Internet of Things (IoT)-based lighting systems are currently receiving a lot of attention around the world. There are many products with new technologies benefiting from the most highly specialized technological research in lighting. The advanced luminaires have very precise photometry; they should be used and installed in an exact way, with advanced lighting software that facilitates proper utilization of the precise photometry.

Currently the electric power generated all over the world is not sufficient to meet the overall demand. Out of total power generated by the power utility companies, approx about twenty percent of it is consumed for the lighting purpose. Reducing the power consumption for the lighting will help in saving great amount of power, which can be utilized in some other areas with more importance. In the recent years with the advent of solid state lighting (LED)

shows a promising future toward attaining that goal. Recently the municipalities in India and throughout the world, are replacing the conventional street lights with LED street lights.

Commissioning, maintenance and revamping of energy-efficient, economical and controllable road lighting systems that satisfactorily cater to the visual requirements of pedestrians and motorists are preferable in the wake of the current global energy crisis. Installation of new road lighting systems or retrofitting of the existing ones would require careful consideration of the design configurations that would maintain road surface average illuminance, uniformity of illuminance, and other parameters in accordance with applicable regional, national, or international standards and guidelines. To facilitate rapid approximation of pertinent road surface illuminance parameters with a view of the prevailing road lighting practices involving common heuristic configurations, photometric simulations of road lighting have been conducted in a software model with photometric data tables of high-pressure sodium (HPS) and light-emitting diode (LED) luminaires possessing different power ratings for a specified set of luminaire mounting height, road width, pole spacing, overhang and tilt values, and a mathematical model consisting of six equations derived by multiple linear regression has been propounded with relevant predictor variables.

Moreover, a framework for LED luminaire power rating selection for retrofitting operations has been proposed to assist manufacturers, electrical contractors and utility operators entrusted with such work.

LED street lights have more potential than conventional street light regarding power saving. Integrating LED Street light with embedded system and communication module will add more functionality to the streetlight. Not only it will save energy but also it will provide information regarding the surrounding environment. This additional functionality has few advantages which have been monitoring the luminaire health status remotely, reduces cost, provides better visual performance, reduces maintenance, provides automatic detection of pedestrian and finally serves citizens intelligently.

The expectation that one can live a life that is both simple and advanced is continually rising due to the rapid advancement of technology, which always has the purpose of serving humanity. The social and educational lives of humans are rendered hopeless in the absence of the internet since it has become such an integral element of those lives. At this point in time, it has been seen that the vast majority of the street lights turn ON throughout the evenings or nights, and they remain in the ON position for the entirety of the night. Because of this, a significant amount of energy is wasted because the lights continue to shine even when there is

no longer any requirement for it (Gorgulu & Kocabey, 2020). In this case, this indicates that street lights have a tendency to remain permanently illuminated even when there are neither vehicles nor pedestrians present on the route. As a consequence of this, there is a significant amount of wasted energy, which is not in the least bit encouraging. Not only do the devices connected to the Internet of Things (IOT) regulate and monitor the electronic, electrical, and various mechanical systems that are utilized in different kinds of infrastructures (Guo, Gu, Wu, & Jiang, 2011), but they also perform these functions. These devices, which were connected to the cloud server, are controlled by a single user and the commands that they issue are again communicated or alerted to all of the permitted users who are connected to that network. Through the use of a variety of network infrastructures, several electronic and electrical equipment can be connected to one another and remotely managed. The use of a web browser that is available on a laptop or smart phone or any other intelligent technology through which it can be operated instead of manually activating switches.

A detail design and development of intelligent street lighting system porotype has been developed and described. Some of the mentioned properties have been implemented and integrated in this work like remote monitoring of the health of the luminaire and communication using Zigbee, long range (LoRa), Global system for mobile (GSM), wireless fidelity (WiFi) protocol. Detail photometric analysis of the porotype luminaire has been done using different photometric instruments.

Prototype designing and controlling of an intelligent street light system through android mobile app has been considered. The main purpose has been to build automatic intelligent street lighting system using suitable controller and communicating through different communication protocols.

Early detection of leaking inflammable gas or smoke plays an important role in detection and reducing calamities due to fire. The developed prototype system can detect presence of inflammable gas or smoke and establishing the communication through GSM network to dwellers involved.

Design, development, and performance analysis of a LED-based Intelligent luminaire have been presented. Illuminance values, Correlated Color Temperature (CCT), Color Rendering Index (CRI), and Spectral power of the light source has been varied wirelessly. Suitable light control logic has been developed. The light control logic has been implemented using the Pulse Width Modulation (PWM) approach and incorporated in a microcontroller to modulate the light outputs of WWLED arrays and CWLED array of a single light source.

Through a WiFi connection, the designed system has been connected to the light source and has been operated by a Smart Phone as a Hand Held Device (HHD). The developed system's performance has been demonstrated by the experimental findings. It has a wide variation in the CCT range, spectral power with improved illuminance level, better CRI, and can provide a controllable soothing night time exterior lighting environment as per requirement and when necessary. Brightness of both cool-white LEDs (CWLED) and warm-white (WWLED) has been controlled by varying the duty cycle in multiple steps.

Machine learning technique has been used to train and analyse various statistical parameters. The developed luminaires have been mounted on street lighting poles for photometric, electrical and environmental parameters measurement, recording and performance analysis at outdoor environment.

Chapter 1: Introduction

Lights are all-permeating and are found lighting up infrastructures such as parking lots, campuses, parks, and streets. Streetlights are an important part of every city because they provide citizens with safety and security. Street lighting networks can be used in a more intelligent way rather than the existing simple on-off mode. Intelligent street lighting systems are gradually emerging as a probable major system for developing smart cities. Lighting control systems have progressed in recent years to reflect the changing lighting needs of the cities. Added intelligence using microprocessors and microcontrollers helped different functionalities of the intelligent street lighting systems so they would now be able to react to operators' specific needs while maximizing energy savings.

According to the Constitution of India one of the most important functions of Urban Local Bodies is to provide street lighting listed at Entry No. 17 of the Twelfth Schedule of Seventy-Fourth Amendment Act, 1992 (D.O.No. N - 11025/89/2011-UCD, 2013). Words of the American Judge Louis Brandeis, that Sunlight is said to be the best of disinfectants; electric light the most efficient policeman". Importance should be given on street lighting and it has been decided that, there is a need for increased focus on street lighting in public places. Civic Bodies must undertake a review of the existing facilities and strengthen these wherever required" in the meeting of the Committee of Secretariat Govt. of India held on 23/01/2013 (D.O.No. N - 11025/89/2011-UCD, 2013). India generates about 334 GW of power (Installed capacity as of January 2018), Out of which more than 60% is generated from Coal and Petroleum products (Ministry of Power, Govt. of India, 2018). Energy generated from coal and Petroleum products contributes high amount of Greenhouse Gases.

Lighting consumes around 17-20% of total energy generation. Energy efficient light sources along with proper lighting design can cut energy consumption to a drastic level. There is remarkable prospective to improve lighting quality while reducing energy consumption, running costs, and greenhouse gas emissions through energy-efficient retrofits for lighting.

In the contemporary world, street lighting is a very important aspect of urban as well as rural life in view of road safety and the consequential improvement of quality of living. The main purpose of the street lighting is to illuminate the road at night time, which reduces traffic accident and street crime. In most of the developed and developing countries, lighting is provided along the streets by poles fitted with grid connected electrically-fed luminaires.

Several research studies are currently being conducted to evaluate the worldwide response to smart lighting systems in order to assert the potential and significant impact of intelligent technology targeted at enhancing street lamp management efficiency. Sensors and control algorithms are integrated into street lights to create autonomous lighting systems that can operate in an Internet of Things (IoT) environment (Castro, Jara, & Skarmeta, 2013). Wi-Fi, GSM, ZigBee too are examples of communication technologies that will play a significant role.

1.1 Traditional Streetlight System and Issues

According to an estimate, in 2012 alone, in the United States, 16% of electric consumption has been used for outdoor lighting with a total cost of 11.6 billion dollars. 30% of that light has been wasted for places where it has been not needed, or when it has been not needed. This waste costs the United States around 3.5 billion dollars each year and resulted in the discharge of 30 million barrels of oil, 8.2 million tonnes of coal, and 14.1 million tonnes of carbon dioxide (CO_2). To reduce the cost and to save energy the countries are retrofitting the traditional streetlights with LEDs (Clowers, 2014). Energy and cost savings have been achieved primarily through the use of LEDs rather than high-pressure sodium (HPS) lights, which are still prevalent in underdeveloped nations. LEDs are more energy-efficient than HPS.

The other problems such as maintenance and billing of the energy consumption are also associated with the traditional systems. It is difficult to find out by the lighting network operator whether a lamp or a part of a streetlight needs to be repaired or replaced. Billing of the traditional streetlights is also imprecise, leading the municipalities to pay for unmetered consumption. LED lamps are a solution because they consume less than half the consumption of HPS lamps. Photoelectric sensors can be used to ensure that the streetlights come out only in the absence of natural light. However, the dust accumulation on the sensors causes them to malfunction. A fundamental drawback of these approaches is that they are disjointed and do not consider the system as a whole; instead, they focus on individual problems (Panchuk, 2009).

In 2016, the US Department of Energy estimated that if all outdoor lighting has been replaced with LED technology, $6 billion a year had been saved (U.S Dept. of Energy, 2016). Besides cost and energy savings, the use of LED also efficiently reduces CO_2 emission, light pollution, light being directed heavenward due to optical control. Among the many ways LEDs increase visibility and safety for the general public are their improved color rendering and

uniform illumination as well as their elimination of dark zones between poles. Streetlights may be improved with controls and sensors to save an additional 20% - 40% on a sliding scale of dimming and operating time thanks to cutting-edge technology.

Table 1-1. Report published by US Dept. of Energy to compare the parameters of several traditional lighting systems with LED

Type of Lamp	Efficacy (Lumen / Watt)	Power Demand (Watts)	Color Rendering Index (CRI)	Correlated Color Temperature (CCT)	Lifetime (in Hours)
Low Pressure Sodium	130 - 170	50 - 180	____	1700 - 1800	16000 - 18000
High Pressure Sodium	80 - 120	70 - 400	22 - 70	1900 - 2200	15000 - 40000
Ceramic Metal Halide	75 - 110	70 - 400	80 - 94	3000 - 4200	10000 - 20000
Compact Fluorescent	80 - 85	20 - 70	80 - 85	2700 - 5000	6000 - 20,000
Metal Halide	40 - 70	70 - 400	60 - 80	3000 - 4200	10000 - 20000
Induction	50 - 85	70 - 250	80 - 85	3500 - 5000	100000
Light-Emitting Diode	up to 145	9 - 1300	42 - 97	2700 - 7000	Above 70,000

Some of the traditional open-air lighting technologies along with their wattage, life-time, CCT, and CRI have been given in Table 1-1 along with that of LED. Potential energy saving with LEDs is given in Table 1-2.

Table 1-2. Potential energy savings with LEDs – an estimate made in 2012 *(U.S Dept. of Energy, 2016)*

Exterior Application	No. of Fixtures (Millions)	Energy Consumption (Source tBtu/Site TWh)	Penetration of LEDs	Potential Energy Savings (Source TBtstBtu/Dollars)
Street Lighting	44	452/43.5	2.3%	238/$2.3 Billion
Parking Structures	38	267/25.7	1%	144/$1.4 Billion
Parking Lots	16	355/34.2	<1%	226/$2.1 Billion
Building Exterior	62	135/12	<1%	54/$0.5 Billion
Other	19	4/3	80%	_____
Total	179	1,213/118	<1%	662/$6.3 Billion

1.2 Necessary Elements of Energy-Efficient Streetlight in Indian Context

Streetlights in India must adhere to the National Lighting Code (NLC), that specifies the minimum intensity of light required for different types of roadways in the country. Roads have been classified according on the volume of traffic they carry. Lighting system components have been classified into categories based on their functions (Report No: AUS7490, 2015):

1. Structural systems consist of poles. Either the old ones have been completely replaced by the new ones or the existing systems have been retrofitted with an upgraded system.
2. As a whole, optical systems are comprised of luminaires that include a lamp, as well as the components needed to distribute and protect that light, as well as a means of securing and connecting the lamp to a power source. There are three components of a luminaire: the reflector, the refractor, and the housing. These components are important to ensure the luminaire's efficiency and cut-off and glare management, to guarantee the proper degree of illumination while avoiding light pollution. Luminaires are categorized according to the degree of glare as defined Bureau of Indian Standard (BIS):
    I. The light distribution of a cut-off luminaire is characterised by a rapid decrease in luminous intensity between roughly 80^{o} and the horizontal. The maximum intensity's direction might vary, but it should be less than 65^{o} degrees. The easiest way to reduce glare is to use this approach.
    II. The light distribution of a semi–cut-off luminaire is defined by a lower intensity drop in the range of 80^{o} to 90^{o}. The maximum intensity's direction might vary, but it should be less than 75^{o}. In terms of location, this method is more flexible than others.
    III. There is no restriction on light dispersion with non–cut-off luminaires. A daylight look is required, and huge and low-brightness luminaries can be used in these situations.

The electrical system consists of lamps and ballasts. There are two components to the electrical system: lights and ballasts. Electricity or power is converted into visual electromagnetic radiation (or light) via the lamps' filaments (lumens). For the most part, however, ballasts have three primary functions: to provide the lamp with the proper open-circuit voltage needed for

initialization, to maintain the lamp's performance within the limits of its specifications, and to familiarise the lamp with the various line voltages that are commonly used.

Novel technologies like Light Emitting Diodes (LEDs) as a light source plays a very good role in energy efficient lighting. There are many socio-economic and technical advantages of LEDs e.g., it has a very good lifespan so maintenance cost is also low, operates at low voltage thereby saving energy cost. LEDs have the capacity to glow instantaneously thereby digitally controllable, it does not contain toxic chemicals inside (e.g., mercury) so special handling and disposal are not required. LEDs does not produce Ultra Violet (UV) radiation that may attract insects, produces directional light there by easy to control light and low glare effect along with high color rendering index. It can be dimmed, providing proper brightness with true colors during night time.

1.3 Intelligent Street Light

1.3.1 What is Intelligent Street Light?

As a public light, an intelligent streetlight is one that incorporates technology such as cameras, light sensors, and other sensors to provide real-time monitoring capabilities. This form of a lighting system, which is also known as adaptable lighting or smart street lighting, is an important development in the development of smart cities. Intelligent street lights also improve peoples' satisfaction regarding security and safety. Non-optimized usage like bright street lights in low footfall areas leads to considerable wastage. There is a need to minimize consumption using smart street lights without compromising the safety of the citizens. In countries like India, even after nightfall, people carry out a lot of outdoor activities. Illumination in areas like parks, main roads, car parks, sidewalks, etc. are thus, required to ensure safety as well as to offer a visually pleasing, glare free environment

In addition to these, smart lighting reduces power consumption drastically (Lewis S. , 2019). Many Internet of Everything (IoE) applications, such as weather, pollution, and traffic monitoring, will rely on outdoor lighting infrastructure as a backbone. LEDs are replacing traditional lighting in many cities, and roughly 20% of these LEDs are deemed "smart" since they can be controlled by existing lighting management systems. Workflow diagram of developed intelligent streetlight has given in Figure 1-1.

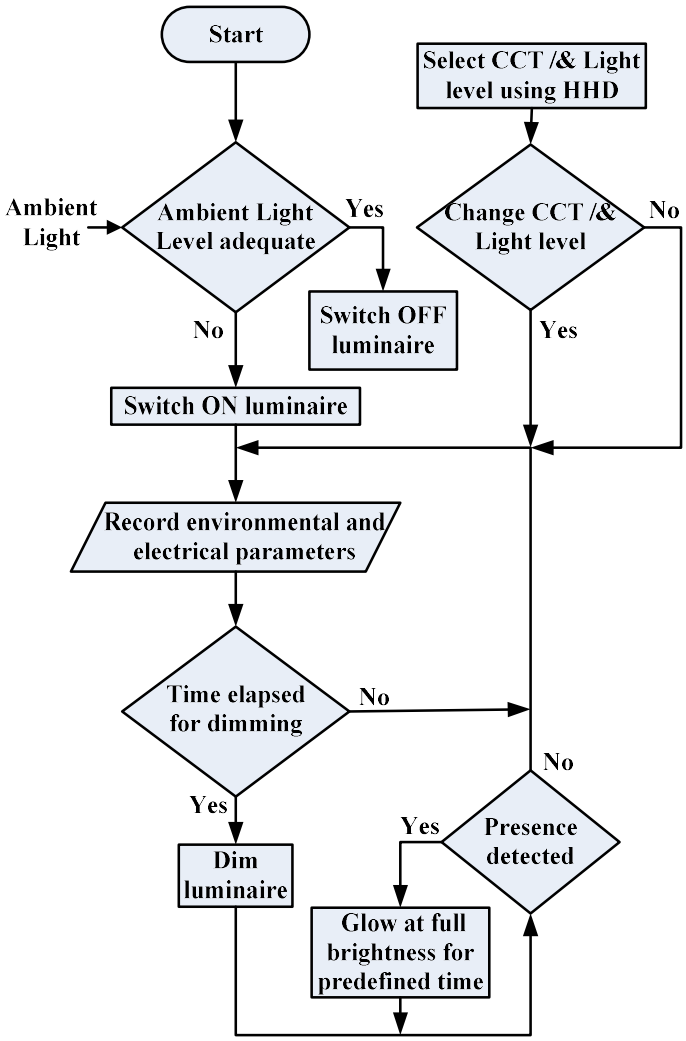

Figure 1-1. Work flow diagram of intelligent streetlight

The work flow diagram Figure 1-1 shows the lighting system starts operating when external power has been switched ON and based on adequate surrounding ambient light level. Whenever the surrounding light level reduces down during dusk condition, the lighting system switches to ON state and remain in that state for five hours as the microcontroller has been programmed and starts data recording. Surrounding light level has to remain dark for fifteen minutes then only the system switches to ON state and avoid any false triggering due to dark clouds during day time or random illumination due to lightning. Data recording of ambient temperature, humidity, air quality, current flowing through a single luminaire is being done on a local web server that has been connected through wireless communication. Alterations to the light output, measured in terms of luminous flux, and adjustments to the colour temperature (CCT) can be made with any laptop or smartphone that is connected to the same WiFi network during initial time duration set through microprocessor programming considering it to be high

traffic movement condition after the lighting system has been turned ON. Any web browser on the HHD can be used to achieve different levels of light output and CCT by searching for the fixed IP address (that has been programmed) of the controller and selecting the required light level and CCT value from the device. After the initial five hours of the lighting system being turned ON, the light output state will change to a dim state i.e. the luminaire will glow at only 20% of the maximum light output level. When the lighting system is operating at a low light output, it is not possible to make adjustments to the luminous flux or the CCT; however, the system continues to record the environmental parameters and the electrical parameters. Whenever any person comes near the controller, the presence detection system using ultrasonic sensors switches the lighting system to 45% lighting output state of the luminaires. The light output of the luminaires stays at the state mentioned for three minutes, after which it reverts to the state where it produces 20% of its total light output if there is no presence detected. When dawn occurs and the ambient light level is high enough, the lighting system goes into the OFF state, and data recording ceases until the level of ambient light drops again.

1.4 Need for Intelligent Streetlight

Electricity consumption worldwide is increasing fast, by around 3% every year. An estimated 15–19% of the world's power is used for outdoor lighting. According to Zissis et al, lighting accounts for around 2.4 percent of yearly energy use and 5–6 percent of greenhouse gas emissions (Zissis, 2016). Outdoor urban lighting may account for up to 20%–40% of total budget expenditures on power, with cities using an estimated 75% of the world's energy (Birol, 2020). Compared to the traditional lighting system, Light-Emitting Diodes (LED) can save energy by 50–70%. Hence, switching to LED lighting can not only save energy but can also be cost-effective. ‘To put it another way, it has been estimated that a global move to LED technology would save roughly 1400 million tonnes of CO_2 and 1250 power plants’ (The Climate Group, 2019). It is critical in this context to deploy solutions that enable the natural environment to be managed effectively. Intelligent lighting may be the answer to these problems.

A. The Indian Scenario

India is expected to have 416 million more urban residents than it has now by 2050 as per the United Nations report. There is an urgent need to improve the conventional infrastructure while simultaneously lowering CO_2 emissions utilising energy-efficient resources as a result of urbanisation and migration. As the world's temperature rises, the demand for environmentally

friendly ways of life has only grown more pressing. The notion of "smart cities" has taken off due to a rise in energy efficiency, renewable resources, and digital technology. 99 cities have already been designated as part of the $14 billion plan by the Indian government to create 100 "smart cities." For sustainability and energy conservation, the lighting industry will play a vital role (Oundhakar, 2019).

Street lighting in India has changed dramatically in recent years as a result of government efforts such as UJALA, the smart cities mission, and the Street Lighting National Program (SLNP). Energy Efficiency Services Ltd (EESL), a subsidiary of the Ministry of Power, has begun the SLNP initiative to replace incandescent street lights with LEDs to explain climate change and improve energy consumption associated with lighting. EESL has set a target of replacing 1.32 crore traditional street lights. EESL has replaced 89.15 lakh street lights with LEDs in 1,400 Indian towns as of April 2019 (Oundhakar, 2019).

Venkatesh Dwivedi, EESL's Director (Projects), is hopeful that this ambitious goal would result in a demand reduction of 1,500 MW yearly energy, saving 900 crore kWh and reducing CO_2 emissions by 62 lakh tonnes. LED lighting makers have geared up to meet the country's growing demand for LEDs. Smart streetlights have been in several cities, including Noida, NCR, Ahmedabad, Nashik, and parts of Kolkata. Delhi already has around 80,000 smart streetlights since August 2019. LED luminaires have been expected to have a 41% smaller environmental impact (such as acidification, climate change, eutrophication, and human toxicity) per kilometre of lit road compared to HPS luminaires (Tähkämö & Halonen, 2015).

The Bureau of Energy Efficiency (BEE) has been assisting towns in India with experimental LED street light systems. BEE has already invested Rs. 90 million in over 30 LED-based street lighting installations across 23 states. Several of the projects in Arunachal Pradesh, Maharashtra, Assam, West Bengal, and Nagaland have been completed. Additional similar initiatives are now being implemented, while others are in the planning phases. Nasik Municipal Corporation has already completed a project of Rs. 400 million which was funded by EESL (The Climate Group, 2015).

Intelligent street lighting system may be equipped for energy savings purposes along with the system may include controlling system for variation of light output and colour of light by varying the CCT of light from the luminaire. The system may be equipped with various environmental sensors like humidity sensor and temperature sensor. The system can be modified by connecting other sensors like surrounding environmental pollution level

measurement sensor, water drip measurement sensor, vibration sensor for movement of vehicle near the streetlight, speedometer and camera system for over speed controlling sound level measurement sensor etc. and accordingly decide the light level of the luminaire and controlling traffic signals and better environmental parameters monitoring and recording will be useful for future works & planning.

1.5 Architecture of Intelligent Streetlight

An intelligent streetlight structure that is shown in Figure 1-2 provides the following facilities (Gagliardi, et al., 2020):

i. A group of streetlights.
ii. IEEE 802.15.4-compliant communication devices constructed utilising the Zigbee high-level protocol.
iii. Detection of traffic as well as pedestrians.
iv. Configuration of the daily lighting routines and remote alarm monitoring through a web application.
v. Using 3G/4G/Wi-Fi connections to communicate between smartphones and the online application.
vi. Controlling and monitoring street light power and dimming level.

The intensity of the LED light is maintained at a pre-set minimum value that is specified by the street lighting requirements when there is no vehicle or pedestrian presence in an area. Otherwise, the LED light is magnified to the most desired value for the region, which is decided by the number of cars, pedestrians, and weather conditions. As a result, the absence of any traffic saves a significant amount of energy. In case the connectivity is lost and the lighting system fails due to some kind of damage, a default condition is activated, i.e. all the intelligent components are deactivated and those function as a conventional lighting system.

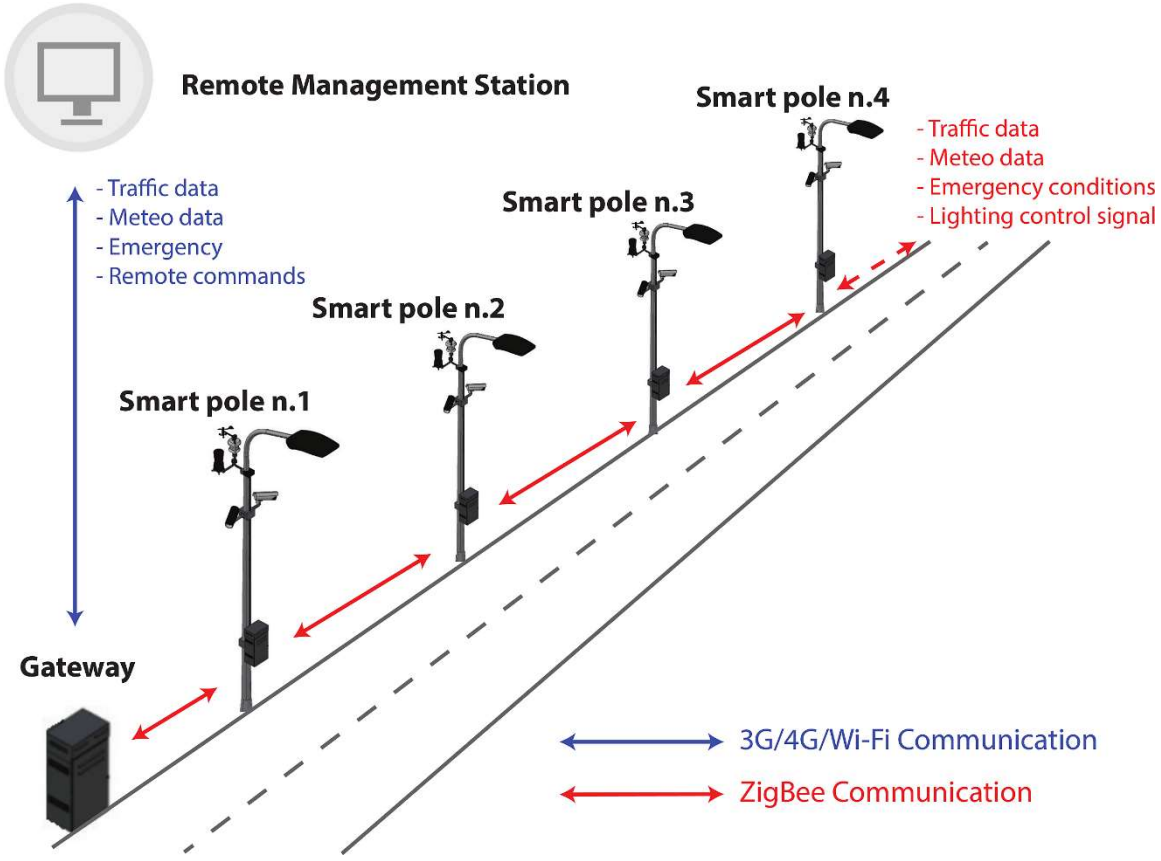

Figure 1-2. Intelligent streetlight configuration *(Gagliardi, et al., 2020)*

1.5.1 Components of Intelligent Streetlight

Main modules of intelligent streetlight are (Barve, 2017):

1. A central server with a firewall for data security.
2. Local control consists of a special communication module that communicates with the streetlight luminaries. This module may also consist of an astronomical clock or sensors to turn the luminaries ON or OFF. This system collects information such as electrical characteristics, the number of hours the lamps are on, the duration of a power outage, etc., in order to provide better service or to conduct future studies.
3. Street light with LEDs Luminaries are equipped with a dedicated communication module that connects them to the local control module, to other Street Lighting Luminaries, or directly to the central server. Additionally, this module accepts other sensors such as a motion sensor, a daylight sensor, and others that are connected to the communication module's input. This module also detects electrical failures such as driver failure, voltage or current exceeding predetermined levels, and communication system faults.

4. Control technique module handles the dimming level of the streetlight based on either timer or sensor. These controls can be done by:
    i. Astronomical timer dim or brighten the streetlight depending on the time of the day or the intensity of natural light.
    ii. Photocell timer that turns the light on or off based on a pre-set light intensity.
    iii. Through a dimmable driver, dimmers adjust the light intensity based on the specified requirements of the user.
    iv. Motion sensor controls the dimming level based on the presence or absence of a vehicle or pedestrian.
    v. Control with an area-based approach in which the proportion of light intensity is decided by the region and its planned use at night. The major road lights often function at 80% intensity, whereas other sections operate at 50%, 30%, or even 0%, i.e. the light is shut off.
5. Additional sensors for detecting noise and air pollution, video surveillance, information display, wireless network, and emergency call can be added to the smart pole.

1.6 Communication Protocols of Intelligent Streetlight

In a streetlight system, there are two variants of communication protocols: long-range communication protocol and short-range communication protocol.

1.6.1 Long-Range Communication Protocol

In the context of an intelligent streetlight system, long-range communication refers to data interchange between the central server and the local control unit, as well as between local control units. For a large city, an intelligent streetlight system consists of several local control units and one central server. After collecting data from the local control units from all over the city, they have been transmitted to a server. Local control units also share information. Due to the homogeneous distribution of local control units across the city, distances between local control units and between local control units and the server can range from a few hundred meters to a few thousand kilometres (Elejoste, et al., 2013). A communication protocol for long-range is thus necessary for carrying out communication between local control units and the server. Wi-Fi, GPRS, Ethernet, Wi-Max, and 3G/4G/5G protocols have been used for communication between local control devices and the server (Rajput, Khatav, Pujari, & Yadav, 2013).

1.6.2 Short Range Communication Protocol

This term refers to the interaction between equipment located at a radius of less than 100 metres. To communicate between the local control units and the light post, short-range protocols have been used. The wired short-range protocols are (Sikder, et al., 2018):

i. The data transfer rate of Power Line Communication (PLC) is 500 Mbps. PLCs convey mostly control messages, and they have been used to control the entire lighting system via power lines (Son, Pulkkinen, Moon, & Kim, 2010).
ii. DALI is an International Electrotechnical Commission-adopted lighting standard (IEC). DALI integrates lighting systems through a star network architecture or use of bus and a standard communication protocol.

IEEE 802.15.4 is the foundation of wireless short range protocols. Protocols for intelligent streetlight systems are:

i. ZigBee is the most extensively used protocol based on the 802.15.4 standard for IoT devices and applications. ZigBee nodes are classified as coordinators, routers, and end devices.
ii. 6LoWPAN is abbreviated form of IPV6 that applies IP suite in the framework of IoT devices that are smaller. Street lighting may exchange sensor data and control messages to other lamps through 6LoWPAN using the same data packet. Faster communication between components using 6LoWPAN technology is achieved for an intelligent streetlight due to its increased data rate.
iii. JenNet-IP was also designed on the IEEE 802.15.4 standard for low-power wireless networks and is an enhanced version of the 6LoWPAN. It enables access to gadget functionality. Its functions include the encryption of outgoing messages and the addition and removal of devices from the network. Its primary benefit is that it can handle over 500 smart light posts, allowing for the creation of a vast network (Lavric & Popa, 2015).

1.7 Variable Color Temperature of Luminaires

Significant differences in the activation zone over the scalp have been identified in Electroencephalogram (EEG) signals for light sources with varying Scotopic to Photopic illuminance ratios (SP ratio). Light sources with a higher SP ratio recorded activity exclusively in the right occipital lobe. On the other hand, light sources with a lower SP ratio caused activation of both the right and left occipital lobe. This may indicate a change in the way visual information is processed and connected with behavioural reactions under two distinct light sources. The spectral composition of light sources has an effect on object recognition since it determines the impression of a lighting environment. Additionally, brain activity varies for the same visual task depending on the lighting situation (Biswas, Chakraborty, & Nath, 2018).

The response times of the various participants indicate early object detection under light sources with higher SP ratio in studies comparing visual performance under metal halide (MH) and high pressure sodium vapour (HPSV) lighting conditions (Lewis A. , 1999) (Fotios, Cheal, & Boyce, 2005) (Akashi & Rea, 2002) (Rea, Bullough, & Akashi, 2009). However, the difference observed is not statistically significant. On the other hand, Akashi et al. discovered a difference in reaction time between metal halide (high SP ratio) at high photopic light levels and sodium vapour at high pressure (low SP ratio) for an off-axis moving target in the actual field. Additionally, different individuals exhibit considerably varying perception-action coupling, implying that there may be variances in human brain processing that have not been reflected in behaviours.

Activities performed with HPS light source have more red and dark blue colors in Electroencephalogram (EEG) signals than tasks performed under MH light source, which implies that the brain is more active in both hemispheres (Chakraborty S. R. D., 2021). Laboratory based effects of peripheral source on on-axis visual performance under variable CCT lighting conditions has been studied (Goswami, Roy, Naskar, & Chakraborty, 2022) (Chakraborty & Mazumdar, 2022). Subjectivity in perceptual experience has a significant effect on object detection under various illumination situations (Akashi Y., 2007) (Lewis A. , 1999) (Boyce & Bruno, An evaluation of high pressure sodium and metal halide light sources for parking lot lighting, 1999) (Eloholma, Halonen, & Ketomuki, 1999).

It is uncertain how the lighting condition affects higher-order brain operations and cortical circuits. Thus, human cognition under low-light situations presents a complicated yet little-studied scenario.

Additionally, the color appearance of streetlights such as MH and high pressure sodium vapour HPSV lamps is taken into account (Biswas, Chakraborty, & Nath, 2018) (Janoff & Havard, 1997) (Rea, Bullough, & Akashi, 2009) (Fotios, Cheal, & Boyce, 2005). Even relatively straightforward object detection becomes extremely complicated.

At 2500 K, the average response time is shorter with a peripheral light source than without one. The 4000 K CCT source has a similar effect, allowing for better visibility. 5000 K CCT has the same good influence. As a result, the observer experiences a beneficial benefit from peripheral lighting for all CCTs. 6000 K CCT, on the other hand, has a negative impact on visibility. The performance of object detection has been affected by the light source's Correlated Color Temperature (CCT). The response time of a light source under CCT of 2500 K, 4000 K, and 5000 K decreased as the CCT increased, whereas the response time of a light source under CCT of 5000 K has been measured. However, the fastest response time has been achieved using a 6000 K CCT light source in both peripheral and non-peripheral circumstances. For both illumination conditions (with and without peripheral), response time has been the lowest under CCT 5000 K, which is the lowest compared to other CCTs. The response time of all individuals remained fastest at 6000 K CCT, however under peripheral illumination, the response time increased even more. The on-axis visibility of the observer has been reduced the most while using a CCT of 6000 K due to the glare effect.

Correlated Color Temperature (CCT) has been shown to have a significant impact on subject performance, both on-axis and off-axis. Even in road lighting conditions, the CCT of the source has a direct impact on the viewer's performance. Color temperature has a significant impact on the user's or observer's ability to see.

1.8 Aims of the Thesis

Currently the street lighting system operates at the night time with manual mode in ON & OFF control mode for groups of poles. At night time the lighting systems provides illumination on the streets and provide visual guidance to the road users from long distances about straight and / or curves of the road. Nowadays conventional street lighting systems with conventional lamps and fixed colour appearance and high power consumptions are being replaced with LED luminaires. And in some cases just by retrofitting the conventional luminaires with LED luminaires without replacing the poles & bracket of the lighting systems. LED street lights have recently been installed in several cities throughout the world, including in India. LED street lights have more potential than conventional street lights regarding power saving. Intelligent

street lighting system offer versatile options over the conventional luminaires. Intelligent luminaire may offer environmental light based control of switching and dimming along with pre-fixed non peak hour light level control. The system may offer occupancy based light level control from the luminaire along with status and power consumption monitoring over large distances using wireless communication network. The same network also provides control of colour appearance from the luminaire. Heavy traffic hours need more attention on the road surface when white coloured light with lumen output is preferred and vice versa. The environmental parameters may be measured and recorded from the sensors attached to the lighting system.

Integrating LED streetlights with embedded system and communication modules will add more functionality to the streetlight. Not only it will save energy but also it will provide information regarding the surrounding environment. This additional functionality has a few advantages which are monitoring the luminaire health status remotely, reducing cost, providing better visual performance, reducing maintenance, providing automatic detection of pedestrians, and finally serves the citizen intelligently. The proposed system aims to:

1. Create a framework for LED luminaire power rating selection for retrofitting operations to assist manufacturers, electrical contractors, and utility operators entrusted with such work.

It is common knowledge that street lighting retrofitting operations are now being carried out in a number of different municipalities and urban local bodies. During the process, conventional luminaires are removed and LED luminaires are installed in their place on existing poles according to the lighting design standards that were in place before, such as pole spacing, tilt angle, bracket length, and so on. The process of retrofitting street lighting can be facilitated with the assistance of a model framework.

2. Design, develop a LED-based intelligent luminaire and analyse performance of the lighting system. Through different communication protocol, the designed system can be controlled and electrical, physical and environmental parameters recording and monitoring within a small area and beyond using hand held device (HHD).

Due to the numerous benefits that are associated with intelligent luminaires, which are outlined in section 1.3, the conventional street lighting luminaires ought to be replaced with intelligent luminaires. On the market, there is a wide variety of intelligent luminaire, each of which comes with a high price tag, a number of different degrees of flexibility, and a range of

operation in terms of the communication distance. Luminaires with low working range coverage is also possible within low cost.

3. Design and develop a lighting system that uses phosphor converted WarmWhite (WW) and CoolWhite (CW) LEDs stacked on a luminaire to provide light output with tuneable Correlated Color Temperature (CCT). Variation of CCT and Light output of the luminaires, which have been obtained by combining radiation from WW and CW LED arrays and its performance analysis.

As covered in section 1.6 within the context of laboratory conditions, research on dynamic lighting environments that have varying CCT and light levels reveal that diverse perceptual capacities seem to be offered during nighttime environments. Under the illumination of artificial light, such as streetlights, humans have mesopic vision. The color temperature of the luminaire would have an effect on the ambient lighting, which in turn affects on visibility, peripheral vision, and variance in fatigue.

1.9 Objectives of the thesis

1. Facilitate rapid approximation of pertinent road surface illuminance parameters with a view of the prevailing road lighting practices involving common heuristic configurations, photometric simulations of road lighting using conventional lighting software.
2. Design and develop an intelligent street lighting system to achieve remote monitoring of the health of the luminaire and communication with a central computer using Zigbee protocol.
3. Development and analyse the performance of a LED-based street lighting luminaire and monitoring, recording and control through suitable communication protocol, using a Smart Phone as a Hand Held Device (HHD).
4. Design and develop a lighting controller system that uses phosphor converted LED based luminaire with tuneable light output and Correlated Color Temperature (CCT).
5. Performance assessment of the dynamic controller for variable CCT white LED light source using Support Vector Machine learning based approach.

Chapter 2: Literature Review

The primary objective of an intelligent outdoor lighting system is to enable more efficient and flexible use of the urban environment, particularly in terms of energy conservation and cost optimization. Many studies and projects on intelligent outdoor light implementations have been discussed in this chapter.

2.1 Introduction

All over the world, rapid urbanisation has led to the implementation of digital infrastructure. This has given rise to an interconnected system of buildings, roads, bridges, and so on. Intelligent lights use a control system that allows connected lights to be monitored remotely via a centralized application online. This technology remotely controls the performance of individual streetlights, detects faults, monitors energy performance, and in combination with sensors, expedites city-wide problems such as traffic flows, parking lots, power outages, and potential accidents by providing real-time alerts. The use of LED streetlights reduces energy consumption by about 50% in metropolitan areas. A smart street lighting system has been used mainly for energy optimization (Signify, 2020).

Time of the day and the season are two main factors that determine the amount of light required. Thus, energy use has been optimised in response to changing environmental and socioeconomic conditions. There has been real-time data collection which allows continuous monitoring. This not only reduces energy consumption but also meets the sustainability goal. Energy saving that occurs due to the use of LED streetlights can pay for themselves. 50% of the energy saving occurs due to LED and another 10% - 20% saving occurs due to dimming. Big cities are the largest consumers of energy, thus, posing a big challenge for the planners while warranting maximum efficacy of the city's energy system. India accounts for 11% of all road accident-related deaths worldwide and is ranked the first out of 199 nations. From 2005 to 2019, the number of road accident deaths grew by an astounding 59.116%, totalling 151113 in 2019 (Transport Research Wing, Ministry of Road Transport and Highways, Govt. of India. Road Accidents in India, 2019). A 2014 case study conducted in Tamil Nadu demonstrates that visual aspects account for 47% of accidents, with light and visibility having the greatest impact on vehicles and pedestrians (Pitchipoo P., January, 2014). This case studies highlights the necessity for appropriate lighting design on Indian roads, particularly highways, in order to guarantee safety and significantly reduce traffic accidents caused by poor visibility.

Comfortable, precise, and fast night-time visibility are the hallmarks of well-designed road lighting. Aside from these benefits, well-designed and installed road lighting can also reduce accidents during the night, help police protect the public, improve user safety and security, manage traffic flow, and encourage the use of public spaces and businesses at night. Furthermore, visual components and tasks such as identifying pedestrians or obstacles in the road, operating a vehicle, identifying signs and traffic signals, figuring out routes, etc., should be easily accomplished in a given road lighting scenario through the use of traffic signals, vehicles' headlights, fixed light at the roadside, etc (ANSI/IESNA RP-8-00, 2000). Since 2016, research has been conducted to develop solutions that are efficient, contemporary, energy-efficient, and human-friendly. Market growth of intelligent streetlights since 2016 has been shown in Figure 2-1.

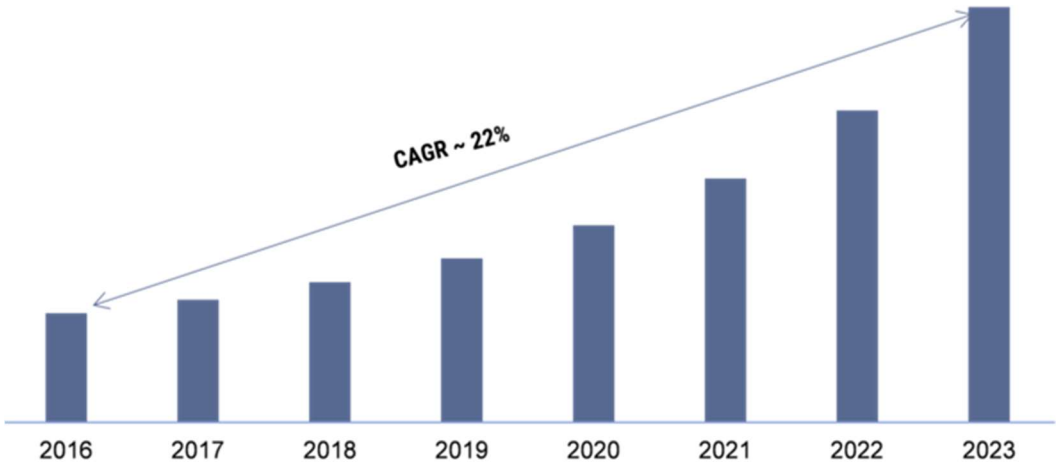

Figure 2-1. Market growth of intelligent streetlight since 2016 and projected till 2023 with compound annual growth rate (CAGR) of 22%

2.2 Commercial Systems in Use

Several intelligent lighting systems that are being used commercially are described below.

2.2.1 InteliLight

Intelligent street lights are flexible and adaptable to the needs. This system uses open communication protocol or combines them in hybrid implementations to construct connected streetlight infrastructure with feedback capabilities. Overall effort required for the management of the grid has been greatly reduced. Even if the communication fails the system can continue to operate the lamps autonomously while trying to re-establish the connection. A vast number

of electrical parameters such as current, voltage, reactive power, active power, etc. have been monitored and an in-depth analytical report has been produced that gives an understanding of the trend in energy loss. This helps improve the lighting policies and this system reduced the energy cost by 35% (InteliLIGHT, 2021).

2.2.2 AAEON Intelligent Lighting System

The streetlight can dim or turn themselves off on a real-time basis (Aaeon, 2020). It is outfitted with the Edge-X Cloud Street Light monitoring and management technology, which features three distinct architectures:

i. Single light control panel,
ii. Loop monitoring panel, and
iii. Loop control panel, depending on the field's size and market need.

It is capable of concurrently powering over 100,000 streetlights. The central administration system enables users to browse the cloud platform in order to examine all of the street's information and to use a set of precise diagnostic engines. It enables managers to speed up the dispatch repair when a fault is detected.

2.2.3 Kanglight

This is an autonomous lighting system that can perform even when there is a communication failure. Lights can be operated autonomously by the controllers till the connection is re-established. Energy consumption is reduced by dimming the light or switching it off. The system can sense a pedestrian or a vehicle and the light switches on automatically. The system can lead to approximately 40% energy saving (Kanglight, 2022).

2.2.4 Interact City

Their software is designed to provide lighting management that allows automatic fault detection and provides real-time response in order to reduce the downtime (Interact, 2022). Information collected from the management system is stored in an on-premise database or in the cloud which can later be used to further enhance and improve lighting operations. Secure APIs facilitate lighting to be synchronized with other city services or activities. The system can also measure energy usage on a real-time basis, thus, reducing carbon dioxide emission. City light can be remotely controlled to increase the lighting in the area of high crimes while dimming in other areas. Light can be dimmed to about 30% to ensure energy saving.

2.3 Case Studies

2.3.1 International Scenario

A. Sheffield, UK

Smart streetlight in Sheffield consists of a three stage network (Dizon & Pranggono, 2021):

i. The Perception Layer (Stage 1) comprises of wireless control nodes known as telecells that has been comprised of sensor nodes that enable Global Positioning System (GPS) functionality along with low-power metering.
ii. Network Layer (Stage 2): A base station operating in the Ultra-Narrow Band (UNB) band offers radio communication up to 5000 sensor nodes.
iii. Application Layer (Stage 3): Instant fault repairing, automated fault diagnosis, reduction in repair time.

Sheffield City Council can now remotely operate streetlights, monitoring them in real time, and automatically detect/diagnose defects, which minimises the number of staff required for maintenance. Energy consumption and carbon footprint have been reduced by up to 65 percent. Because the system lacks autonomy and self-adaptation, it exhibits stagnant behaviour. They used Dynadimmers that dimmed the light at different times of the day at five different levels. This resulted in further energy saving.

B. Edinburgh. Scotland

Edinburgh City Council introduced smart streetlight in 2018 (Telensa, 2020). A centralized system connected 64,000 streetlights. Yearly spending of £3.2 million has been reduced by 50% due to the use of smart LED streetlight. Installation of wireless nodes provided the advantage of real-time and remote monitoring. However, a common fault has been luminaire driver failing which became difficult to manage as they have many different driver types across their fleet of streetlights.

C. Doncaster, UK

Doncaster had 450,000 streetlights covering 220 square miles. To reduce the wastage of energy, the city council opted for smart lighting system. The energy saving achieved had been of worth £1.3 million annually. They achieved the saving the following ways:

i. Based on external factors the light levels are dimmed.

ii. Reducing the time period for which streetlights remain turned on during the dawn and dusk

iii. Adapting the power consumption to maintain light output in the face of slow LED lumen degradation and dirt accumulation in between cleaning cycles.

By modifying the lighting schedule, energy consumption has been lowered from 67,087 to 51,474 kWh, resulting in a 19% energy and 23% kWh savings.

D. Uppsala, Sweden

Uppsala municipality of Sweden have been installing smart streetlights since 2015. A smart control system regulates or adjusts the intensity according to the needs, place, and the time of the day. Control systems can make adjustments to optimize the dimming curve. The system is able to handle many different dimming curves for different parts of the city. The dimming curves stay constant over the year, but there are options to lower the intensity during a period with snow covering the ground. To ensure safety in the paths through dark forests, the armatures are continuously on full effect. With smart control system the energy saving is around 80%.

The software used with the control system has a module called 'dusk relay' that measures the daylight to regulate when the control box should turn the power on or off. The model takes as input data from the user and computes the energy consumption. Expenditure is calculated by taking input from the users and the supplier and the final outputs are the amount of energy savings, reduction in carbon dioxide emission, and cost savings.

E. Los Angeles, USA

LA started replacing streetlights from 2009. The city currently has 180,000 streetlights equipped with LED luminaires, resulting in a 65 percent energy savings, or EUR 8.17 million in cost and 65,000 tonnes of carbon dioxide equivalent each year. In 2015, 100 smart poles with LED lights and 4G LTE wireless connectivity have been erected. By 2020 another 500 smart poles have been erected leading to a cost savings of EUR 2.45 million in maintenance. Energy savings of around 50%–70% have been achieved when connected LED lighting has been used, and up to 80%–90% when sensors, smart controls, and Internet of Things (IoT) technologies have been used (Bachanek, Tundys, Wiśniewski, Puzio, & Marouškova, 2021).

F. Copenhagen, Denmark

Copenhagen aims to become carbon dioxide emission free by 2025. As an initiative they have installed 20,000 connected LEDs for street lighting. LED lamps are equipped with intelligent module which when detects a vehicle or pedestrian turns the light brighter; otherwise the light is dimmed. They have achieved 65% energy savings (Bachanek, Tundys, Wiśniewski, Puzio, & Marouškova, 2021).

J. Jakarta, Indonesia

With 90,000 LED streetlight Jakarta has the largest LED streetlight system in the world. Their lighting system is integrated with other smart city technologies and can be remotely regulated, as can the entire city. They achieved an energy saving of 70% (Bachanek, Tundys, Wiśniewski, Puzio, & Marouškova, 2021).

K. Buenos Aires, Argentina

The city of Buenos Aires has 126,000 lights. LEDs have replaced 55% of the total. The system can be monitored at the light level. Due to these changes, the luminous flux will decrease. When compared to a standard lighting system, this results in savings of 50 to 80 percent (Bachanek, Tundys, Wiśniewski, Puzio, & Marouškova, 2021).

L. Singapore

LED lamps have been installed by Singapore's Land Transport Authority (LTA) since 2013, which are about 25% more energy efficient than traditional lighting and require less frequent repair. (SLAT, 2017). Since 2014, LTA has erected 29,000 LED streetlights, and traditional lighting are planned to be phased out by 2022 in the remaining locations. Remote Control and Monitoring (RCMS) is a crucial module for lighting because it enables the system to adapt more effectively to changing weather conditions.

M. Birmingham, UK

Birmingham is Europe's largest metropolitan LED installation project, with 90,000 street lighting covered. Energy savings of 50% have been predicted, along with a EUR 2.2 million decrease in yearly operating expenses. The additional expenditures associated with establishing

smart control are more than offset by the savings in energy usage and maintenance and renewal costs. A real time tracking system has been implemented to collect information on the system's performance. It is possible to adjust the intensity of light according to current requirements. This will result in a substantial reduction in energy use. (Bachanek, Tundys, Wiśniewski, Puzio, & Marouškovᡠ2021).

2.3.2 National Scenario

India planned to change 35 million streetlights to LED by the end of 2020. This has been supposed to save 4.9 billion euros per year in terms of reduction of electricity consumption. Adaptation of smart LEDs for streetlight has been growing rapidly and has reduced 6.2 million tons of carbon emissions each year (Nhede, 2019).

A. Pune, Maharashtra

Pune is the first city in India to use technology to illuminate the streets. Around 80,000 of the city's halogen streetlights has been replaced with energy-saving LED luminaires that could be operated remotely. A group of light can be dimmed and these commands are broadcast over the power supplies to the LED luminaires. This had gotten rid of the conventional voltage step dimming and two-way power line communications technology. Faulty streetlights can be detected remotely and the automatic notifications are sent to the registered mobiles to minimize the downtime. Feedback can be provided by the people about road lighting or luminaires that are not functioning properly (Interact City, 2019).

The project is self-financed due to energy savings and reductions in maintenance costs brought about by LED technology. Thus, as far as, streetlight is concerned, Pune Municipal Corporation has no extra financial burden. LEDs dimmed in a group can save up to 40% on electricity.

B. Jaipur, Rajasthan

Largest sensor based case study in India was in Jaipur (TviLight, 2021). This not only reduced the carbon dioxide emission, and light pollution, but also reduced the energy consumption by 72%. Automated diagnosis and reporting system facilitates the tracking of luminaire performance. Motion sensors and wireless controllers enable the adjustment of the brightness levels of streetlights based on real-time human presence. Lighting profile can be created from

the collected data that can be used to determine the unique illumination requirements of particular locations in the city.

Open API allow integration with other Smart City applications. These include several smart city applications such as smart parking nodes, environment sensors etc. The city can collect data to create the lighting profile and use that to determine the illumination requirements of particular locations in the city.

C. Jamshedpur, Jharkhand

Industrial town of Jamshedpur needs intelligent streetlight implementation to ensure energy conservation, reduction in carbon dioxide emission, and automated fault detection (Tata Communications, 2018). With the help of LoRa devices and wireless radio frequency technologies, Low Power Wide Area Network (LPWAN) enabled the smart lighting. LoRa technology is capable of monitoring each streetlight and repair faulty lights on a real-time basis. Energy consumption has been tracked and optimised by automatically switching off streetlights. The streetlights are controlled by a command centre which operates centrally and monitors, and optimizes the streetlights using a web-based application. Reduction in power consumption was of 27%.

2.4 Major Research Works

2.4.1 Intelligent Streetlight

Using IEEE 802.15.4 short-range communication technology, Pasolini et al. highlighted the technical aspects of designing and implementing smart streetlight systems. As part of their research, they have also produced an example of a smart building application that uses the low-rate (LoRa) and long-range communication protocol (Pasolini, et al., 2018). Instead of the traditional streetlights the use of LED DC lamps are more cost-effective with circuit-efficiency above 92%. An LED streetlight module driver with power factor modifications for the American voltage range of 100V–120V has been presented as a revolutionary single-stage, highly efficient, and cost-effective driver (Cheng, Chang, Chung, & Yang, 2015). LEDs have lower maintenance costs, higher efficiency, longer lifetime, and, over and above all, they are easily disposable as it is mercury-free. As a result of LED streetlight luminaries' technology, they have an explicit communication module that may either link to the local control module or directly to the Central server. In order to control, a certain driver must be used. There might be a motion sensor, daylight sensor, or other sensor attached to the communication module's

input to obtain the desired illumination level. Elements for detecting electrical problems such as driver failure, voltage/current exceeding predetermined levels, and flaws in the communication system have been included also (Barve, 2017).

A prototype of smart street lighting system has been proposed by El-Faouri et al. (El-Faouri, Sharaiha, Bargouth, & Faza, 2016). Photovoltaic (PV) panels have been used to power a number of DC street lights in this prototype. A motion sensor and a battery have been used to store extra energy generated by the solar panel. As a result, an intelligent and efficient lighting system has been developed.

Using the Global Positioning System (GPS) and an Internet-enabled cell phone, Müllner and Riener presented a pedestrian-alert smart street lighting (SSL) system. The GPS signal from the pedestrian is utilised to switch on or off the lamps (Müllner & Riener, 2011).

Communication between streetlights take place using ZigBee protocol. Leccese suggested intelligent LED lamps with remote control (Leccese F. , 2012). Solar panels have been installed to conserve energy by utilising ZigBee devices, sensors, and protocols to regulate intelligent streetlights. This system was said to be useful for street lighting in locations with low traffic during a specified time period. In another publication, the same author used ZigBee sensors with WiMAX to create fully automated smart street lighting for use in smart city applications (Leccese, Cagnetti, & Trinca, 2014). Local sensors have been used to turn the lights on or off. The coordinated lamp posts have been provided with computing power by Raspberry Pi. In both the works the authors did not mention the percentage energy saving. Both the systems consist of

a. Monitoring Station in each lamp post and they consist of the following modules:
    i. A presence sensor detects the passing of a vehicle or person and activates the lamp.
    ii. In the early morning or at twilight, a light sensor analyses the brightness of the sunlight and uses this information to guarantee that the roadway is properly illuminated.
    iii. Fault management and system upkeep have been made easier with the help of operating control.
    iv. To assess the system, a controller receives the data from the control unit and processes it.

b. Entire lighting system is visualized through Base Control Station. A Zigbee module collects light status data and transmits it to a central station. Flowchart of the control software is shown in Figure 2-2.
c. A wireless communication technology called ZigBee Network that is based on IEEE802.15.4 standard.

Kaleem et al. (Kaleem, Ahmad, & Lee, 2014) proposed a ZigBee mesh network for communication with streetlights, gateway nodes, and management software enabling real-time monitoring and control of an intelligent, energy-efficient LED streetlight system. Modification of the illumination status of streetlights have been implemented with light sensors.

Distributed Traffic-Aware Lighting Scheme Management Network (TALiSMaN) had designed to monitor pedestrian and vehicle traffic using a Wireless Sensor Network (WSN) (Lau, Merrett, Weddell, & White, 2015). Simulation has been done using Street Light Sim. Illuminance can be reduced to a predetermined value at a predetermined time Depending on the traffic about 45% reduced energy savings has been obtained. There are four different functioning states of Luminaire:

i. ON by delay
ii. ON by sensor
iii. ON by neighbour
iv. Lamp OFF

Operational states is depicted in Figure 2-3 state diagram.

Shahzad et al. presented an energy-efficient intelligent LED street lighting system (Shahzad, Yang, Ahmad, & Lee, 2016) to implement traffic-adaptive control. ZigBee mesh network has been used to facilitate communication between different streetlight nodes. The brightness of the LED streetlights adjusted in response to the density of traffic on the road during the day. LED street lamps' brightness may be adjusted by adjusting the density of people at various nodes in the traffic flow. The system consisted of light sensors, temperature sensor, and power metering sensor. Savings ranged from 68 to 82%, depending on the length of sunshine in summer vs winter.

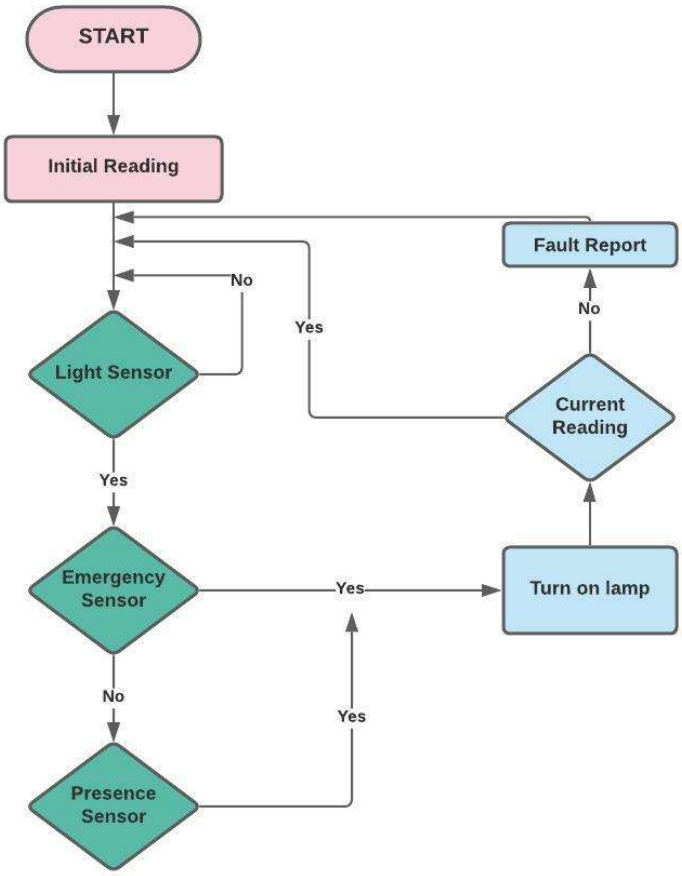

Figure 2-2. Control software flowchart *(Leccese F. , 2012)*

Using the DALI protocol and IEEE 802.15.4 for communications and streetlight control, a smart streetlight system has been suggested by Bellido-Outeiriño et al. (Bellido-Outeiriño, 2016). Energy saving and carbon dioxide emission was about 30% - 40%. This system also allows the integration of lighting network with other Smart City solutions. In addition, the illuminance level can be adjusted in response to changes in the reflectivity of the road surface, the volume of traffic, and the weather, all of which contribute to decreased energy usage without diminishing the luminaire's lifespan (Domenichini, La Torre, Vangi, Virga, & Branzi, 2017) (Guo, Gu, Wu, & Jiang, 2011). Compared to HPS lighting, LED lighting has a significantly lower energy efficiency index (by about 40-62%), meaning that the utility saved money by switching to LED (Yoomak, Jettanasen, Ngaopitakkul, Bunjongjit, & Leelajindakrairerk, 2018) (Davidovic & Kostic, 2022). ‘According to the life cycle cost analysis, the 80 W LED and 150 W HPS luminaires have about the same cost effectiveness for a new road lighting application assuming a 30-year operation period and the M2 road lighting class. In contrast, the overall cost of 153 W LED luminaires is less than that of 250 W HPS and

MH luminaires in the M1 road lighting class' (Ayaz & Ozcanli, 2021). When used in conjunction with a reflector module, LED lighting follows the CIE's standards for road illumination (Unlu, 2022). Daely et al. (Daely, Reda, Satrya, Kim, & Shin, 2017) presented a smart city streetlight system based on ZigBee and 3G technologies. ZigBee device collisions have been mitigated using Collision Sense Multiple Access (CSMA/CD). LEDs have been controlled using TCP/IP protocol.

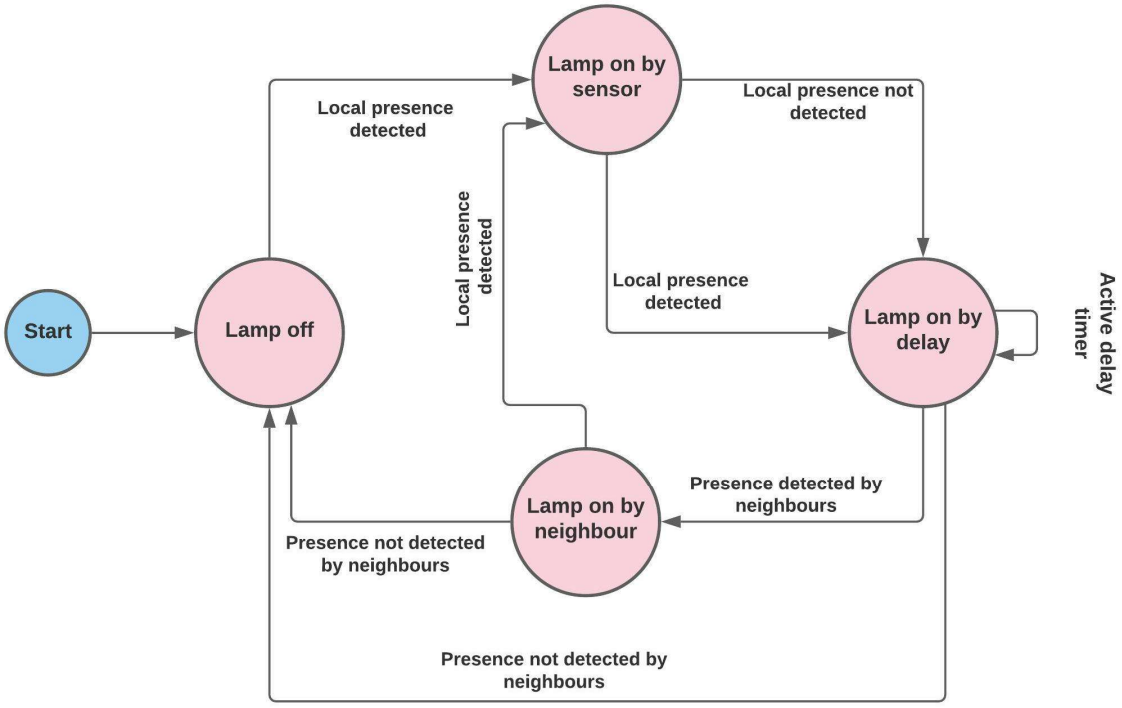

Figure 2-3. State machine diagram of the four operational states *(Lau, Merrett, Weddell, & White, 2015)*

Mohandas et al. (Mohandas, Dhanara, & Gao, 2019) presented a smart streetlight system based on an artificial neural network (ANN). Streetlight brightness levels have been controlled using fuzzy logic depending on the variations in luminance. The system's effectiveness has been tested in residential areas in five distinct situations. Energy consumption has been reduced by 13.5%. Power utilisation of a smart city can be optimised by integrating traffic management with intelligent street lighting (Novak, Pollhammer, Zeilinger, & Schaat, 2014). Najim et al. (Najim , Al-Omari , & Said , 2008) employed an ANN-based technique to assess the load curve both during the day and at night, taking into account variables like temperature and the time of day.

Adaptive LoRa-based approach for intelligent streetlight has been proposed by Bingol et al. (Bingöl, 2019). The system architecture consists of LED fixture or node, LoRa network server and gateways, and central unit with GUI. LED nodes integrated with controllers receive data from a central unit that includes an alert system, a persistence layer, and a control unit.

For intelligent control of streetlights Fernandes et al. (Fernandes, et al., 2014) proposed a solution that made use of smart grid control. For wide-area networks, IEEE standards-based wireless protocols have been used in the development of the core. However, this approach is not possible in Indian scenario. ZigBee networks linking streetlight nodes have been offered as a solution by Shahzad et al. (Shahzad, Yang, Ahmad, & Lee, 2016) . LED street lighting' brightness may be adjusted based on the number of people using them by exchanging data about traffic flow. The complexity of this approach has been increased by using a layered communication protocol structure to secure and implement it.

Energy consumption and waste may be minimised using an Infrared (IR) Sensor & Moonlight-based method, according to research work by Jagdish et al. (Jagadeesh, Akilesh, & Karthik, 2015). Brightness of the light has been reduced based on the moonlight and the use of Proximity IR help measure the intensity to control the lamp. Even though the technology is basic, it uses a lot of energy. In addition, it can't be utilised to determine the exact time of the day. Image processing has been reportedly employed in another research. In addition to a basic on/off switch, a camera module monitors the density of vehicles and people on the street, allowing it to regulate the lamps in real time. Because it can only hold a single light source, its use might be prohibitively costly (Veena, et al., 2016).

The dust as well as mist factor is strong in some regions where street lights are located. Akin et al. (Akin, Sisiopiku, & Skabardonis, 2011) compared the results between different environmental conditions. However, it has been found that in rainy seasons, not only does the speed of automobiles decrease but traffic volume decreases as well. Vehicle speed is approximately same in mist or dusty circumstances to that in a clear environment. LED lights are advantageous in this case because they eliminate glare and, as a result, minimise driver and pedestrian fatigue due to visual tiredness. In addition, there is no need for a warm-up period, allowing for immediate optimum brightness levels. Flexibility is the most crucial component in allowing lowering of light to be achieved (Mathur, 2010).

LEDs require an extremely short switching interval period compared to HPS luminaires; therefore, they can be utilised for implementing smart street lighting (SSL) systems in which

lighting poles can be attached with ZigBee-based radio devices and these can be controlled by multi-hop routing from a central SSL server that receives information of pedestrian locations and performs dynamic switching of LED luminaires (Müllner & Riener, 2011). LED-based SSL systems can be operated for different classes of roads and their energy efficiency can be evaluated and optimized based on the normalized power density criterion. A large-scale study focusing on exploring the feasibility of retrofitting conventional road lighting luminaires with LEDs found definitive environmental and economic benefits, primarily a simple payback period (SPP) of 16 months, savings to investment ratio (SIR) of 4.49 and electrical energy saving of about 36,880 MWh/year, which reinforces the perceived benefits of retrofitting street lights with LEDs (Bamisile, Dagbasi, & Abbasoglu, 2016). Therefore, it can be aptly posited that road lighting systems with LED luminaires would ultimately be advantageous when compared to the existing HPS-based road lighting installations (Todorovic & Samardzˇija, 2017) and it would become the perdurable standard of road illumination in the face of a global energy crisis.

Roads can be classified in accordance with a validated real-time traffic and road condition data-based weighted sum model (Chakraborty S. B. P., 2018) and road lighting systems can be categorized into five energy-efficient classes A, B, C, D and E based on the normalized power density levels for different road surface types such as smooth and granular surface bituminous, asphalt, porous concrete, etc. (Chakraborty S. B. P., 2018).

Streetlights that are dimmable and have motion sensors and ZigBee or Bluetooth wireless connection can save energy as well as adaptive dimming when combined with ambient light level sensors. When there are no cars or people passing by the streetlights, dimming and tele-management of streetlight systems is beneficial (Johnson, Phadke, & Stephane, 2014).

In another work, Satvaya et al. (Satvaya, Mondal, Sur, & Mazumdar, 2018) designed and developed of a smart street lighting system prototype that uses Zigbee communication protocol to transmit data between two xbee modules that has been utilized to make the system intelligent and self-operative. The system has the limitation of poor communication distance which can be upgraded by other version of xbee module. It also enables supervisory control of the system from local control station. Raspberry Pi module with specific IP address has been connected with the system to transmit and receive information using internet network. In that sense the system can be accessed from any place with internet connection. In that scenario

encryption & decryption methodologies become very important to make the system secure enough and fault free in future, not allowing unauthorized access.

2.4.2 Dynamic Light Controller

A simple dynamic light controller (DLC) has been suggested, designed, and built to enable the practical implementation of a white light emitting diode (WLED) light source with changeable correlated color temperature (CCT) but constant light output by Maiti et al. (Maiti P. K., 2015). For a set of CCT points that fall within 2840–5750 K and a fixed illuminance of 300, the DLC's performance was empirically confirmed. For warm white and cool white zones, the maximum divergence in CCT had been 160 – 194K. Compared to a reference illuminance of 300 lx, the measured illuminance values varied by just 9.7 percent to 8.3 percent. Using a dynamic light controller (DLC), the authors in another study looked at the performance of LED arrays with warm and cool white LEDs to create a dynamic light source (Maiti & Roy, 2018). There are two methods for varying the CCT and the light output of DLC: step variation and continuous variation. 16 potential combinations of four CCT values between 2900–5600 K and four illuminance values between 100–300 Lux have been examined for step variation performance. It has been found that the measured illuminance values has a variance of roughly 16 percent, which is so little that it cannot be seen by the naked eye and is not noticeable to the human eye. The DLC's performance has been determined to be good, although the light output of discrete WLED arrays at lower duty cycles affects the performance.

Maiti et al. developed a microcontroller-based electronic dimmer employing pulse width modulation (PWM) in a separate study. An infrared (IR) remote control can be used to operate the dimmer, which can be linked between the LED module and the driver. Commercially available warm and cool LED luminaires used for indoor lighting applications have been used to test the performance of the developed LED dimmer. Light output of the white LED luminaire could be changed from 25% to 100% without a significant change in its photometric and color properties using a dimmer. When dimmed to 25 percent, the efficiency of the warm and cool white luminaires has been reduced by 17 and 14.7 percent respectively (Maiti & Roy, 2017).

In another paper Satvaya and Mazumdar (Satvaya P., 2014) discusses the different criteria of advanced luminaires and different methods used these days in road lighting, which has been categorised as advanced luminaires. A software model has been created by Roy et al. (Roy, et al., 2022) to facilitate rapid approximation of pertinent road surface illuminance parameters with a view of the dominant road lighting practices involving common heuristic configurations.

Photometric simulations of road lighting have been conducted with photometric data tables of high-pressure sodium (HPS) and LED luminaires possessing different power ratings for a specified set of luminaires with features such as mounting height, road width, pole spacing, overhang and tilt values. A mathematical model comprising of six equations derived by multiple linear regression was proposed with relevant predictor variables. A framework for LED luminaire power rating selection for retrofitting operations was proposed for the assistance of the manufacturers and the utility operators.

Stability analysis was done on LED driver system based on buck-boost topology. LED modules have been satisfactorily operated with power rating in the range of 6W – 24W (Ganguly, Gupta, & Satvaya, 2019). A microcontroller-based smoke and gas detector technology was implemented with mobile communication and a LED emergency light. The system can detect fire or gas within 5 minutes and sends alert SMS so that people can evacuate easily with the help of emergency light (Mukherjee, Satvaya, & Mazumdar, 2019).

Light sources' spectral composition has an impact on object recognition since it affects how a lighting environment appears. Furthermore, even when doing the same visual task under the same lighting conditions, brain activity varies (Biswas, Chakraborty, & Nath, 2018).

In research comparing visual performance under metal halide (MH) and high pressure sodium vapour (HPSV) lighting conditions, the response times of varied participants reveal that early object detection occurs under light sources with a higher SP ratio (Lewis A. , 1999) (Fotios, Cheal, & Boyce, 2005) (Akashi & Rea, 2002) (Rea, Bullough, & Akashi, 2009). As an example, Akashi et al. discovered that for an off-axis moving target in the actual field, a difference in reaction time between metal halide (high SP ratio) at high photopic light levels and sodium vapour at high pressure (low SP ratio) was seen. Individual differences in perception-action coupling are also seen, showing that there may be differences in human brain processing that are not represented in behavioural differences across individuals. Electroencephalogram (EEG) data from tasks conducted under an HPS light source show more red and dark blue colors than signals from tasks performed under an MH light source, indicating that the brain is more active in both hemispheres during the tasks performed under the HPS light source (Chakraborty S. R. D., 2021). A major influence on object detection under a variety of illumination conditions can be attributed to subjective perception of the environment (Akashi Y., 2007) (Lewis A. , 1999) (Boyce & Bruno, An evaluation of high pressure sodium and metal halide light sources for parking lot lighting, 1999) (Eloholma, Halonen, & Ketomuki, 1999). Effect of light spectrum on the detection of off-axis targets suggest that there is a significant effect of light colour relevant to road lighting. Specifically, (He Y., 1997) carried

out a laboratory experiment in which HPS and MH light sources were compared for their effects on the reaction time to the onset of a 2° diameter disc with the centre either on-axis or 15° off-axis, for a range of photopic luminances from 0.003 to 10 cd/m².

In the photopic state, the cones are dominant, but as the mesopic state is reached, the rods begin to have an impact on spectral sensitivity until in the scotopic state, the rods are completely dominant. Given the different balances between rod and cone photoreceptors in different parts of the retina and under different amounts of light, it should not be surprising that the MH light source produces shorter reaction times for off-axis detection than the HPS in the mesopic range because it is better matched to the rod spectral sensitivity (Boyce P. R., Human Factors in Lighting,, 2014).

The effect is that light sources that provide greater stimulation to the rod photoreceptors, that is, with a higher S/P ratio, ensure better off-axis visual performance (Akashi Y., 2007). Given that both on- and off-axis vision are important to drivers, a responsible approach to introducing the effect of light spectrum into road lighting practice would be to use light sources with high S/P ratios i.e. high CCT, without reducing recommended road surface luminances expressed in photopic measures (Boyce P. R., Human Factors in Lighting,, 2014).

Higher-order brain activities and cortical networks are not known to be affected by the lighting condition, which is now under investigation. As a result, human cognition in low-light environments provides a complex, yet understudied, scenario. Further consideration has been given to streetlights with different color appearances, such as metal halide (MH) and high pressure sodium vapour (HPSV) lamps (Biswas, Chakraborty, & Nath, 2018) (Janoff & Havard, 1997) (Rea, Bullough, & Akashi, 2009) (Fotios, Cheal, & Boyce, 2005) With increasing complexity, even very simple object identification might become incredibly difficult to do.

Using a peripheral light source at 2500 K, the average response time is significantly shorter than when not using one. The CCT source with a 4000 K color temperature has a similar effect, providing for improved vision. The same positive affect has been exerted by 5000 K CCT. As a result, for all CCTs, the observer receives a good benefit from peripheral lighting as a result of this. However, visibility is negatively affected with a color temperature of 6000 K CCT. The Correlated Color Temperature of the light source has been shown to have an impact on the performance of object detection (CCT).

A considerable impact on subject performance has been demonstrated to be caused by Correlated Color Temperature (CCT), which can be measured both on and off-axis. Even in

low-light settings, the color rendering index (CRI) of the source has a direct impact on the performance of the viewer. Color temperature has a considerable impact on the capacity of the user or observer to see under different lighting conditions.

In summary the literatures shows different types of LED based luminaires with separate control logics. Luminaire developed by Mullner et al controls the light levels based on GPS signals from pedestrians have been used for light level control of luminaires. The Luminaire system developed by Leccese F et al does not provide any solution for power computation methodologies. Simulation based lighting system has been developed by Lau et al for pedestrian and vehicle traffic and accordingly control illumination level. Most of the literature addresses the light level control and reduction of power consumption by the luminaires based on traffic situations. Some literature like Maity et al, Chakraborty et al, Rea et al addresses the visual performance issues under different CCT light from the luminaire. Variable CCT lighting conditions have been discussed mostly in laboratory conditions. Performance parameters dynamic CCT light from has not been discussed.

The commercial lighting systems mentioned like InteliLight, Aaeon Intelligent Lighting system, Kanglight etc., does not provide flexibility over the control of the colour of light emitting from the luminaire for choosing the proper visibility level and ability to observe small objects by varying the scotopic and photopic illumination level ratio.

Present thesis addresses the mentioned issues and research gaps in detail along with development of the proposed system.

Chapter 3: Estimation of Road Surface Illuminance Parameters

Various local bodies, municipalities and transportation authorities at governmental and semi-governmental levels have been retrofitting existing High Pressure Sodium (HPS) luminaires with LED luminaires of lower power ratings. This may be attributed to several perceived advantages of installing LED-based road illumination systems which are energy-efficient and the luminous efficacy of such illumination systems is expected to increase in the near future (Brons, Bullough, & Frering, 2021) (Beckwith, Zhang, Smalley, Chan, & Yand, 2011). This would result in almost 83% decrease in electrical energy consumption when compared to HPS luminaires (Chenani, Rasanen, & Tetri, 2018). LED luminaire optical systems can be customized to deliver lights to intended areas (Eichelberger, 2010), and individual lenses may distribute the luminous flux output from one or a string of LEDs.

White LED-based illumination systems not only reduces greenhouse gas emissions to a significant extent (Mills, 2002), but also LED-based road illumination systems can easily be controlled, dimmed and integrated with the internet-of-things (IoT) based local or regional network systems (Anguraj, Balasubramaniyan, Kumar, Rani, & Ashwin, 2021), (Satrya, et al., 2017). Solar energy harvested from daylight and stored in battery banks can be fed to LED-based street lighting systems at night to ensure higher luminous flux delivery per watt of consumed power (Ciriminna, Meneguzzo, Albanese, & Pagliaro, 2017), (Bhattacharya, 2022), (Muhaisen, Khan, Habaebi, Ahmed, & Ahmed, 2021). Finally, the spectral power distribution of the luminous flux emitted by white LEDs has more relative spectral power in lower wavelengths in the ‘blue’ region (Brons, Bullough, & Frering, 2021) and this may render a road illuminated by such LEDs to seem brighter when compared to the yellowish illumination of HPS luminaires as white light is perceived to be brighter than yellowish light at equal photopic light levels (Rea, Bullough, & Akashi, 2009).

To install new lighting poles, lighting fixtures or retrofitting the existing ones, it is appropriate to estimate essential road surface illuminance parameters and luminaire power requirements beforehand so as to maintain compliance with local, regional, or national level lighting codes, regulations and standards, calculate the costs involved with new or retrofit installations and analyse the bids received in a tender with specific technical requirements. Consequently, photometric simulations of road lighting have been conducted for both LED and HPS luminaires, and a road lighting model was promulgated which could facilitate simple

estimation of road surface average illuminance, uniformity of illuminance and diversity of illuminance levels for different luminaire power ratings of both LED and HPS luminaires. In addition, an overview pertaining to the selection of appropriate LED luminaire power ratings corresponding to different HPS luminaire luminous flux output values has been provided to maintain constant road surface average illuminance levels upon retrofitting.

3.1 Road Lighting Simulation

Photometric simulations of road lighting have been conducted with a software model created in Relux, a validated tool for general-purpose road lighting simulation that has also been used for community street lighting simulation with the 'Crime Prevention Through Environmental Design (CPTED)' approach (Kim & Park, 2017). The photometric quantity illuminance (S.I. unit: lx or lm/m2), considered as the pre- dominant quantity for road lighting design and analysis, was prioritized in this work as the light distribution on a road surface can be thought of as the spatial variation of this quantity (Moreno, Avendaño-Alejo, Saucedo-A, & Bugarin, 2014)]. By default, the road width and luminaire pole spacing have been assumed to be uniform along the road strip for photometric computation (Sedziwy, 2016). In the software model, every road strip was considered with two lanes and without any central reservation. The chosen luminaires had type II lateral distribution (50% candlepower iso-intensity trace remains within 1 to 1.75 times the mounting height on the street side with respect to the luminaire position), and short-medium range longitudinal distribution (i.e., the tip of maximum candlepower can be located within 1 to 3.75 times the mounting height on both sides longitudinally with respect to the luminaire position) (Rea M. S., 2000). Five luminaire power ratings, inclusive of magnetic ballast/ integrated driver power dissipation, have been chosen for simulation with HPS luminaires (Cooper, GE Lighting Solutions and Hubbell): 100 W, 150 W, 250 W, 468 W and 675 W, and six luminaire power ratings have been chosen for simulation with LED luminaires (GE Lighting Solutions, Rab Lighting, Decrolux Lighting, Signify and Hubbell): 43 W, 93 W, 123 W, 180 W, 294 W and 347 W. Consequently, necessary luminaire luminous intensity files (.ies file format) have been introduced into the created software model.

The polar luminous intensity curves of the chosen HPS and LED luminaires have been depicted in Figure 3-1 and Figure 3-2, respectively. The system design parameters, specified in Table 3, have been chosen with a view of the prevailing practices involving common heuristic configurations (Czyzewski D., 2020) (Karmakar, Aruna, Rao, & Yaragatti, 2006) (Kostic, Kremic, Djokic, & Kostic, 2013) (Pracki, 2011) and they have been applied to conduct photometric simulations with the created road lighting model and the aforementioned

luminaires. A maintenance factor (MF) of 0.8 was designated in order to take account of the lamp luminous flux output (lumen) depreciation over time and accumulation of dirt over the luminaire light-emitting surface. The outputs have been compiled in a tabular form for statistical analysis.

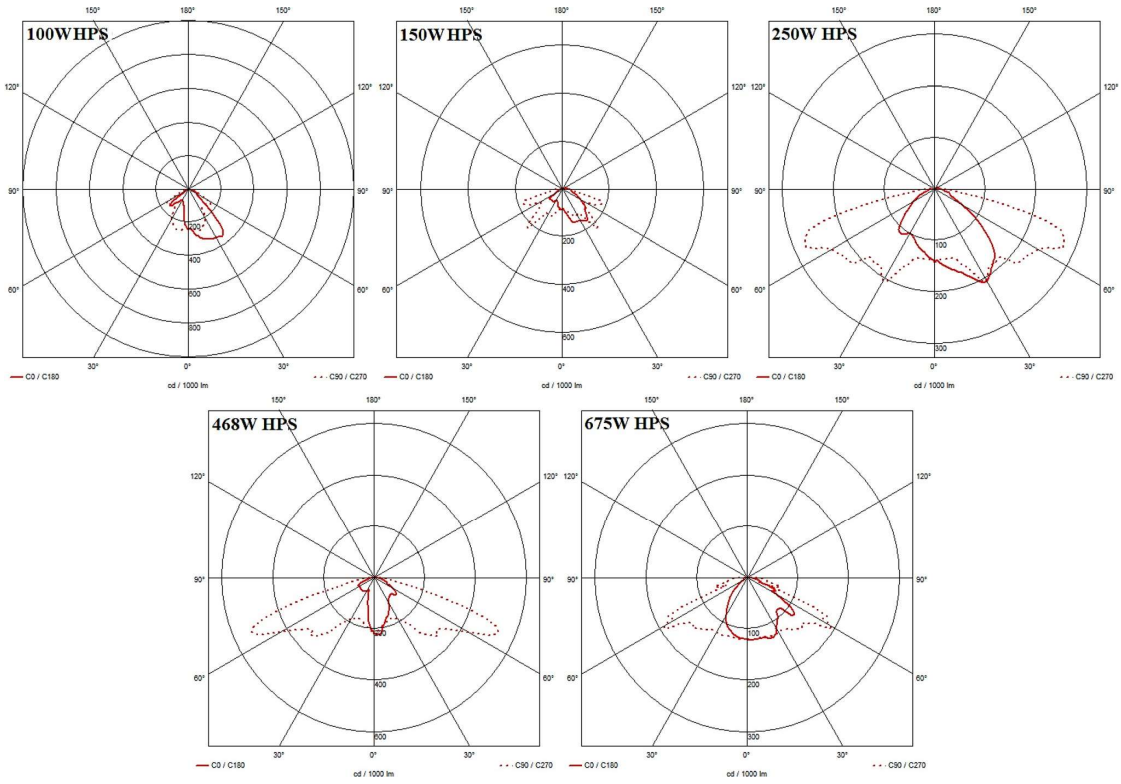

Figure 3-1. Polar luminous intensity curves of the chosen HPS luminaires for photometric simulation of road lighting

Table 3-1. System design parameters and constraints in the created road lighting simulation model with single- sided pole arrangement

System design Parameters/constraints/variables	Values/description
Luminaire type	HPS and LED
Luminaire power rating (W) for LED	43, 93, 123, 180, 294 and 347
Luminous efficacy range (lm/W) for LED	79.9 to 142.6
Luminaire power rating (W) for HPS	100, 150, 250, 468 and 675
Luminous efficacy range (lm/W) for HPS	64 to 86.6
Luminaire mounting height (m)	9 and 12
Road width (m)	8 and 10
Pole spacing (m)	30, 40 and 50
Overhang (m)	1.5 and 2.5
Luminaire tilt (degrees)	5 and 10

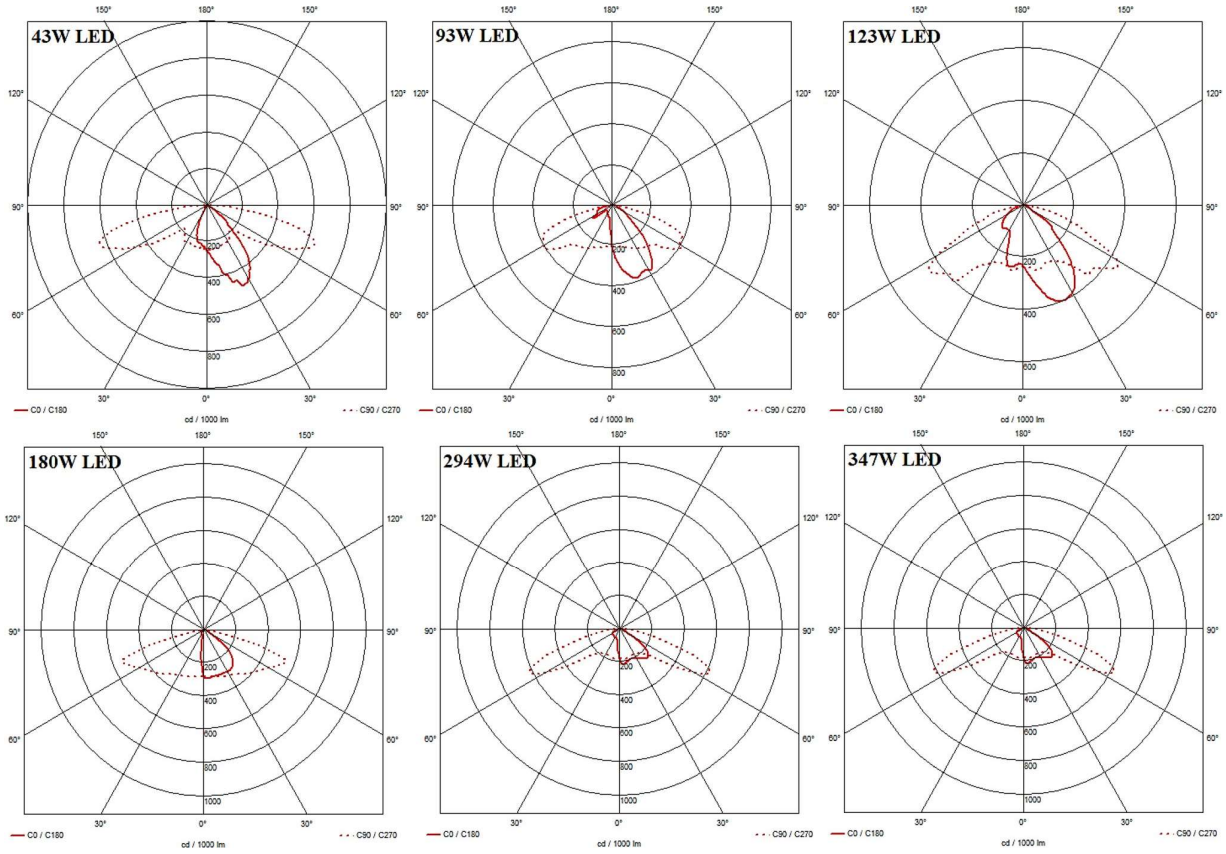

Figure 3-2. Polar luminous intensity curves of the chosen LED luminaires for photometric simulation of road lighting

3.2 Linear Model for Estimation of Road Surface Illuminance Parameters for existing lighting system design configurations

The compiled output data, obtained from photometric simulation of road lighting for the design parameters specified in

Table *3-1*, have been utilized to formulate a simple linear model of estimating road surface mean (average) illuminance, uniformity of illuminance ($U_0 = E_{min}/E_{avg}$), and diversity of illuminance ($U_D = E_{min}/E_{max}$). Evidently, road surface average illuminance (E_{av}), minimum illuminance (E_{min}) and maximum illuminance (E_{max}) have been taken as the respective outcome variables and the following eight variables have been chosen as the predictor variables: luminaire power or wattage rating (W), pole mounting height (h), the width of the road (b), spacing between adjacent poles or span (S), luminaire overhang (y_l), luminaire tilt (d), luminous efficacy (g; unit: lm/W) and luminaire power per unit road length (S; unit:

W/km). Multiple regression analysis was conducted to predict E_{av} and E_{max} from all the aforementioned predictor variables except S, and E_{min} from all the eight predictor variables including S. Regression Equations (1) to (3) have been derived from the photometric simulation of road lighting with HPS luminaires (F = 525.3196, p < 0.0005 and R^2 = 0.9406 for $\widehat{E}_{av}$; F = 380.4946, p< 0.0005 and R^2 = 0.9198 for$\widehat{E}_{max}$; F = 410.4953, p< 0.0005 and R^2 = 0.9342 for$\widehat{E}_{min}$), and regression Equations (4) to (6) have been derived in a similar manner from photometric simulation of road lighting with LED luminaires (F = 586.945, p< 0.0005 and R^2 = 0.9361 for $\widehat{E}_{av}$; F = 573.7986, p< 0.0005 and R^2 = 0.9348 for $\widehat{E}_{max}$; F = 444.4643, p< 0.0005 and R^2 = 0.9272 for $\widehat{E}_{min}$).

$$\hat{E}_{av} = 33.1308 + 0.04037 * W - 1.18472 * h - 0.36017 * b - 0.37692 * S + 0.507 * y_l + 0.00793 * \delta - 0.02533 * \eta \quad (1)$$

$$\hat{E}_{max} = 40.40382 + 0.129281 * W - 8.13722 * h - 0.08 * b - 0.01687 * S + 0.618333 * y_l + 0.129 * \delta + 0.648056 * \eta \quad (2)$$

$$\hat{E}_{min} = -11.5217 - 0.02124 * W + 0.4445 * h - 0.07242 * b - 0.001349 * S + 0.058167 * y_l + 0.0097 * \delta - 0.096909 * \eta + 001182\tau \quad (3)$$

$$\hat{E}_{av} = 12.6886 + 0.054607 * W - 0.98345 * h - 0.26351 * b - 0.30838 * S + 0.405764 * y_l + 0 - 0.01001 * \delta - 0.117198 * \eta \quad (4)$$

$$\hat{E}_{max} = 50.96216 + 0.20287 * W - 7.83354 * h - 0.09003 * b - 0.01229 * S + 0.195347 * y_l + 0.28579 * \delta + 0.321898 * \eta \quad (5)$$

$$\hat{E}_{min} = -8.08252 - 0.03203 * W + 0.240301 * h - 0.03837 * b - 0.053279 * S + 0.026181 * y_l + 0.002792 * \delta + 0.030307 * \eta + 001655\tau \quad (6)$$

However, it was noted that at α=0.05 significance level, not all the predictor variables contributed statistically significantly to the prediction of E_{av}, E_{max} and E_{min} for both HPS-based and LED-based photometric simulation of road lighting. Therefore, the contributions from those predictor variables which have been deemed insignificant at α=0.05 significance level in predicting E_{av}, E_{max} and E_{min} have been omitted from further statistical analysis. Considering only those predictor variables which contributed statistically significantly at α=0.05 significance level, multiple regression analysis was further conducted to predict E_{av}, E_{max} and , E_{min} and therefore, regression Equations (7) to (12) have been obtained. Regression Equations (7) to (9) have been derived from the photometric simulation of road lighting with HPS luminaires (F = 913.6757, p<0.0005 and R^2 = 0.9395 for E_{av}; F = 900.2257, p< 0.0005

and $R^2 = 0.9196$ for E_{max}; $F = 827.4611$, $p < 0.0005$ and $R^2 = 0.9337$ for E_{min}), and regression Equations (10) to (12) have been derived in a similar manner from photometric simulation of road lighting with LED luminaires ($F = 818.9805$, p\0.0005 and $R^2 = 0.9355$ for E_{av}; $F = 1344.051$, $p < 0.0005$ and $R^2 = 0.9342$ for E_{max}; $F = 715.53$, $p < 0.0005$ and $R^2 = 0.9269$ for E_{min}).

$$\hat{E}_{av} = 32.09542 + 0.040605 * W - 1.18472 * h - 0.36017 * b - 0.37692 * S \quad (7)$$

$$\hat{E}_{max} = 41.21299 + 0.129281 * W - 8.13722 * h + 0.648056 * \eta \quad (8)$$

$$\hat{E}_{min} = -11.9304 - 0.02113 * W + 0.4445 * h + 0.096909 * \eta + 001177 * \tau \quad (9)$$

$$\hat{E}_{av} = 13.42053 + 0.054607 * W - 0.98345 * h - 0.26351 * b - 0.30838 * S + 0.117198 * \eta \quad (10)$$

$$\hat{E}_{max} = 52.19431 + 0.202868 * W - 7.83354 * h + 0.321898 * \eta \quad (11)$$

$$\hat{E}_{min} = -8.35453 - 0.03203 * W + 0.240301 * h + 0.058279 * S + 0.030307 * \eta + 001655 * \tau \quad (12)$$

Equations (7) to (12) constitute the proposed road lighting model. Table 3-2 and Table 3-3 demonstrate the analysis of variance (ANOVA) results with relevant predictor variables in connection with the conducted multiple regression analysis with outputs emanating from HPS-based and LED-based road lighting simulations, respectively.

Table 3-2. ANOVA results of the regression model pertaining to HPS-based photometric simulation of road lighting

ANOVA, HPS Luminaires, α = 0.05							
Outcome	Variable	df	SS	MS	F	p-value	sig
$\hat{E}_{av}$	Regression	4	21,245.62	5311.404	913.6757	6.8E-142	Yes
	Residual	235	1366.108	5.813227			
	Total	239	22,611.72				
$\hat{E}_{max}$	Regression	3	209,013.1	69,671.05	900.2257	7.4E-129	Yes
	Residual	236	18,264.72	77.39286			
	Total	239	227,277.9				
$\hat{E}_{min}$	Regression	4	2620.092	655.0231	827.4611	3.7E-137	Yes
	Residual	235	186.0274	0.791606			
	Total	239	2806.12				

However, it should not be construed that those predictor variables which did not contribute statistically significantly (at α = 0.05 significance level) to the prediction of the outcome variables in the preceding analysis have no bearing to or cannot influence the outcome variables

under any circumstances or illumination system design configurations. To expound upon the rationality behind this supposition, let two predictor variables y_l and δ be considered which did not contribute statistically significantly in the foregoing analysis.

Table 3-3. ANOVA results of the regression model pertaining to LED-based photometric simulation of road lighting

ANOVA, HPS Luminaires, α = 0.05							
Outcome	Variable	df	SS	MS	F	p-value	sig
$\widehat{E}_{av}$	Regression	5	17,938.7	3587.74	818.9805	1.4E-165	Yes
	Residual	282	1235.369	4.38074			
	Total	287	19,174.07				
$\widehat{E}_{max}$	Regression	3	229,351.6	76,450.52	1344.051	2E-167	Yes
	Residual	284	16,154.1	56.88065			
	Total	287	245,505.7				
$\widehat{E}_{min}$	Regression	5	1470.382	294.0763	715.53	6.9E-158	Yes
	Residual	282	115.8994	0.410991			
	Total	287	1586.281				

Those two predictor variables could not contribute statistically significantly in the foregoing multiple regression analysis principally due to their relatively lower variability (δ varied from 5^0 to 10^0 and y_l varied from 1.5 m to 2.5 m), the light output distribution patterns of the chosen luminaires and the chosen significance level. Additional simulations have been conducted to illustrate the effects of δ (δ was varied from 5^0 to 70^0 with an interval of 5^0) on road surface illuminance parameters considering the following design specifications: Wattage = 294 W (for LED) and 468 W (for HPS), h = 9m; b = 8m; S = 30m; y_l = 1.5m. Likewise, the effects of y_l (y_l was varied from 0.5 m to 7 m with an interval of 0.5 m) on road surface illuminance parameters have been explored considering the following design specifications: Wattage = 294 W (for LED) and 468 W (for HPS), h = 9m; b = 8m; S = 30m; δ = 5^0. Figure 3-3 portrays the association between δ and road surface illuminance parameters E_{av}, E_{max} and E_{min}, and Figure 3-4 portrays the association between$y_l$and road surface illuminance parameters E_{av}, E_{max} andE_{min}. It may be seen that the respective curves can be fitted with polynomial mathematical functions and the coefficient of determination (R^2) values have been 0.90 in each scenario. The association between E_{av} and δ has been expressed by quadratic functions (^{R2}> 0.93), that between E_{max} and δ has been expressed by quartic functions (R^2> 0.97) and that between E_{min} and δ has been expressed by cubic functions (R^2 > 0.99).

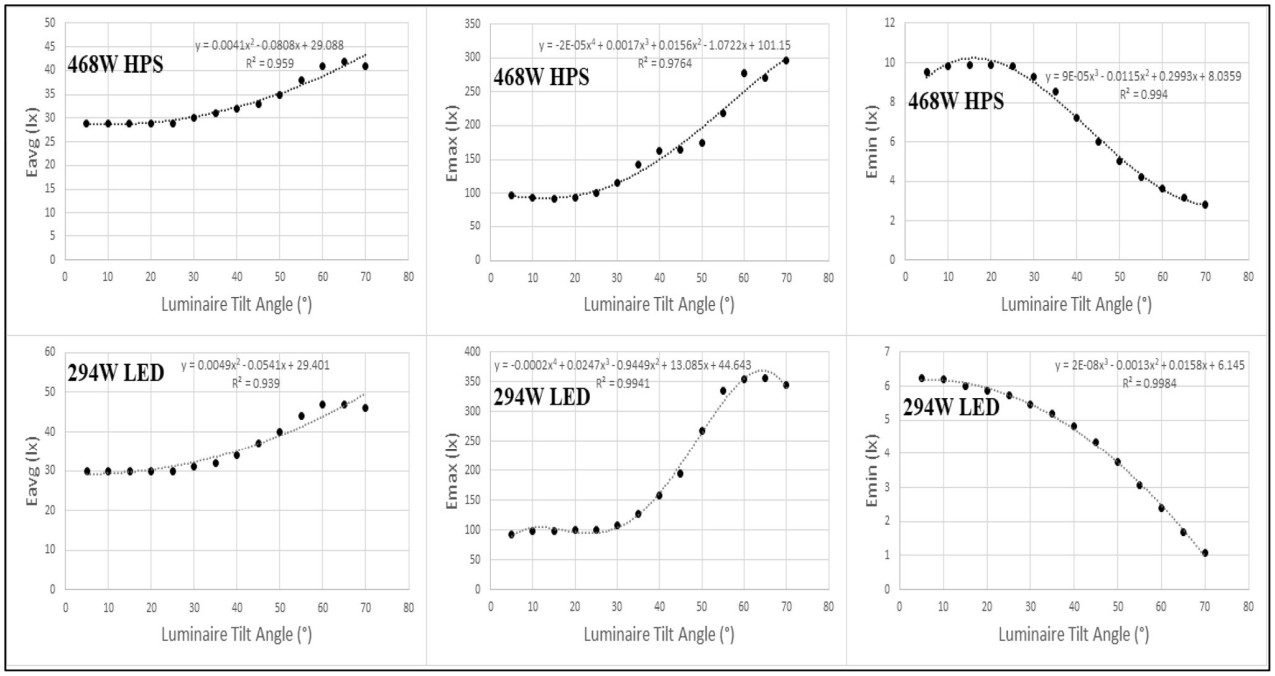

Figure 3-3. Characteristic curves of the association between luminaire tilt and road surface illuminance parameters (average illuminance, maximum of illuminance and minimum of illuminance) for a particular system design specification

Yet, the aforementioned associations demonstrate predominantly linear characteristics for the sub-domain $\delta = 5^0 – 20^0$ and E_{av}, E_{max} or E_{min} undergo modest levels of variation (< 7.5%) along the ordinate for the aforementioned sub-domain of δ. Likewise, in Figure 3-4, the association between E_{av} and y_l has been expressed by quadratic functions (R^2> 0.96), that between E_{max} and y_l have been expressed by quartic functions (R^2>0.91) and that between E_{min} and y_l have been expressed by cubic functions (R^2>0.93). It might be inferred that the aforementioned associations demonstrate predominantly linear characteristics for the sub-domain $y_l = 0.5 – 2.5$ m and E_{av}, E_{max} or E_{min} undergo modest levels of variation (<10.5%) along the ordinate for the aforementioned sub-domain of y_l.

3.3 Maintain Constant Road Surface Average Illuminance Levels Upon Retrofitting

Manufacturers, municipal authorities and electrical contractors look for a rational basis for choosing the most appropriate LED luminaire power ratings to retrofit existing HPS luminaires under different circumstances. The common practice in road lighting has been to refer to heuristic guidelines in selecting a luminaire power rating for local-level implementation which may leave uncertainties in documenting the implementation of regional and national level energy policies. Thus, the output data obtained from photometric simulation of road lighting

have been curated and analysed to introduce a framework for selecting appropriate power ratings of LED luminaires that would maintain road surface luminous flux packages comparable to pre-retrofit conditions. The relationship between luminaire power rating or wattage (W) and road surface average illuminance level (lx) was explored for both LED and HPS luminaires and it was found that the relationship followed a linear pattern with coefficient of determination (R^2) values being greater than 0.91.

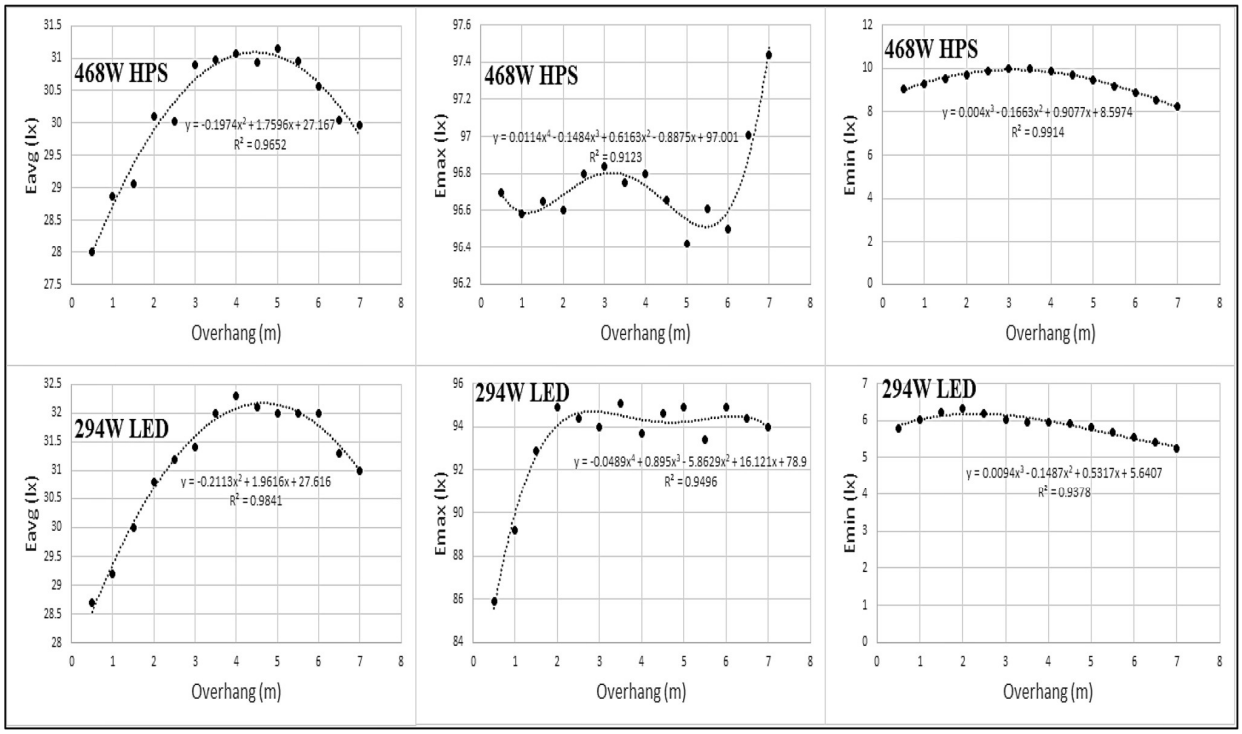

Figure 3-4. Characteristic curves of the association between luminaire overhang and road surface illuminance parameters (average illuminance, maximum of illuminance and minimum of illuminance) for a particular system design specification

This is also an indicator that the luminous flux linkages with the road surface from luminaires (having the type-II lateral and short-medium longitudinal distribution of emitted luminous flux in the context of this work) with nearly identical power ratings are fairly similar. Figure 3-5, Figure 3-6 and Figure 3-7 demonstrate the luminaire wattage-average illuminance trend lines for pole spacing of 30, 40 and 50 m, respectively. With a view of prevalent road lighting system configurations, the width of the carriageway or the road strip in this analysis was fixated at 8 m and it could consist of one or more lanes, as it may be specified. The mounting height for all luminaires was kept at 9 m above the road surface. The overhang was chosen to be 1.5 m, and the luminaires have been tilted at an angle of 5^0.

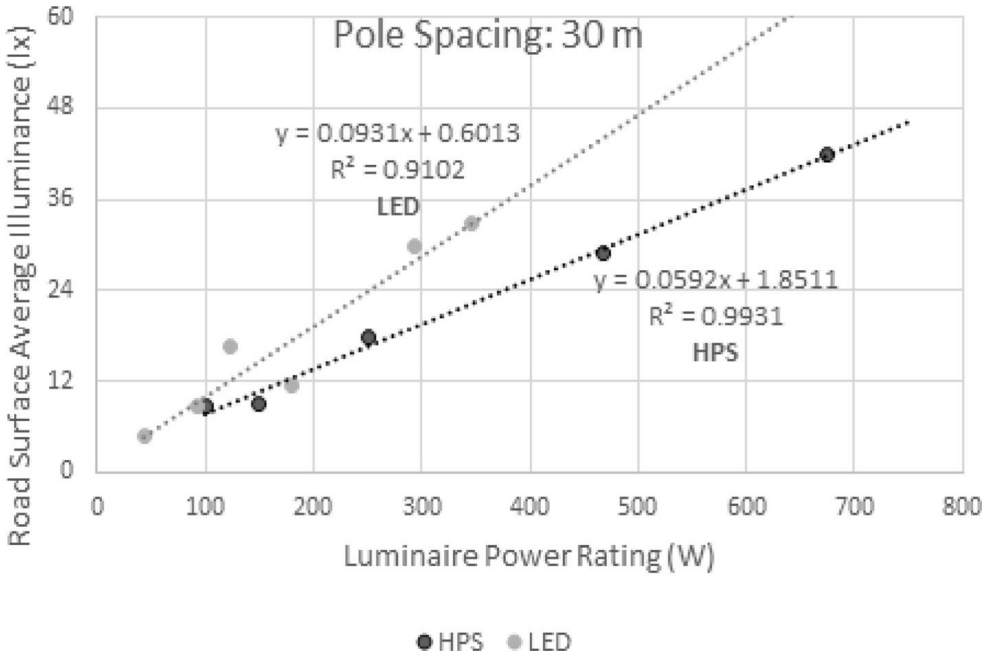

Figure 3-5. Exploration of the relationship between road surface average illuminance and luminaire power rating with HPS and LED luminaires for a conventional system configuration with a single-sided pole spacing of 30 m

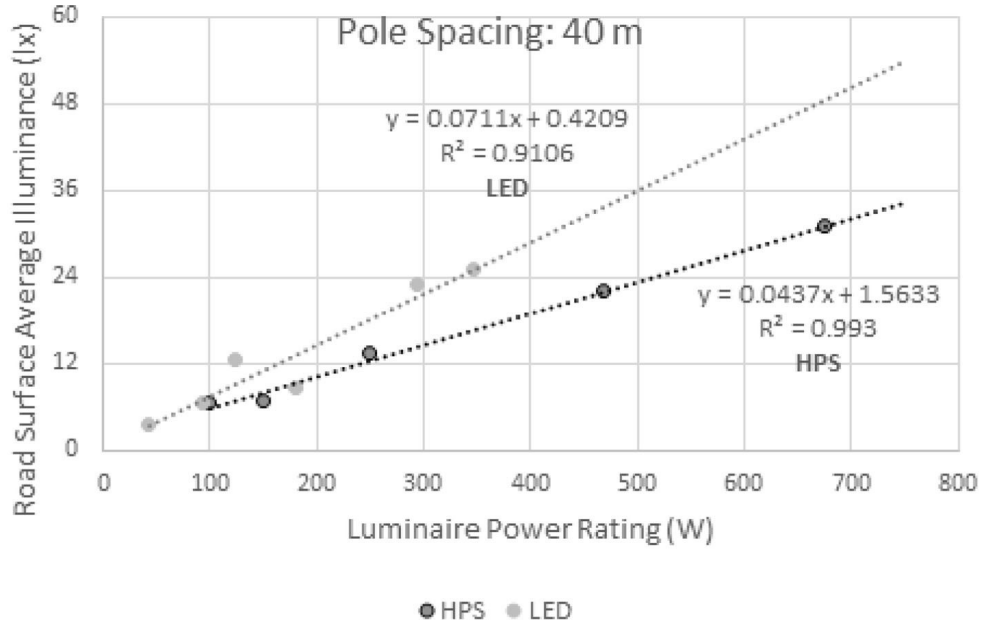

Figure 3-6. Exploration of the relationship between road surface average illuminance and luminaire power rating with HPS and LED luminaires for a conventional system configuration with a single-sided pole spacing of 40 m

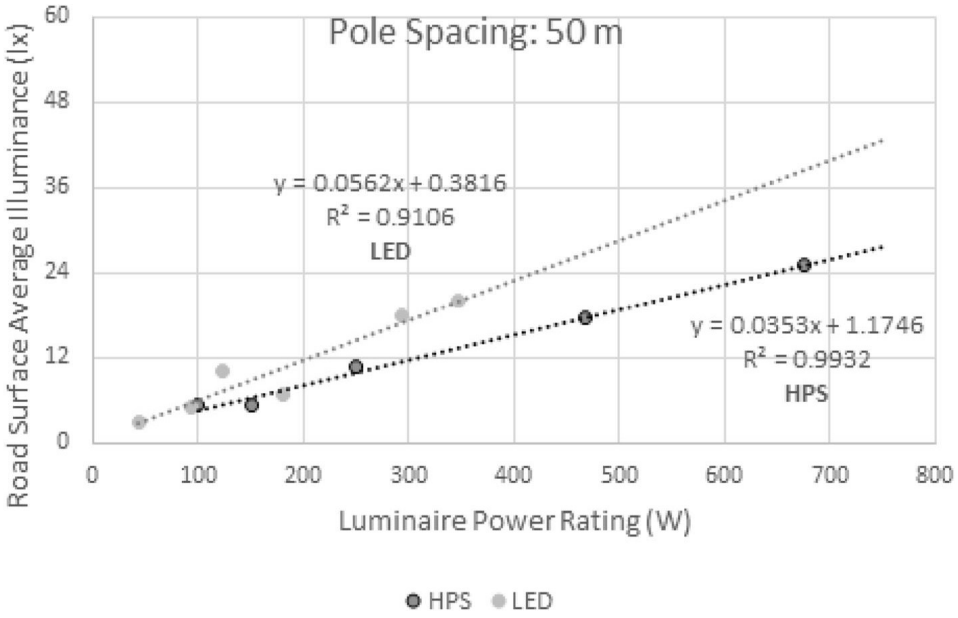

Figure 3-7. Exploration of the relationship between road surface average illuminance and luminaire power rating with HPS and LED luminaires for a conventional system configuration with a single-sided pole spacing of 50 m

It has been observed that the trend lines are in the slope-intercept form of $y = m * x + c$ and are extrapolated till the abscissa value of 750. It can be perceived that the gradient values (m) are slightly higher for LED luminaires, indicating that the increment in average illuminance level, per unit increment of luminaire power, has been higher in the case of LED luminaires utilized in this study. The intercept (c) has been a measure of the error in the devised trend line equations as road surface average illuminance should be zero when luminaires emit no luminous flux or are cut-off from the power supply. The error values in the trend line equations of LED luminaires are less pronounced and may be considered negligible for common system design configurations. It can further be noted from Figure 3-5 that the HPS and LED luminaire trend lines shall cross each other at three different points between abscissa values 0 and 100 as the trend lines are not parallel. The hypothesized existence of those points, at least theoretically, indicates that for a pre-defined pole spacing, while keeping other design parameter constant, the road surface average illuminance level will be theoretically unchanged at a particular power rating of both HPS and LED luminaires. In other words, the luminous flux linkage with the road from a luminaire of a particular operating power rating will not vary with the category of the luminaire. Equating the HPS and LED-based trend line equations would reveal that retrofitting HPS luminaires with LEDs would still maintain a constant road surface average illuminance level in each scenario: at 4.03 lx for a luminaire wattage of 36.87 W and pole spacing of 30 m; at 3.39 lx for a luminaire wattage of 41.70 W and pole spacing of

40 m; and at 2.51 lx for a luminaire wattage of 37.94 W and pole spacing of 50 m. However, this is of little practical significance as HPS power ratings below 50 W are not commonly chosen for general road lighting systems. Table 3-4 provides a compilation of proposed LED luminaire power ratings, after rounding up decimals, if any, to the immediate higher whole number, corresponding to HPS luminaire luminous flux packages to maintain constancy in road surface average illuminance levels upon retrofitting for a commonly chosen luminaire mounting height in road lighting practice (9 m), luminaire overhang (1.5 m) and luminaire tilt (5^0).

Table 3-4. Proposed LED luminaire power ratings for retrofit operations to maintain constancy of road surface average illuminance level for typical design parameters

Road width (m)	HPS luminous Flux (lm)	LED power rating (W) For pole spacing		
		30 m	40 m	50 m
8	9500	78	78	77
	16,000	109	109	109
	27,500	173	170	172
	51,000	312	304	309
	90,000	443	431	439
10	9500	79	79	79
	16,000	109	109	109
	27,500	170	169	169
	51,000	302	299	299
	90,000	428	422	423

3.4 Discussion

Despite the advantages of selecting LED luminaires for illuminating the streets and roads, several restraints exist that prevent LED luminaires to be readily commissioned for road lighting projects.

1. The cost of electricity per unit (kWh) varies widely across a country and the unit cost of a majority of LED luminaire products in a catalogue or product inventory might exceed that of conventional road lighting luminaires such as HPS and metal halide (MH) by as much as six times (Onaygil, Guler, & Erkin, 2012).
2. The theoretical return on investment (ROI) period for a completed LED-based retrofitting project can be between six and seven years, as estimated by an exploratory study conducted in Casarabonela, Spain (Marı´a Morillas & Ramo´n de Andre´s, 2019) and it can surpass the manufacturer-specified performance warranty period.

3. The lamp luminous flux output (lm) and spectral irradiance ($W * m^{-2} * nm - 1$) depreciation for LEDs can be hastened by inimical ambient thermal and humid conditions and this is known to affect chip-on-board (COB) and surface-mounted-device (SMD) type LED luminaires possessing higher power ratings (Raul & Ghosh, 2019).
4. Any public lighting project of retrofitting with LEDs would require the sanction of a competent authority which may be guided by the availability of skilled manpower at its disposal and the credentials of the bidders.

Often, the post-retrofit maintenance strategy, involving luminaire cleaning, lamp replacement, rewiring of electrical connections etc., may have to be conceived in a manner that has been different from the pre-retrofit maintenance strategy owing to the differences in electrical and optical characteristics between pre-retrofit HPS and post-retrofit LED luminaires. A maintenance factor value of 0.85 can be correlated with a maintenance interval of 3 years and an intermediate degree of air pollution (Marı´a Morillas & Ramo´n de Andre´s, 2019). The net economic and energy savings can be influenced by the ownership of the retrofitted LED luminaires. It was found that the electricity consumption in four electrical panels (supplying municipally-owned LED luminaires post-retrofit) in Casarabonela, Spain (Marı´a Morillas & Ramo´n de Andre´s, 2019) reduced from 3,10,931 kWh in 2012 (pre-retrofit) to 1,56,222 kWh in 2015 (post-retrofit) which equated to 49.76% in annual energy savings and 48.25% in annual monetary savings. It has been estimated that municipal-owned LED luminaires deployed for road lighting can result in 50% savings in terms of financial incurrences but that margin can be much lower for LED luminaires leased by municipalities from contractors or lighting utilities (Brons, Bullough, & Frering, 2021).

Thus, local bodies, municipalities and road transport authorities aiming to upgrade existing HPS-based road lighting systems ought to consider the aforementioned points and conduct a feasibility analysis before devising a comprehensive lighting retrofit blueprint with LED luminaires. The road lighting model proposed in this work can approximate the road surface average illuminance level, uniformity of illuminance and diversity of illuminance based on common input parameters for both HPS (Equations 7 to 9) and LED luminaires (Equations 10 to 12) and this can assist contractors or other stakeholders entrusted with a road lighting retrofitting project to compare the pre-retrofit (HPS) and post-retrofit (LED) road lighting parameters and make reasoned choices regarding the installation procedure.

The software simulation of road lighting with validated software tools and models has been predicated on the fact that the results can be processed to provide a comprehensive picture of road lighting quality metrics, energy efficiency, maintenance costs, financial accrual, and adherence to national and international road lighting standards prior to project commissioning (Pen˜a-Garcı´a, Go´mez-Lorente, Espı´n, & Rabaza, 2016) (Bhattacharya, 2022). In addition, new simulations of road illumination have led to the development of linear regression-based mathematical models with energy-efficiency functions (Rabaza, Gómez-Lorente, Pérez-Ocón, & Peña-García, 2016). By performing road lighting simulations based on luminance parameters such as average luminance, adaptation luminance (essentially for a fixed area of measurement), longitudinal uniformity of luminance and overall uniformity of luminance, and by introducing visibility as a quality parameter in road lighting designs with single sided, opposite, staggered, and twin-bracket central pole arrangements, new insights regarding road lighting design criteria can be gained (Sahana, Paul, & Roy, 2019) (Güler & Onaygil, 2003).

Chapter 4: Stages of Luminaire Prototype Development

This chapter presents different stages of development of luminaire prototypes using different communication protocols. Communication methods like Zigbee, Bluetooth, LoRa, GSM and WiFi protocols have been used to develop different prototypes of luminaires. LED based luminaire has been designed and developed for outdoor street lighting applications. Lighting controller for dynamic control of light level and CCT of luminaire has been designed and developed. Digital version of luminaire has been generated for different combination of light level and CCT of light from luminaire. Digital version of luminaire has been used to software based simulation of lighting application. Control software logic has been developed for controlling light level & CCT of light and recording of environmental parameters on local server. The developed luminaire has been mounted on street lighting poles for onsite measurements of light level applications and CCT parameters.

4.1 Intelligent Luminaire System Prototype Design

To design and develop an intelligent streetlight system, some properties of IoT has been implemented to remotely monitor the health of the luminaire and communicate with central computer using Zigbee protocol. To do that, an 18 Watt LED Luminaire system prototype has been developed with dusk/dawn sensor to sense night time and accordingly switch on the luminaire with a dimming control from the microcontroller attached to it. The dimming of the luminaire has been done by controlling the Pulse width modulation (PWM) duty cycle from the microcontroller (Satvaya, Mondal, Sur, & Mazumdar, 2018).

4.1.1 Microcontroller

A Microcontroller has been the heart of the system. Microcontroller along with different circuits connected the sensors with dimming circuit and LED driver before installation on luminaire. The block diagram and the circuit has been shown in Figure 4-1 and Figure 4-2 respectively. Main functions of the microcontroller has been to send the status information and receive commands from local control room. In this process, microcontroller collects different data from the sensors for status information and transmits through the connected xbee module and receives the information from the xbee module & accordingly processes those information

and dim down light output level of the luminaire. Zigbee protocol has been used for wireless communication between the modules.

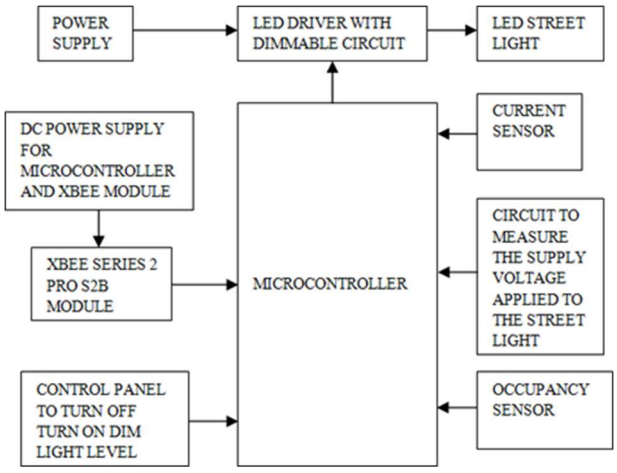

Figure 4-1. Block diagram of Luminaire lighting controller unit

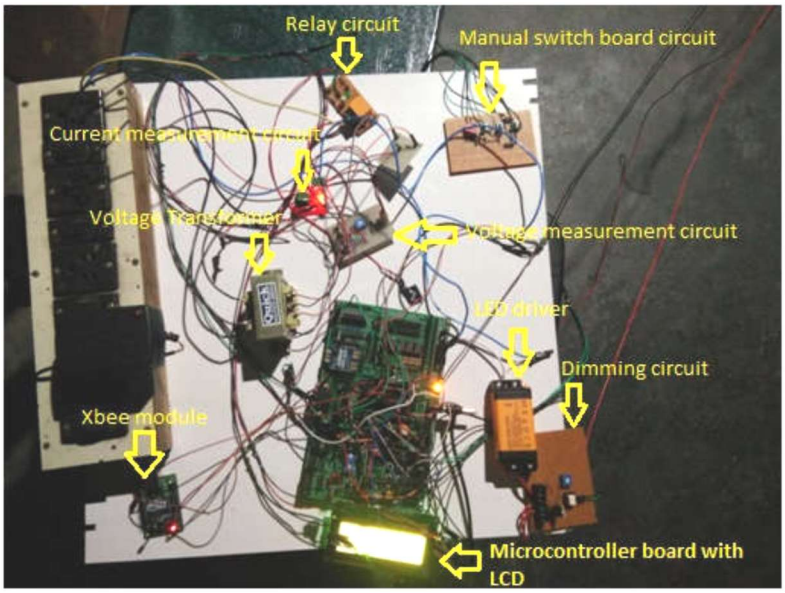

Figure 4-2. Diagram of Microcontroller unit with circuits for different sensors before installation at luminaire

An intelligent streetlight system is also required to detect the presence of a vehicle or human being, in which case the luminaire is expected to shift to full brightness level from the dim condition. A diagram of the luminaire glowing on a flexible pole inside Illumination lab has been shown in Figure 4-3. Xbee module was used as router to obtain status information of the luminaire pole system and transmit to another xbee module in local control unit side which is also known as coordinator.

Command from the local control unit (LCU) has been sent to the luminaires from a computer in the local control room using Raspberry Pi module. LCU, which is the coordinator block receives data from the Luminaire, which is the router side block. ATMEGA 32, which is a microcontroller manufactured by Atmel has been used for the controlling purpose. All the required servers and the xbee module, Xbee Pro S2B, has been attached to the luminaire for serial communication. At the receiver end Xbee has been used in Application Programming Interface (API) mode for transmitting or receiving data to or from another Xbee module. Figure 4-4 shows the 60% PWM duty cycle of microcontroller output. Figure 4-5 shows Screen shot of the luminaire status data received by the xbee module at coordinator side. Communication and data transfer established has been represented in the mentioned figure.

Figure 4-3. Diagram of the luminaire glowing on a flexible pole inside Illumination lab. Grid Mat has been used for measuring isolux at different PWM duty cycle

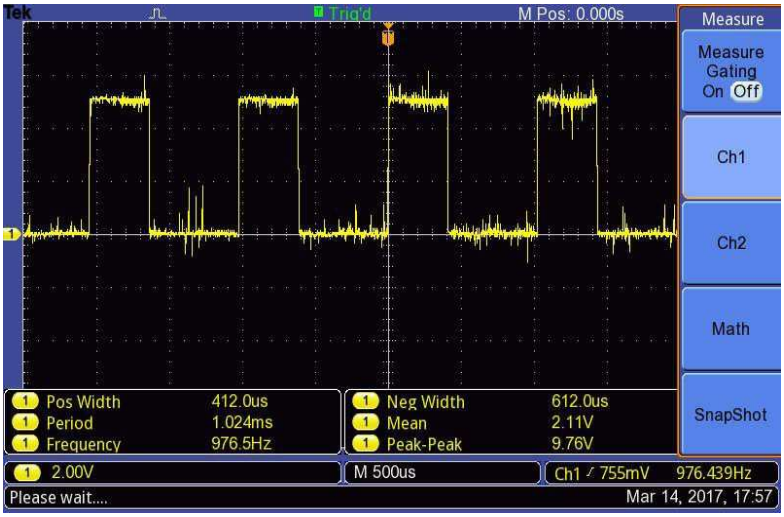

Figure 4-4. Microcontroller PWM output duty cycle 60%

Raspberry pi Model 3 has been used as internet gateway. It acts as a bridge to access the luminaire status data being uploaded to it. Figure 4-6 shows Raspberry Pi connected to xbee module. Figure 4-7 shows Raspberry Pi module has been also connected to internet network through mobile handset. Raspberry pi Model 3 also acts as a central hub for receiving and storing all data (for certain period of time). All the information regarding the status of the luminaire can be accessed by any computer having a proper IP address and connected to the local network.

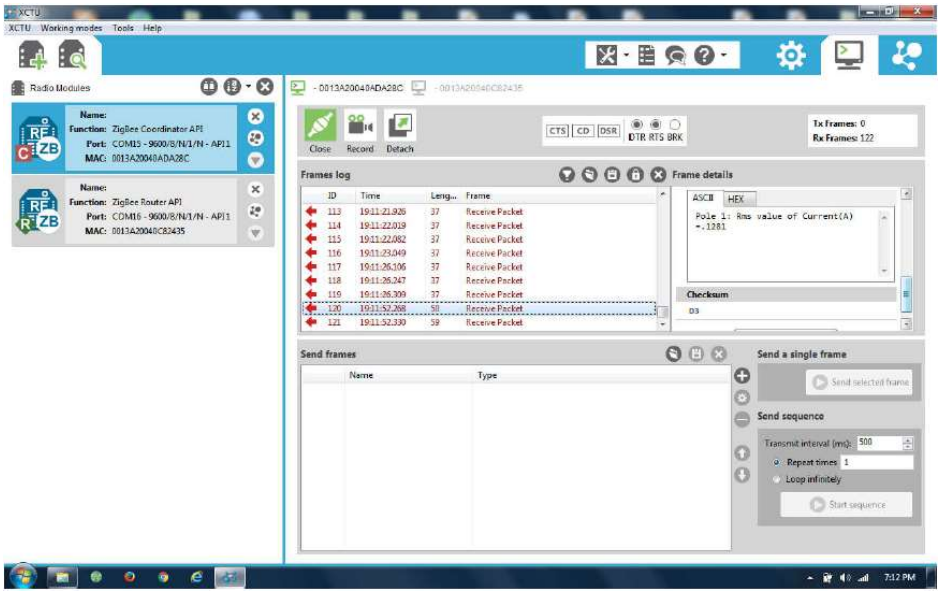

Figure 4-5. Screen shot of data receiving by Xbee module

A dusk to dawn sensor has been connected to sense low day light during the evening and switch on the luminaire. Current and voltage sensors have been used to detect illumination conditions of lamps as status intimation. The sensors have been used to detect luminaire on or off status by the current flowing through it. The sensor measures less current while the

luminaire has been in dimmed condition. Voltage sensor measures terminal voltage at connecting terminal of the luminaire. Current and voltage sensors together measure lamp failure status by proper voltage signal but no current signal by the microcontroller. A dimming circuit has been used to dim the light level after getting the dim signal sent by the microcontroller. In peak hours luminaire will glow at full brightness level for four hours, then it will be dimmed by controlling Pulse Width Modulation (PWM) duty cycle. In non-peak hours while in dimmed condition the luminaire will glow to its full brightness level by an interrupt signal from the passive infra-red motion sensor, if any human movement has been detected.

4.2 Global system for Mobile communication based lighting system with smoke detection facilities

An emergency lighting system with smoke detection and mobile communication facilities has been developed. This has been achieved using smoke and gas detector technology and added intelligence utilizing integrated microcontroller, mobile communication and a LED emergency light. Here a LED has been used as emergency light, this light has been operated at 3V DC, 0.25A battery source. Figure 4-8 shows the circuit diagram of using Microcontroller to interface of Gas and smoke sensor with emergency light.

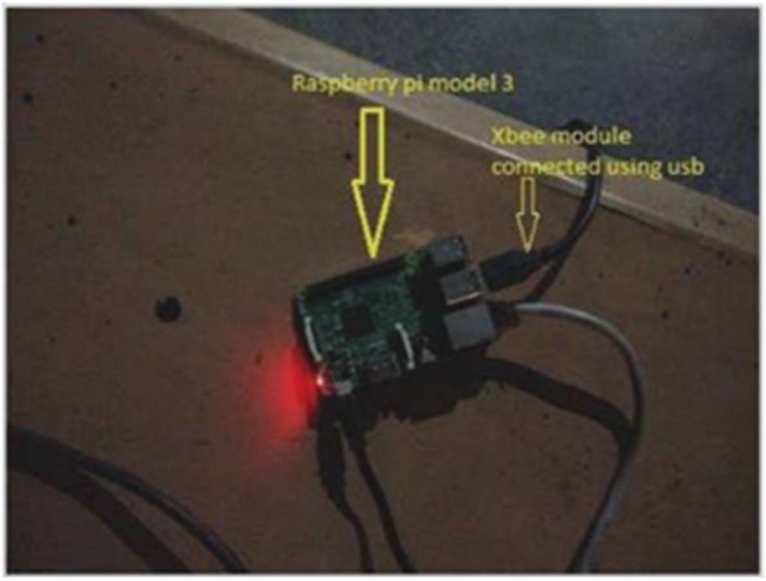

Figure 4-6. Screen shot of data receiving by Xbee module

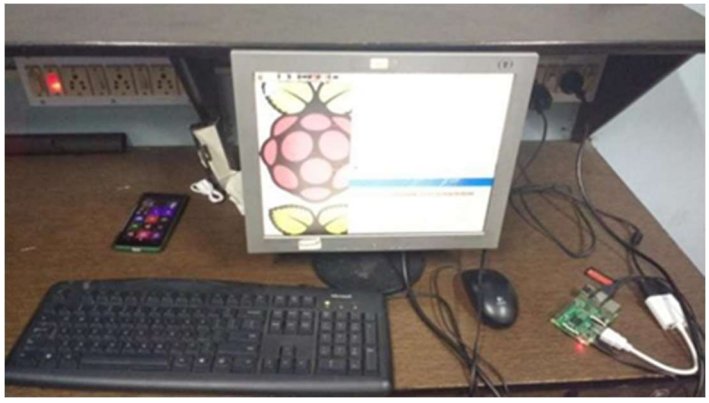

Figure 4-7. Raspberry Pi module connected to internet network through mobile handset

The combined smoke detector system with emergency lighting and communication system can monitor the smoke from the fire or gas leakage continuously. This has been achieved by scanning the digital output (Do) of the sensor continuously. When the air is clean that is there has been no smoke or gas leakage, the Do of the sensor has been high as well as the conductivity between the electrodes of the sensor is less. If there occurs a smoke or gas leakage at any time, the conductivity between the electrode of the sensor will be high as well as the digital output Do of the sensor will change to low status and that time SMS alert, buzzer and emergency light will be activated (Gas Leakage Detector using Arduino and GSM Module with SMS Alert and Sound Alarm,).

When the emergency situation arises, Short Message Service (SMS) has been sent by using AT commands through a Global System for mobile (GSM) module. The SMS alert set in the programme and the base of the transistor Q1 gets the high pulse due to detection of smoke or gas, the transistor would turned ON or forward biased and turns ON the buzzer, which has been connected to the specified pin of the microcontroller. Once smoke or gas leakage has been detected by the system, the set numbers of SMS alert have been sent. When this situation arises, humans should take proper action to stop the gas or smoke problem.

After sending the SMS alerts, the system will activate the emergency light. When the smoke or gas leakage has been stopped and system will automatically reactivate its SMS alert setting by resetting SMS counting variable back to zero. Figure 4-9 shows the flow chart to interface gas and smoke sensor with emergency light.

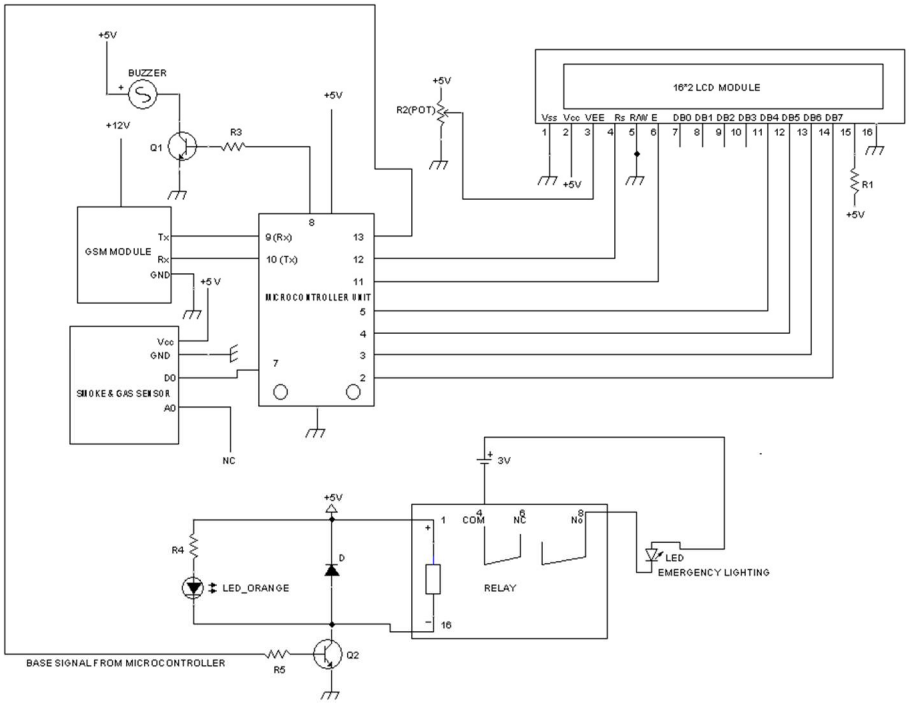

Figure 4-8. Circuit diagram of using Microcontroller to interface Gas and smoke sensor with emergency light

When the base of the transistor Q2 gets the high pulse due to detection of smoke or gas, the transistor turned ON or forward biased. The relay also gets energized and 'NC' (Normally Closed) terminal of the relay changes to 'NO' (Normally Open) terminal, the relay circuit is completed. The emergency light would turned ON.

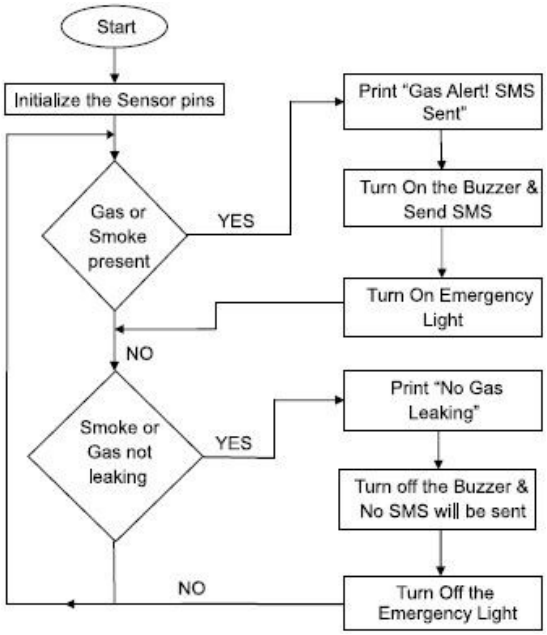

Figure 4-9. Flow chart to interface Gas and smoke sensor with emergency light

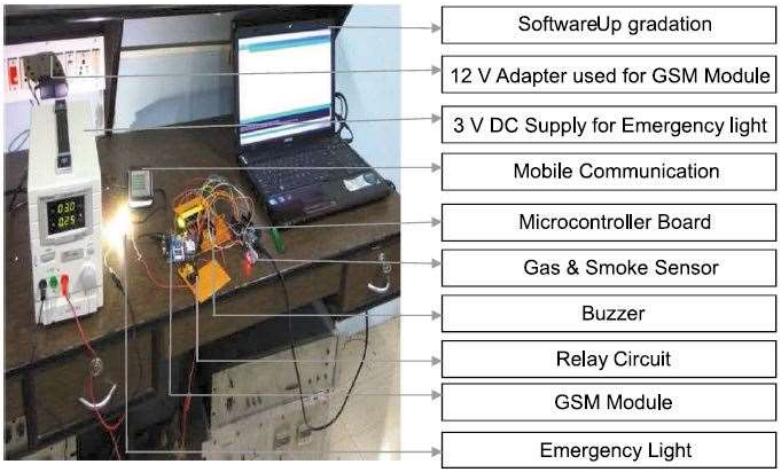

Figure 4-10. Experimental setup using Microcontroller to interface gas and smoke sensor with emergency light

In the circuit an orange color small LED has been used to check the status of relay circuit. The relay circuit has been energized properly during the presence of smoke or gas. When there is no gas leakage or smoke, the base of the transistor gets low pulse, the transistor has been reverse biased, and the relay also gets de-energized, and in such case the 'NO' terminal of the relay changes to 'NC' terminal. Figure 4-10 shows the experimental setup using microcontroller to interface gas and smoke sensor with emergency light.

The developed combined smoke detector with emergency lighting system has the following specifications:

– The LED emergency light has long life, small size, good efficacy and good visibility having monochromatic yellow LED light. The whole system requires proper maintenance and can be sustained for a long period of time.

– This system is easy to install and very simple to operation.

– This system is more reliable in domestic, industrial and commercial interiors.

– This system detects the different gas leakage like LPG leak, methane leak, butane leak, or any such petroleum based gaseous substance and smoke that can be detected using smoke and gas sensor.

The developed combined smoke detector with emergency lighting system has the following disadvantages:

– The smoke and gas sensor with emergency light has been driven by battery power. So, regular checking, maintenance and replacement of the battery system is necessary. A smoke detector and emergency light with dead battery saves no live.

– Water steam is very harmful for smoke and gas sensor. Smoke detector should be protected from rain shower or near steam rooms or over ovens of kitchens.

– The smoke and gas sensor should not install near smoky areas. If sensors have been installed in such a place, this may give false alarm. But those areas are the most important areas where need of careful monitoring for fire hazards, installation of the system in a proper wall or ceiling is very much necessary (Chase).

4.3 Development of lighting controlling and monitoring system using different communication protocol through Android application

The lighting system prototype has been designed and implemented consisting of Passive Infrared (PIR) sensor considering detection of road user and smd LEDs have been used to illuminate the pathway. To interface with mobile app Bluetooth and WiFi module have been used. In addition, communication through LoRa also worked out. While Bluetooth interface, Atmega328 microcontroller has been used. When at WiFi interface nodemcu esp8266 has been used. Movement of road users when detected, LED will get ON. There has been a dimming option too. When there is a no movement for a period LED will get dimmed when at dimming mode otherwise will get OFF.

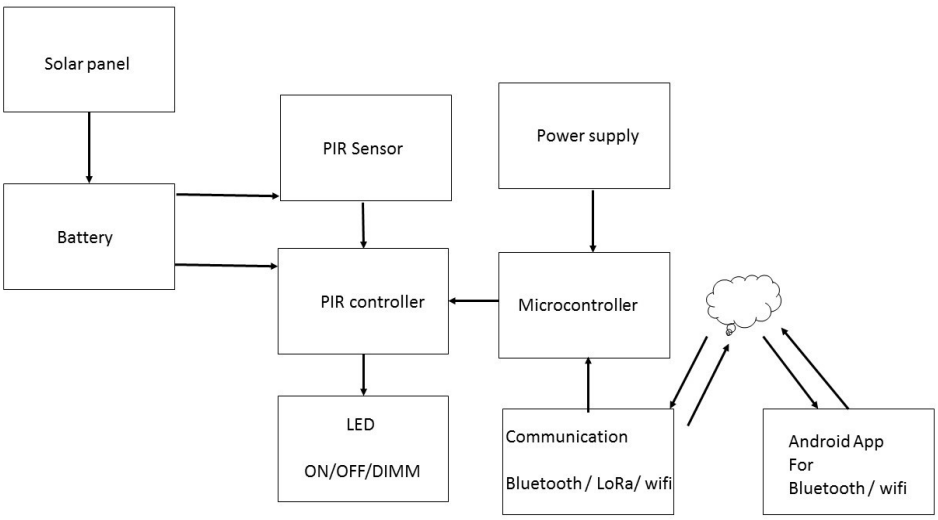

Figure 4-11. Block diagram of developed solar street lighting system

The Figure 4-11 shows the block diagram of developed solar street light system prototype for controlling through android-based mobile application. The system has been setup

so that light will be ON when required. Then light will go to OFF position when there is no movement. Here the main aim has been to monitor the status and control the solar street light system. Bluetooth/ LoRa / wife wireless module for the communicating with android mobile application, Atmega328p acts as control board and motion/occupancy sensors have been used for detection purpose, and communicating with PIR controller and Atmega328p to control the LED street light. Light dependant resistor (LDR) has been used to detect status of luminaire i.e. the luminaire has been glowing or not.

4.3.1 Occupancy / Movement detection

The Figure 4-12 shows schematic circuit diagram of the PIR controller which is based on AS085 and PIR sensor RE200B. AS085-SD3 is a CMOS Process integration PIR (Passive Infra-Red) Controller IC, with low-power consumption. Its internal architecture has Analog and digital hybrid circuit Mixed-mode, using in each case are very stable. AS085-SD3 The third generation PIR Human pyroelectric infrared detection aspect, it designed with built-in high-precision arithmetic unit, self-adaptation. The current environment, filtering out interference environment, it has been an efficient extraction of body signals, the farthest sensing distance of twenty meters.

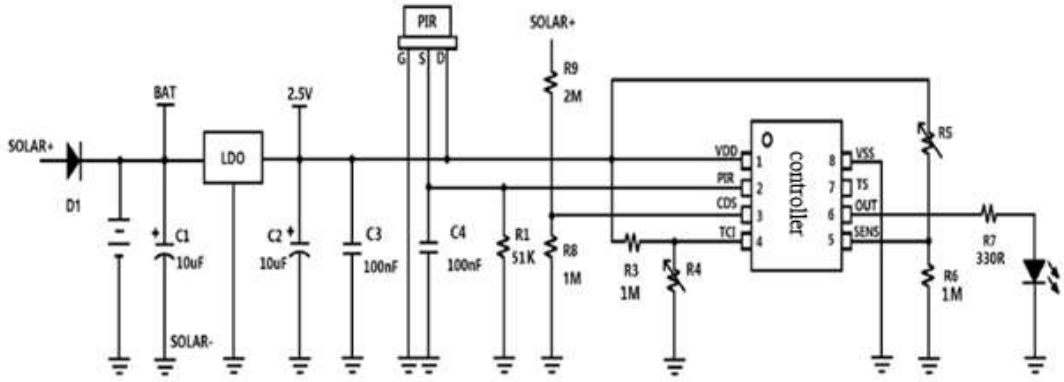

Figure 4-12. Schematic of PIR controller

4.3.2 Experimental circuits

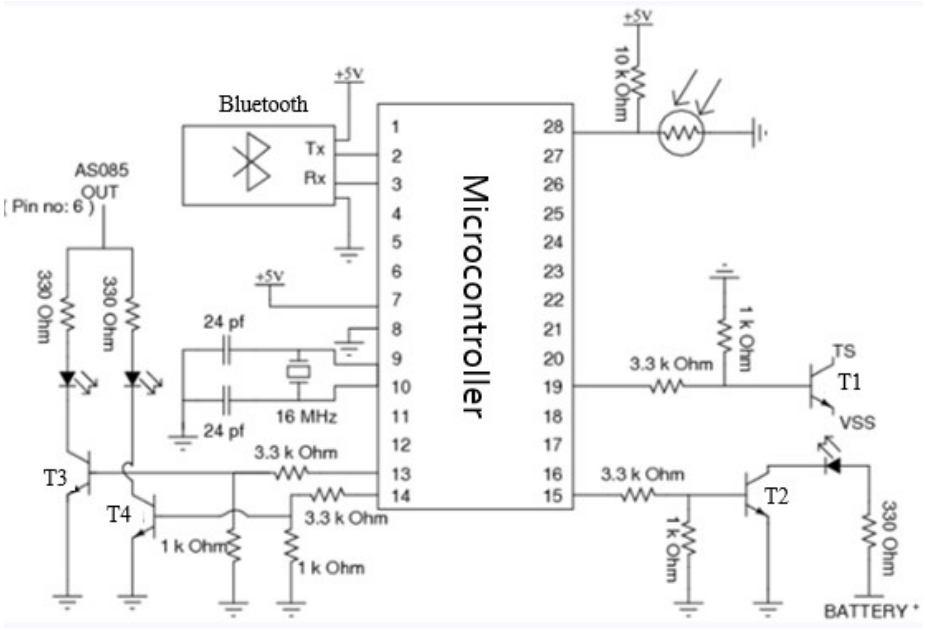

Figure 4-13. Schematic diagram of Bluetooth based controller circuit

Figure 4-13 shows schematic circuit diagram of Bluetooth based controller with micro controller (Atmega328P), solar panel and battery. An External 5-volt power supply has been used to power up the microcontroller and wireless communication (like Bluetooth, LoRa and WiFi). Transistor 2N3906 has been used as switch. Transmitter/Receiver (Tx / Rx) terminal in microcontroller has been used to integrated with wireless communication system (Bluetooth). Datasheet of AS085 shows that shorting of TS and VSS pin would change the mode of PIR controller (ON/ OFF/ DIMMIMG). In the figure transistors 2N3904 (T1, T2, T3, T4) has been used to switch the mode. Output pins (13, 14, 15, 19) of ATMEGA328P has been used to switch ON/OFF the transistors.

Figure 4-14 shows schematic circuit diagram of LoRa based experiment (transmitter end) external 5-volt power supply has been used to power up the microcontrollers ,wireless communication (LoRa) and Bluetooth (HC-05). In this circuit, microcontroller2 has been connected with Bluetooth to communicate with mobile app. And digital output pin (14) s connected to analog input pin (23) of microcontroller1. Transmitter LoRa has been connected with microcontroller1. Microcontroller2 has been already paired with mobile phone as hand held device (HHD) for controlling and monitoring purposes.

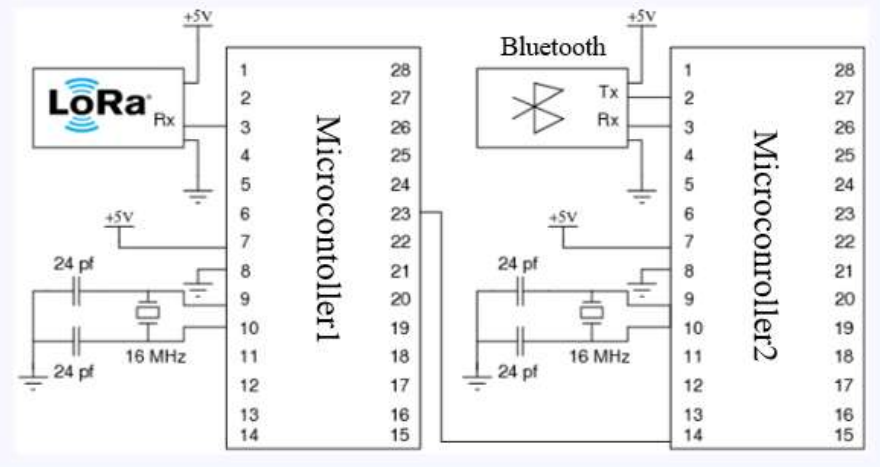

Figure 4-14. Schematic diagram of LoRa based controller circuit transmitter end

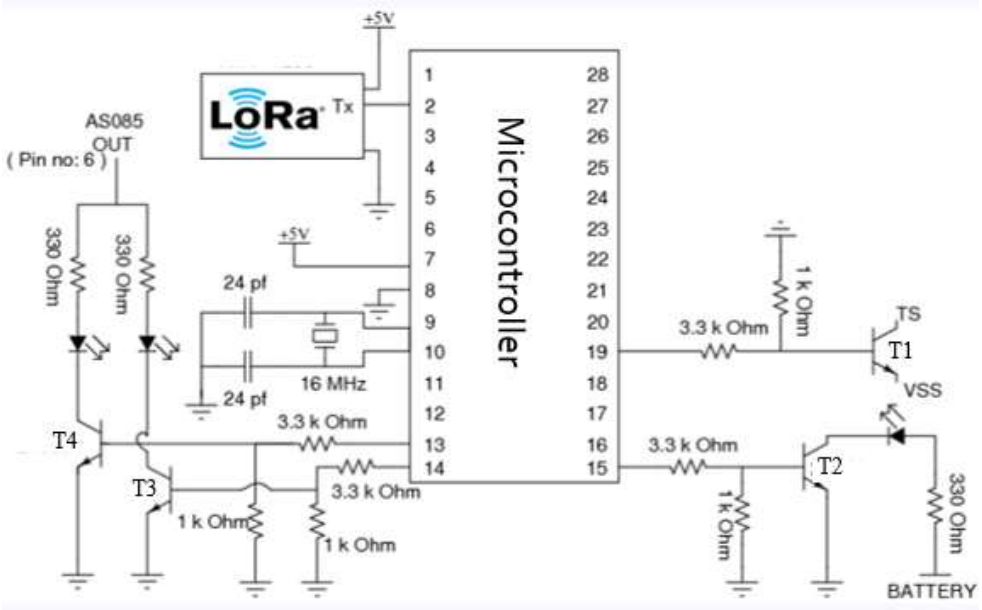

Figure 4-15. Schematic diagram of LoRa based controller circuit receiver end

Figure 4-15 shows schematic circuit diagram of LoRa based controller circuit (receiver end) external 5-volt power supply has been used to power up the microcontroller and wireless communication module (LoRa). As in Bluetooth experiment switching transistors have been used here. Output pins (13, 14, 15, 19) of ATMEGA328P have been used to switch ON/OFF the transistors. Since the output voltage of ATMEGA328P has been of 5V, voltage divider has been used to bring down the voltage to 1.1V. Here the ON voltage has been 1.1V (> 0.7V) and OFF voltage has been 0V (< 0.7V). Figure 4-16 shows developed prototype based on communication protocol.

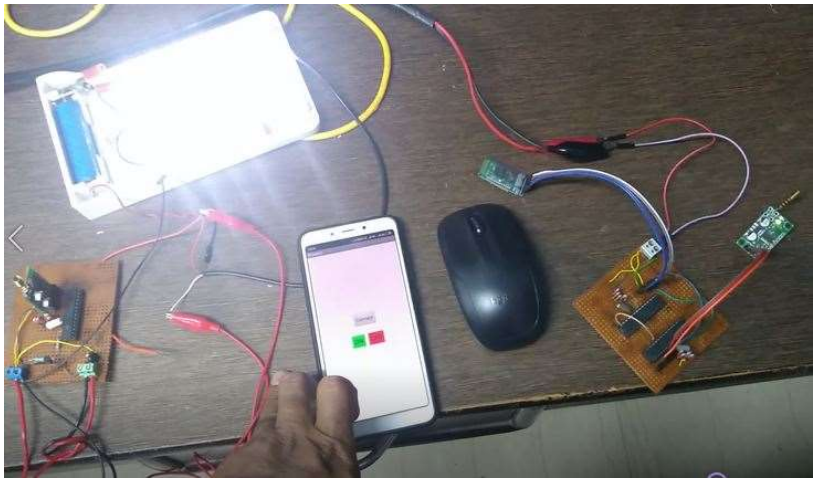

Figure 4-16. Developed LoRa communication based protype

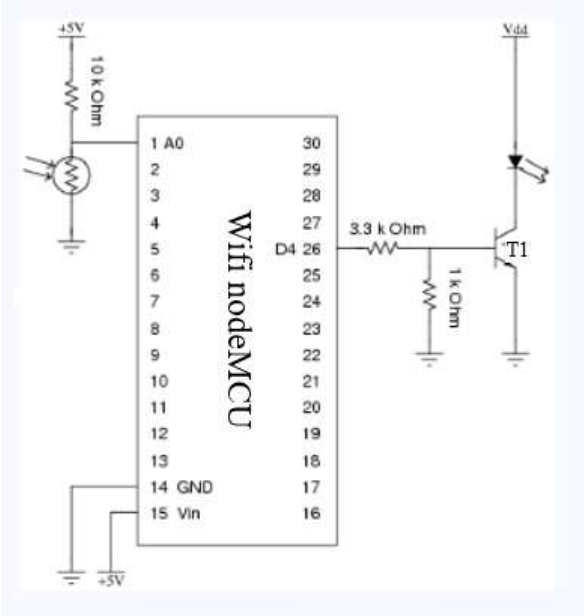

Figure 4-17. Schematic diagram of WiFi based experimental circuit

Figure 4-17 shows schematic circuit diagram of WiFi based experimental circuit, external 5-volt power supply has been used to power up the nodemcu with WiFi. As in other experiments switching transistors have been used here. Output pin (26) of ESP8266 nodemcu has been used to switch ON/OFF the transistor. Since the output voltage of ESP8266 is of 3.3V, a voltage divider has been used to bring down the voltage 1.1V. Here the ON voltage has been 1.1V (> 0.7V) and OFF voltage has been 0V (< 0.7V).

4.3.3 Working of the Automatic lighting system

In general working of solar light system has been to ON the light when it is night and OFF the light when it becomes morning. Further comes an improvement to street light system with a

sensor detecting the presence of pedestrian so that the light turns ON automatically and turns OFF when there have been no road user using the road. However, in some cases, it has to monitor the status whether the street light system has been working properly or not. Whenever there has been a problem, the administrator has to know and rectify the problem. Therefore, real time monitoring of a system has been useful for smooth function of automated street light system. Here when it comes to working of intelligent street light system, it has a status monitoring system which can send real time status to android mobile application, so that technician can keep on monitoring the installed system at any time.

Initially the motion sensor solar street light system has been developed using solar panel, battery production IC, PIR sensor and PIR controller. Here solar panel has been used to detect the light level so that the whole system can ON at low light (at night) and OFF at high light (In day).

Firstly, solar panel senses the light level. If the light level has been low solar panels would turn on the circuit and switching has no effect at high light. Here PIR sensor has a detecting range 1-8m and sensing angle of 120 degree. Then the PIR controller switch ON the LED. The system has dimming options too. PWM signal of 20% and 60 % dimming signals, which can be selected by switching. Each switching would change this feature mode, it would cycle to beginning. Here LDR has been used to detect the LED status. A resistor has been used in series with LDR as voltage divider. So the voltage would vary with respect to light level, this voltage has fed into microcontroller where the lookup table has already been loaded. This voltage has been compared with the lookup table and transmitting corresponding LED status to mobile application by through Bluetooth or WiFi module. This is how status monitoring mechanism works.

To get the real time status of LED android mobile-based app has been designed by using MIT app inventor. For a Bluetooth integrated system, Bluetooth in a mobile has been used to interface with Bluetooth module HC-05 which has been trans-receiver side of street LED light. In case of WiFi, firebase has been used to interlink the mobile app and installed street light. NodeMCU esp8266 in street light system and mobile app have the authentication of firebase system.

4.3.4 Flowchart of the lighting system

The flow chart in the following figure explains that the system has been started initially by giving power, and then the solar panel is sensing the light level. When surrounding light level

has been low the whole system will switch ON. For monitoring status LDR has been used series with the resistor and kept like facing of LED. Output voltage has been fed to microcontroller analog input. This voltage will compare with preloaded lookup table, and the corresponding LED status has been transmitted through serial pin which has been connected to the HC05 bluetooth module. In case for WiFi the status has been send to firebase real time data base. And the paired/ authenticated mobile app can monitor at any time.

4.4 Modified Controller for outdoor application

A modified circuit diagram has been designed and developed as shown in Figure 4-20 for outdoor application. The developed system has been equipped with dusk–dawn detector for switching ON or OFF luminaire based on presence of surrounding light in the environment. The controller has been also equipped with sensors to detect lighting status for the luminaire along with voltage across and current measurement through the luminaire.

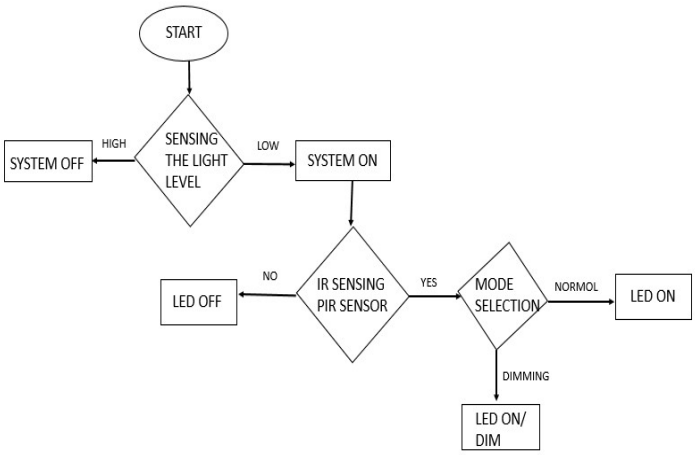

Figure 4-18. Flowchart of the lighting system

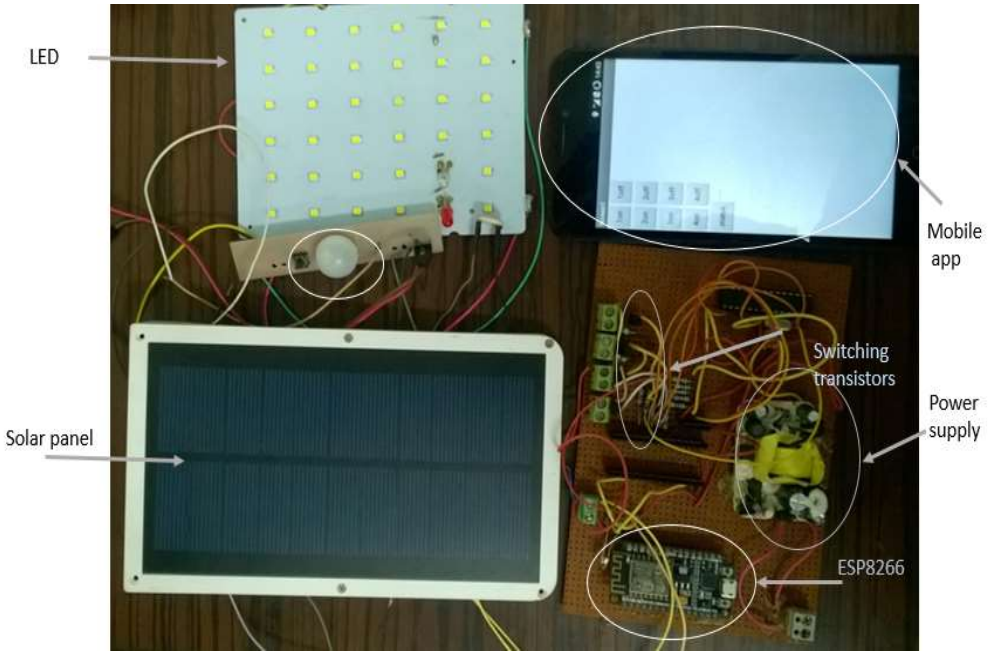

Figure 4-19. Experimental setup of the lighting system

Figure 4-19 shows the developed lighting system diagram with wifi based communication module.

The modified controller circuit has been equipped with a presence detector using ultrasonic detection method. The microcontroller has been programmed to switch ON luminaire in absence of sufficient ambient light. The controller circuit allows to glow luminaire for a pre-defined time. After the pre-defined time the luminaire glows at 50% of the light output level. During operating at dimming level the controller activates the presence detector to detect presence of any human being or moving object like car etc. In case presence of moving object the luminaire glows at the full brightness level for three minutes, then it returns back to 50% brightness level. The electronic circuit continuously measures the voltage across the luminaire and current through the luminaire.

4.5 Analysis of LED Luminaire

Because LEDs are current controlled light sources, their light output varies approximately linearly with their forward current (Schubert, 2003) (Zukauskas, Shur, & Gaska, 2002), they are suitable as dimmable light sources. Dimmer switches are often used in a variety of lighting applications because they allow you to modify the light level according to your visual needs, resulting in energy savings. The electrical performance (harmonic problem) of a pulse width

modulation (PWM) dimmer employing MOSFET for LED has been documented in comparison to a phase controlled dimmer.

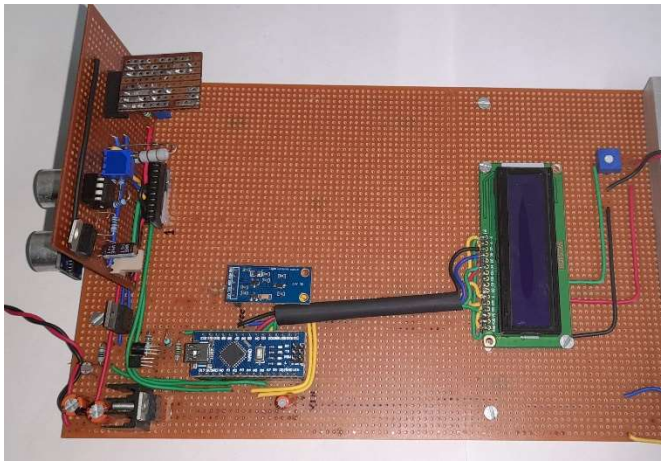

Figure 4-20. Modified lighting controller

The light source has been designed and developed using three arrays of yellow phosphor converted blue color emitting LEDs having 3V forward voltage. As per the electrical Parameters, and the procured LED driver, Printed Circuit Boards (PCB) have been designed and developed as shown in Figure 4-21. Figure 4-23 shows the PCB module with LEDs and lenses mounted on it along with a complete lminaire.

The proposed system aims to develop a dynamic CCT varying lighting system and its performance analysis. Experiments have been done with the developed, variable CCT luminaires. The designed light emitting panel of the luminaires use total 72 numbers of 3V LEDs. The light emitting panel having three arrays of LEDs, each with 24 LED chips have been connected in series. Separate LED drivers have been used for each array of LEDs. Out of the three arrays of LEDs, two arrays of WWLEDs have been placed in two sides and one array at the middle has been of CWLEDs in one of the luminaires S1 to provide warmer CCT variation. Similarly, two arrays of CWLEDs placed in two sides and one array of WWLEDs have been placed at the middle in the luminaire S2 to provide cooler CCT variation.

The brightness of LEDs has been controlled by controlling the duty cycle of PWM 1 KHz signal. A smartphone has been used as Hand Held Device (HHD) to control the duty cycle of PWM signal from microcontroller unit. The microcontroller unit and the HHD have been connected wirelessly to Wi-Fi router. PWM signal from the microcontroller unit has been of 3.2 V peak value. An electronic circuit was used to step up the PWM signal to 10V peak value. Brightness of the LEDs have been controlled in steps by controlling the duty cycle (0, 12.5%, 25%, 37.5%, 50%, 67.5%, 75%, 87.5% & 100%).

Figure 4-21. Designed and developed PCB module for LED light source

Experiments have been conducted and data collection have been done when all three arrays of LEDs have been glowing for both the light sources S1 and S2 with CWLEDs along with WWLEDs. Figure 4-24 shows the block diagram and Figure 4-25 shows developed circuit for the designed lighting system. Each of the LEDs has a secondary lens at the top of the LED chips.

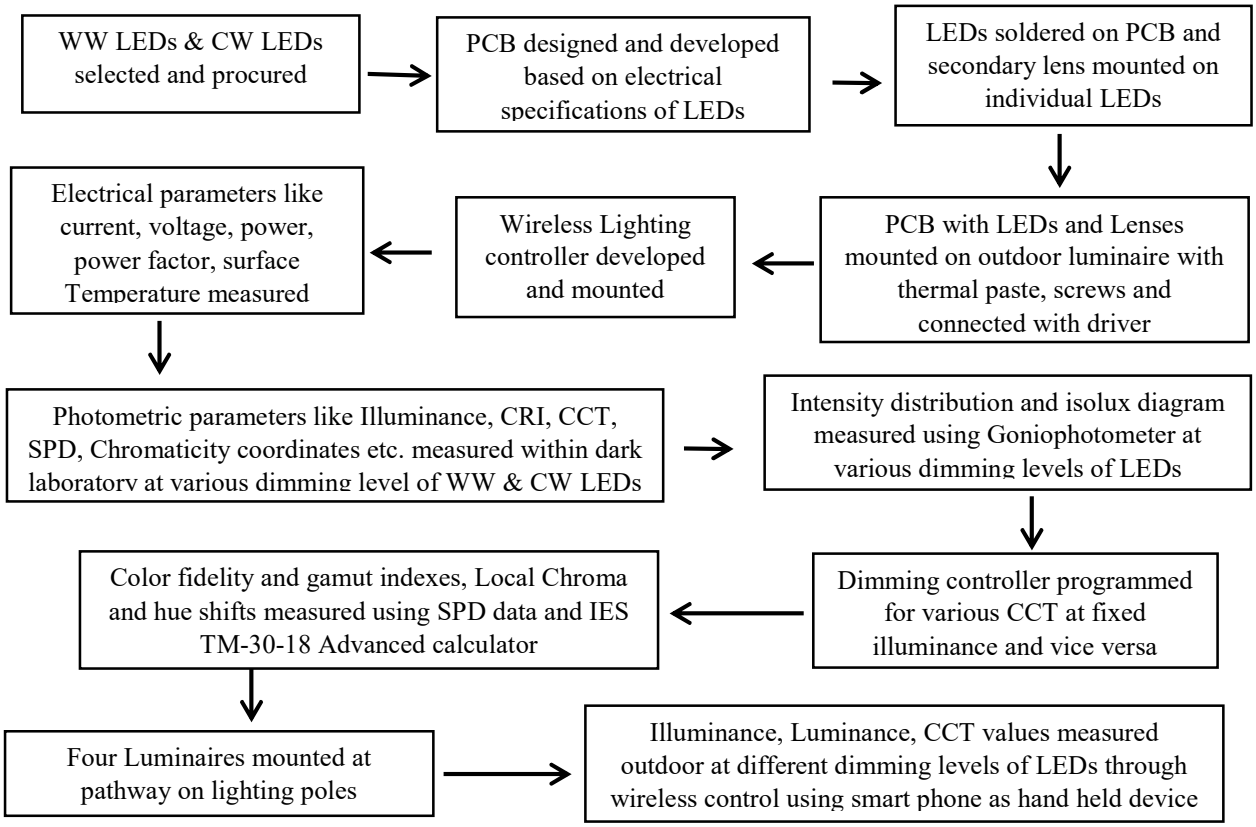

Figure 4-22. Flow chart of the development and experimental steps

Steps of the experiments and measurements are mentioned below:

Step 1: WWLEDs and CWLED procured from the market and their photometric and electrical parameters have been measured using CL-70F (Make Konika Minolta, Japan) photometer and Yokogawa (WT 210) digital power meter.

Step 2: Based on the electrical parameters LED drivers have been procured, a printed circuit board (PCB) has been designed and developed to meet the electrical requirements of the LEDs. Each PCB is having three arrays of LEDs.

Step 3: The LEDs have been soldered on the PCB at proper orientation for the two types of luminaires as mentioned.

Step 4: The PCB with LEDs on them has been mounted on luminaire housing with heat sink arrangement so that while the LEDs glow it can properly dissipate the heat generated over there.

Step 5: A wireless based controller has been developed for variable light output and CCT values from the lighting system. The WWLED and CWLED arrays have been controlled individually for variable CCT values.

Step 6: Photometric measurements have been done on the lighting systems and compared keeping it within a dark laboratory without any external stray light from other sources.

Step 7: Chromaticity coordinates (x, y) of individual CWLEDs and WWLEDs have been calculated at desired points and compared with the measured values.

Step 8: Color fidelity index (R_f) and Color Gamut Index (R_g) have been measured for a few combinations of WW and CW LEDs dimming levels of both luminaires from their spectral power distribution.

Step 9: Local chroma shift at various hue angle bins and local hue change at various hue angle bins have been measured for similar combination of dimming levels.

Step 10: Developed luminaire has been mounted within a dark laboratory and Iso-Lux lines have been drawn based on the photopic and scotopic illuminance values on the horizontal plane.

Step 11: The intensity distribution of the developed luminaire was measured using a C-γ type Goniophotometer for a different combination of dimming levels of developed luminaires based on the developed logic for variation of CCT value for pre-set illuminance levels.

Step 12: Digital version of the intensity distribution data for different pre-set illuminances have been used for outdoor lighting simulation using lighting design software. Results have been compared for achieving the best results.

(a) (b)

Figure 4-23. (a) PCB module with LEDs and lenses mounted, (b) complete Luminaire

Step 13: Luminaire surface temperature has been measured for different preset illuminance levels.

The light output of LEDs has been controlled by controlling the amount of current through them. The optical conversion non-linearity increases as forward current increases, but photopic output efficacy declines beyond the linear range (Schubert, 2003) (Zukauskas, Shur, & Gaska, 2002).

The light output from LEDs have been controlled by controlling the average current through it. The average current has been controlled by PWM signal generated from a 32-bit ESP 8266 Wi-Fi enabled Tensilika L106 microcontroller based embedded system module. This method keeps the amplitude of the current through the LEDs constant for every duty cycle. Constant current through LEDs keeps the photometric parameters stable. Supply current through LEDs have been of fixed amplitude but pulsating in nature. The PWM signal has been of 1 KHz and variable duty cycle. The average Current (Iav) of the PWM signal will be Peak Current (Ip) times of the duty cycle (DC). Peak current through individual segments has been of 700 mA, fixed from the driver.

$$\mathrm{Iav} = \mathrm{DC} * \mathrm{Ip} \tag{13}$$

Utilizing PWM dimming with high modulation frequency has been employed to prevent the appearance of individual pulses, resulting in flickering (Gacio, et al., 2010). This dimming strategy allows for a wider variation of dimming by obtaining lower current levels and linear light output control down to zero percent (Dyble, Narendran, Bierman, & Klein, 2005).

4.6 Development of Wireless Dimming Controller

A microcontroller-based electronic dimmable controller circuit enables PWM-based dimming. The light intensity controlling circuit has been created and built for Warm White LEDs (WWLEDs) and Cool White LEDs (CWLEDs), and it can be controlled wirelessly via a smartphone as an HHD. Figure 4-24 and Figure 4-25 illustrates the block diagram and schematic of the developed dimmable controller circuit.

Purpose of the different blocks of the dimming controller are as follows:

1. Power Supply Unit has been used for providing electrical power to different working units from an AC to DC converter, converting the 230V, 50Hz AC power supply to +5V and +10V DC supply unit for other functional units of the dimming controller circuit.
2. Pulse Width Modulation Signal Generator has been used for generating PWM signal based on the signal received from a Hand-Held Device (HHD). A 32-bit ESP 8266 Wi-Fi enabled Tensilika L106 microcontroller based embedded system module has been used to generate the PWM signal of 1 kHz. The module has been connected to a Wi-Fi router with a specific IP address as shown in the block diagram of Figure 4-24 (Gacio, et al., 2010). When HHD has been connected to the Wi-Fi router and the same IP address has been searched on a web browser in the HHD, it shows the option to switch ON or OFF the light source. Multiple time switching by touching the ON key of the touch screen display of HHD changes the duty cycle from DC = 12.5, 25, 37.5, 50, 62.5, 75, 87.5, and 100%. Switching the ON key repeats the process. Switching the OFF key sets the duty cycle to zero (DC = 0; No PWM signal output). The light output of the developed light source varies accordingly. Brightness of LED arrays changes accordingly.
3. PWM Signal Amplifier unit has been used to amplify the 3.3V signal. The LED driver operates at 10V PWM signal. A signal amplifier circuit using two-stage transistor has been used to level up the 3.3V PWM signal from the microcontroller unit to 10V PWM signal output for the LED driver.

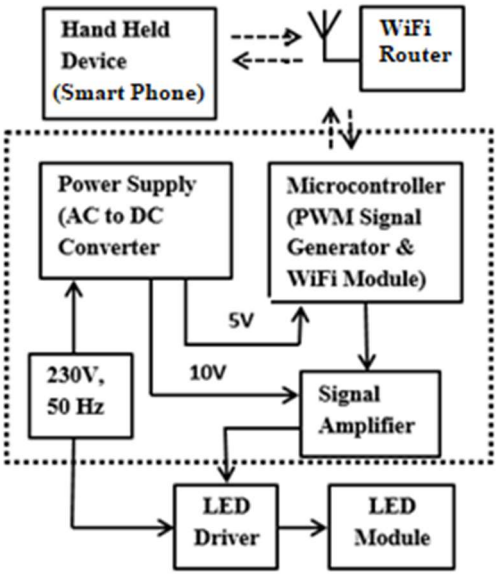

Figure 4-24. Block diagram of the developed dimmable controller circuit

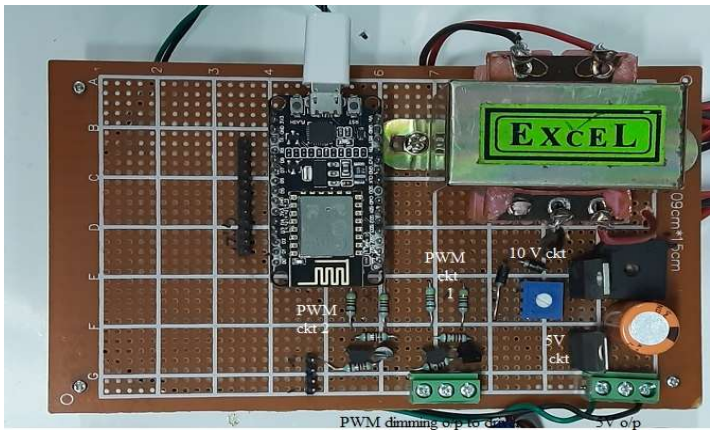

Figure 4-25. Developed dimmable controller circuit

4.7 Development of a Dynamic CCT Varying Lighting System

Photometric parameters have been measured using CL 70-F (make Konika Minolta, Japan) within a Dark Laboratory so that no stray light can come inside other than the designed light source. Measurements has been done at the nadir point of the luminaire at a distance of 2.476 meter from the luminaire. Figure 4-23(a) shows the diagram of the designed PCB layout with LEDs and lenses mounted and Figure 4-23(b) shows diagram of a complete luminaire where developed PCB module with LEDs and lenses has been mounted within a housing using scrues and thermal paste. Each LED having a secondary lens at the top of the LED chip. Figure 4-26 shows two individual Microcontroller unit generating 1 KHZ Pulse width modulated signal. The microcontroller has been powered from 5V supply and it generates 3.3 V PWM signal. PWM signal from the microcontroller converted to 10V PWM signal using a signal booster.

Individual PWM signal have been used to control brightness of WWLEDs and CWLEDs. A smart phone has been used to control the Width of the PWM signal.

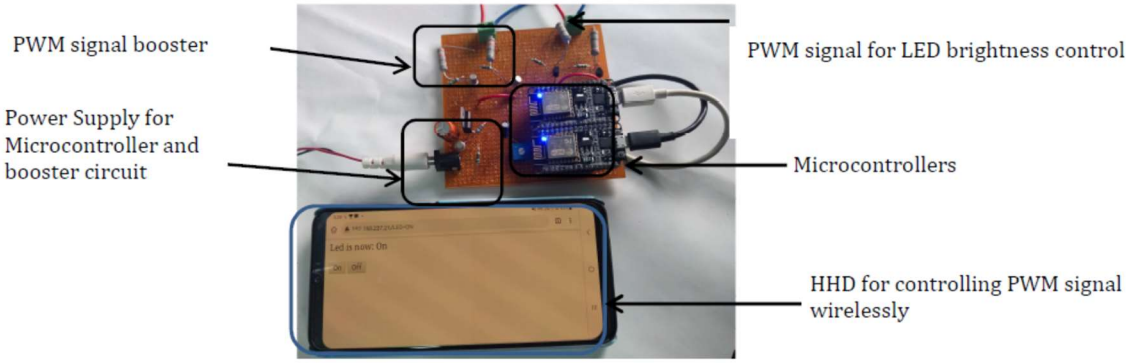

Figure 4-26. LED brightness controlling unit with HHD

The proposed variable Correlated Color Temperature (CCT) luminaire uses Warm White Light Emitting Diodes (WWLED) sources along with Cool White Light Emitting Diodes (CWLED). Both the WWLEDs and CWLEDs have been yellow phosphor converted blue color emitting LEDs. Experiments have been done with variable CCT luminaire. The designed light emitting panel of the luminaire uses total 72 numbers of 3V LEDs. The light emitting panel having three arrays of LEDs, each with 24 LED chips connected in series. Separate LED drivers have been used for each array of LEDs. Out of the 3 arrays of LEDs, 2 arrays have been of WWLEDs and 1 array at the middle has been of CWLEDs.

Brightness of LEDs have been controlled by controlling the duty cycle of pulsed width modulated (PWM) 1 KHz signal. A smart phone was used as a hand held device (HHD) to control the duty cycle of PWM signal from microcontroller unit of Nodemcu. Microcontroller unit and the HHD have been connected wirelessly to Wi-Fi router. PWM signal from the microcontroller unit was of 3.2 V peak value. An electronic circuit was used to step up the PWM signal to 10V peak value. Brightness of the LEDs have been controlled in steps by controlling the duty cycle (12.5%, 25%, 37.5%, 50%, 67.5%, 75%, 87.5% & 100%). While controlling the brightness of the CWLEDs in different steps.

Experiments have been conducted and data collection was done once when all three arrays of LEDs have been glowing i.e., two arrays of CWLEDs along with one array of WWLEDs. Another set of experimental data have been collected when one array of CWLEDs along with one array of WWLEDs have been glowing.

4.8 Luminaires and Controller Mounting

Modified controller along with the sensor and relay modules have been mounted within a controller box as shown in Figure 4-27(a) and mounted on the intelligent street lighting poles.

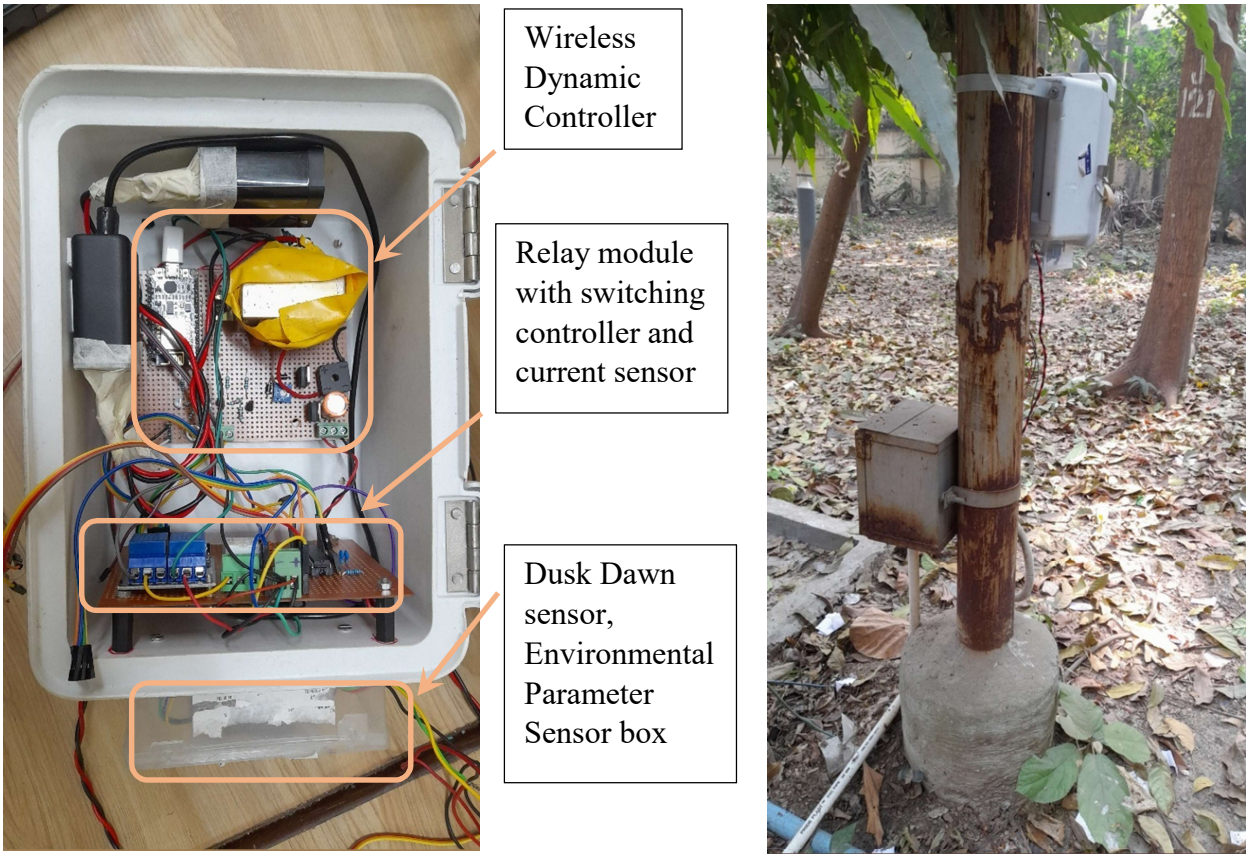

(a) (b)

Figure 4-27. Modified controller box with sensor, relay module and mounting on poles

The lighting controller box includes developed dynamic controller that can be controlled from wireless hand held device (HHD). It also includes switching controller for dusk dawn sensor and presence monitoring system during dimming condition of the luminaire. The dusk dawn sensor has been attached with the system to monitor presence / absence of surrounding light and accordingly switch ON / OFF the lighting system. The presence monitoring system works during the dimming condition of the luminaire. When presence has been detected near the luminaire within the range of 7.63 meter near the local controller. Figure 4-27(b) shows wireless controller box mounted on street lighting poles along with the electrical junction box. Figure 4-28 shows the luminaires mounted on the poles at the garden at the side of the pathway. Figure 4-29 shows one of the installed luminaires with variations of lux level and CCT. Different steps of development and experimental measurements can be seen in Figure 4-30.

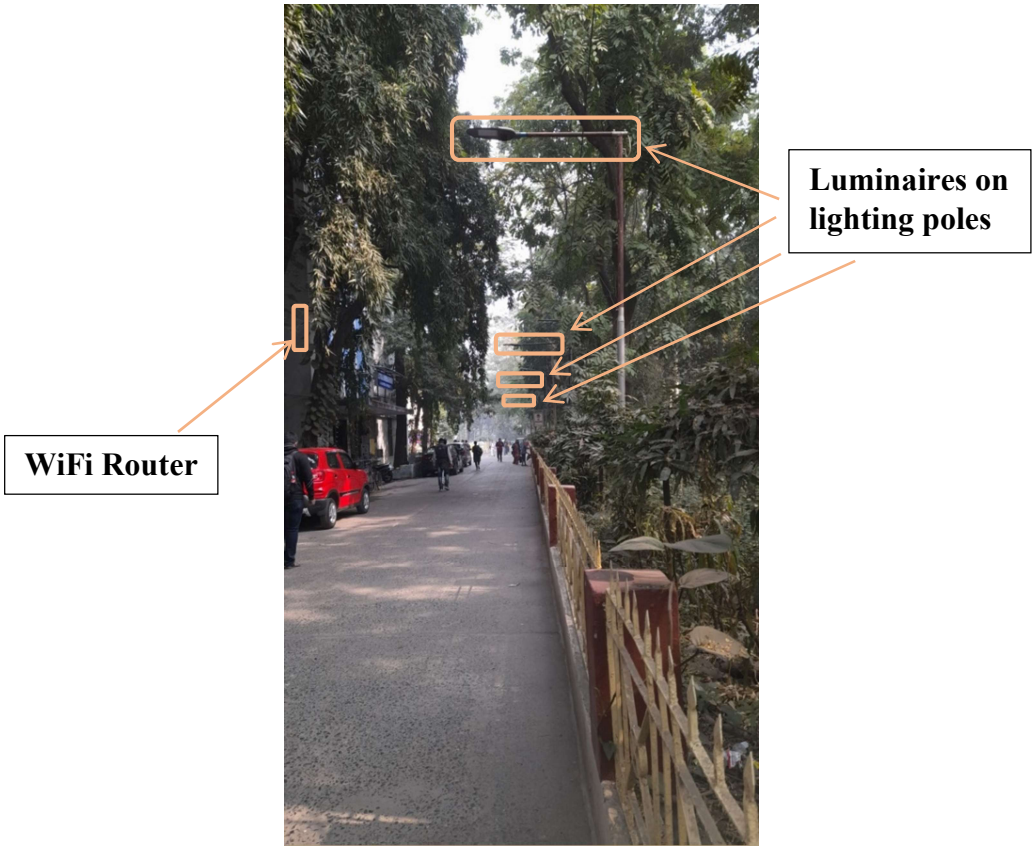

Figure 4-28. Luminaires mounted on street lighting poles

Figure 4-29. Installed Luminaires with Flux and CCT variations

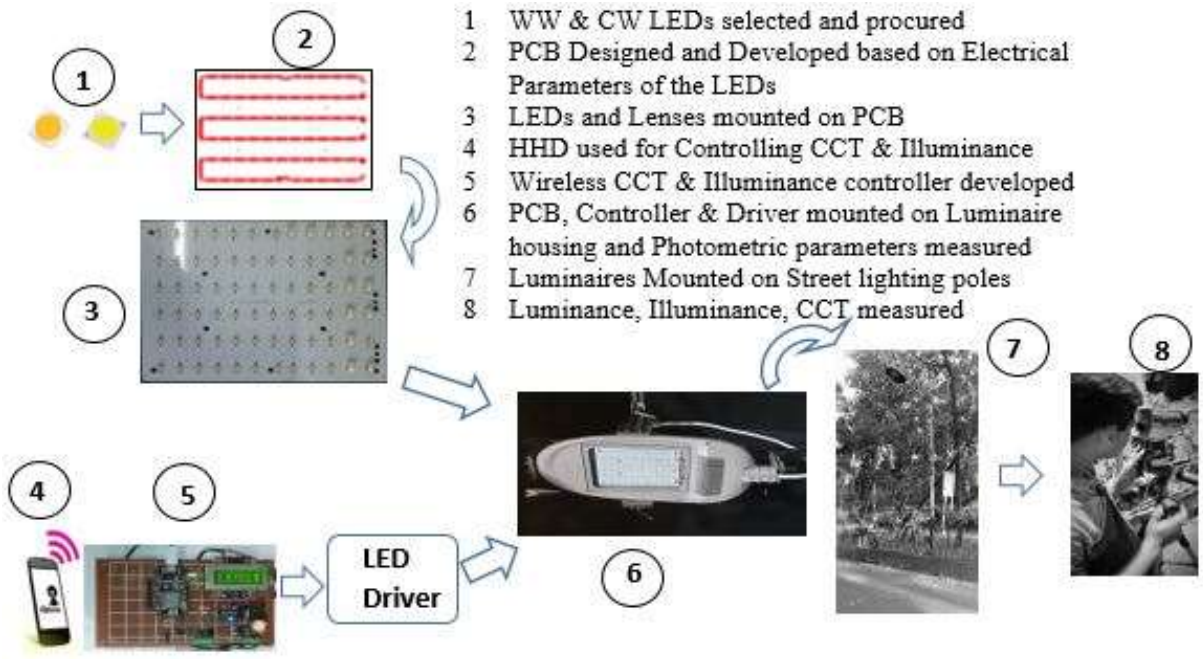

Figure 4-30. Different steps of development process of the Luminaire and measurements

The working flow diagram of the developed intelligent lighting system has been shown in Figure 4-31. The flowchart shows the lighting system starts when external power has been switched ON and then it would go switch OFF state based on adequate surrounding ambient light level. Whenever surrounding light level reduces down during dusk condition, the lighting system switches to ON state and remain in that state for five hours as the microcontroller has been programmed and starts data recording. Surrounding light level has to remain dark for fifteen minutes then only the system switches to ON state and avoid any false triggering due to dark clouds during day time and vice versa during dawn time. Data recording of ambient temperature, humidity, air quality, current flowing through a single luminaire is being done on a web server that has been connected to a laptop on the same WiFi network through the use of wireless communication. Alterations to the light output, measured in terms of luminous flux, and adjustments to the colour temperature (CCT) can be made with any laptop or smart phone that is connected to the same WiFi network within the first five hours after the lighting system has been turned on. Any web browser on the HHD can be used to achieve different levels of light output and CCT by searching for the fixed IP address (that has been programmed) of the controller and selecting the required light level and CCT value from the device. After first five hours of the lighting system being turned ON, the light output state will change to a dim state. his means that the luminaire will glow at only 20% of the maximum light output level. When the lighting system is operating at a low light output, it is not possible to make adjustments to the luminous flux or the CCT; however, the system continues to record the environmental

parameters and the electrical parameters. Whenever any person comes near the controller, the presence detection system using ultrasonic sensors switches the lighting system to 45% lighting output state of the luminaires. The light output of the luminaires stays at the state mentioned for three minutes, after which it reverts to the state where it produces 20% of its total light output if there is no presence detected. When dawn occurs and the ambient light level is high enough, the lighting system goes into the OFF state, and data recording ceases until the level of ambient light drops again.

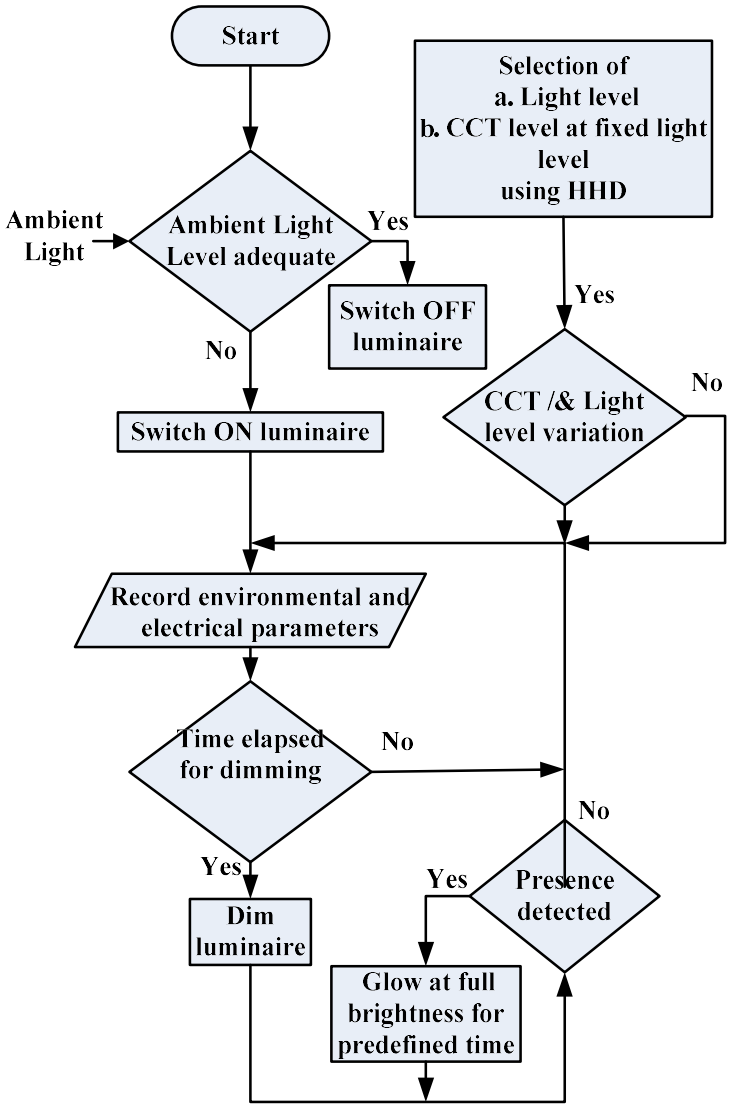

Figure 4-31. Work flow diagram of developed intelligent streetlight

The lighting system can control the light output level at fixed CCT level of only Cool White color temperature, only Warm White color temperature or at mixed CCT levels and vice versa. Illuminance level on the road surface, as well as cool white or warm white light i.e.,

CCT values can be varied using a hand held device during surrounding dark condition for a stipulated duration of few hours and then the light output of the lighting system will dim down for rest of the night time except in presence of any person nearby for fixed duration of three minutes. The lighting system monitors energy consumption of the luminaires along with surrounding environmental parameters like Temperature, Humidity, air quality etc. and the system has provision to monitor other environmental and physical parameters when needed.

Chapter 5: Experimental Results and Analysis

5.1 Prototype Luminaire

A prototype of streetlight system was designed by a luminaire with LED arrays. Different sensors have been used to acknowledge the status of different conditions of the luminaire. An occupancy sensor has been used to detect any human presence near the luminaire and consequently control action of the illumination levels have been provided. System has been attached with an Occupancy sensor to detect any person near it and accordingly shift the brightness to full illumination level during the non-traffic hours. Wireless communication has been used to transmit data between two Xbee modules that worked as router and coordinator. Coordinator module has been connected to a Raspberry Pi unit and a computer working as local control unit as shown in Figure 5-1. Router side module has been connected with a microcontroller working as brain for the lighting system as shown in Figure 4-1.

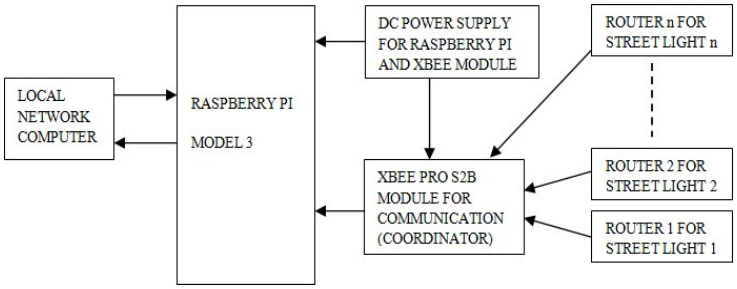

Figure 5-1. Block Diagram of the Local control unit side (Coordinator)

As the luminaire shifts to full brightness when human presence has been detected, this status information of the luminaire pole system has been transmitted by the Xbee module working as router from pole lighting system to another xbee module working as coordinator in local control unit side.

Diagrams below show different illuminance distribution values transmitted from local control unit to the luminaire and accordingly microcontroller provided that output to the driver of the luminaire. To determine the isolux plot of the 18W LED street light, rectangular area of 3m X 5.5 m has been used to collect the illumination values in front of the streetlight pole. This area has been subdivided into 0.5m X 0.5m area grid square. Grid points have been 0.5 m apart from each other.

The height of the street lighting Luminaire has been kept at 3m with bracket length of 0.5 meter. Thereby nadir point has been 0.5 meter away from the vertical axis in the following diagrams. Iso-lux plots at four PWM duty cycle levels have been shown here. Figure 5-2 shows isolux diagram based on the illuminance values on horizontally illuminated surface in front of the lighting pole at pulse width modulation (PWM) duty cycle 100% i.e. when there is no dimming. Figure 5-3 to Figure 5-5 shows isolux diagram under similar conditions, when PWM duty cycle has been 80%, 60% & 40% respectively i.e. when the lighting level have been dimmed and lower illumination achieved. Horizontal and Vertical axis represents grid layout with consecutive grid distance of 0.5 meter each with 5 m x 2.5 m area. There have been total eight dimming level changes for changes in duty cycles, summary of which have been shown in Table 5-1. Change in maximum and minimum illuminance for change of PWM duty cycle has been shown with bar graph in Figure 5-6. Photometric test report of 18W cool white streetlight Luminaire has been shown in Table 5-2.

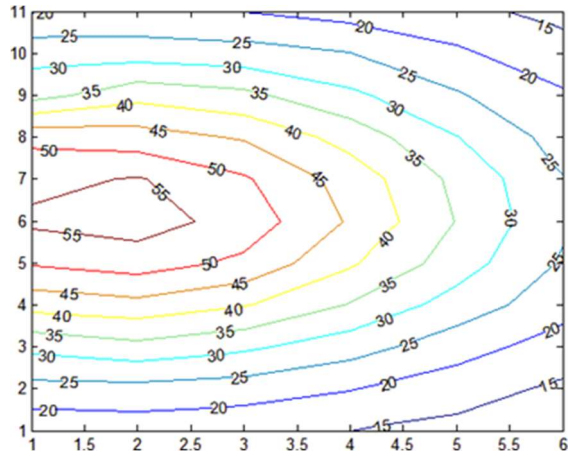

Figure 5-2. Isolux Diagram at PWM duty cycle 100% in lux values

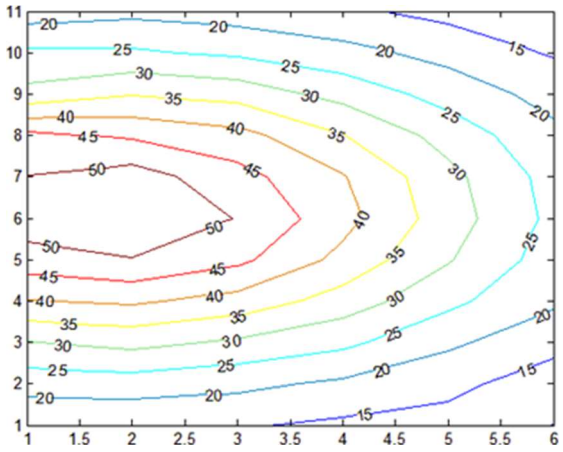

Figure 5-3. Isolux Diagram at PWM duty cycle 80% in lux values

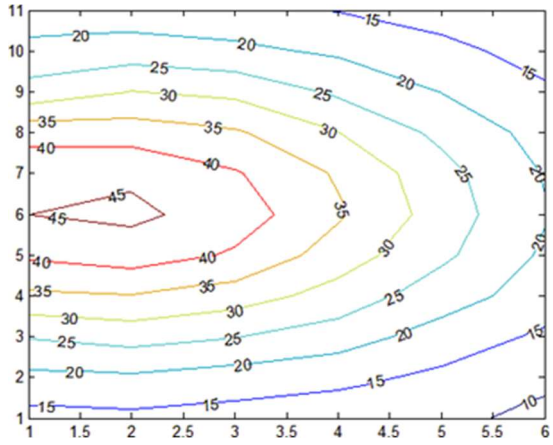

Figure 5-4. Isolux Diagram at PWM duty cycle 60% in lux values

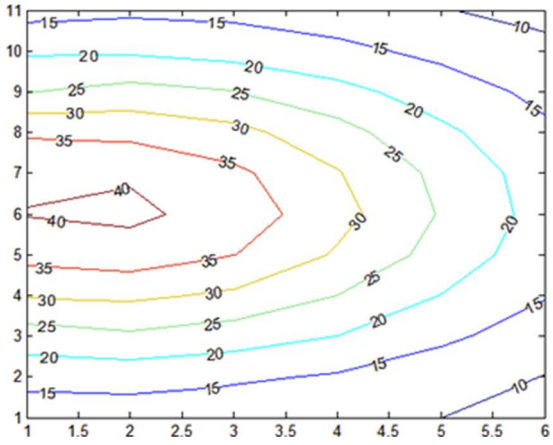

Figure 5-5. Isolux Diagram at PWM duty cycle 40% in lux values

Table 5-1. Light distribution values

	PWM Duty Cycle							
	100%	90%	80%	70%	60%	50%	40%	30%
Illuminance (Max) Lux	57.3	55.4	54	47.9	46.1	44	41.1	37.5
Illuminance (Min) Lux	10.6	10.2	9.9	8.8	8.5	8	7.5	6.9

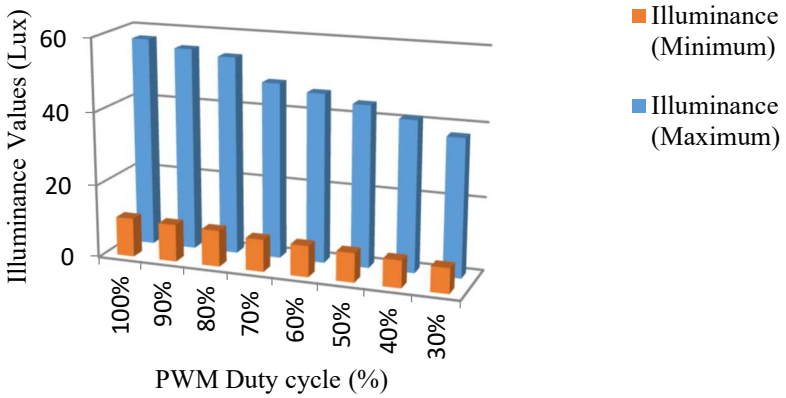

Figure 5-6. Bar graph of the luminaire illuminance maximum and minimum values at different PWM duty cycle values

Table 5-2. Photometric test report of 18W cool white streetlight Luminaire

Voltage (V)	230.05
Current (A)	0.1693
Power (W)	18
Power Factor	0.465
Frequency (Hz)	49.88
Lux	342.4
Luminous Flux (Lumen)	1711.6
CCT (°K)	5969.5
x	0.3452
y	0.3401
Efficiency (lumen/W)	95.088
Sphere Diameter	1 meter
Stabilization Time	10 minutes
Globe Internal Temperature	34^0 C
Communication Distance	5.2 meter

The system uses Zigbee as communication protocol to transmit data between two Xbee modules that hasbeen utilized to make the system intelligent and make the whole system self-operative. The system has the limitation of poor communication distance which can be improved by other version of xbee module. It also enables supervisory control of the system from local control station. Raspberry Pi module with specific IP address has been connected with the system to transmit & receive information using internet network. In that sense the system can be accessed from any place with internet connection. In that scenario encryption & decryption methodologies become very important to make the system secure enough and fault free in future, not allowing unauthorized access.

5.2 Performance Assessment of the Lighting System

Photometric parameters have been measured using CL 70-F illuminance meter within a Dark Laboratory so that no stray light can come inside other than the designed light source. Measurements have been done at the nadir point with luminaire height of 2.476 meters. The performance of the developed system has been evaluated based on photometric parameters. The parameters have been measured on the developed luminaire of Warm White LED (WWLED) and Cool White (CWLED). Two LED arrays of the developed lighting system have been used for measurements. The electrical parameters of the driver has been as mentioned below.

Dimming levels of 0, 12.5, 25, 32.5, 50, 62.5, 75, 87.5, and 100% refer to the percentage of light output from LED arrays when driven by their driver at the rated supply voltage in a dark environment with no stray light have been considered.

5.2.1 Electrical Measurements

Variations of electrical parameters have been measured at the input and output terminals of the drivers used for a single array of WWLEDs and CWLEDs at different dimming levels and shown in Figure 5-7 and Figure 5-8. The electrical parameters have been measured using a digital power meter Yokogawa (WT 210). Figure 5-7 shows the variation of input and output current and Figure 5-8 shows the variation of input and output power due to the variation of duty cycle of the PWM signal on WWLEDs and CWLEDs.

5.2.2 Photometric Measurements

Variation of Illuminance levels has been shown in Figure 5-9 due to change in the duty cycle of the CW and WW LED arrays. Illuminance values have been measured for both the luminaires S1 & S2 for photopic and scotopic illuminance using SOLAR LIGHT illuminance meter. When both CW & WW LED arrays have been at 0% dimming level no light output has been there. Maximum illuminance value achieved of 1054 lux and 629 lux for scotopic and photopic illuminances respectively for the luminaire with two arrays of CWLEDs and one array of WWLEDs when all LED arrays glowing at 100% duty cycle. Variation of scotopic to photopic illuminance measured value ranging from 1.25 to 1.839.

Figure 5-10 shows the variation of CCT values in terms of Tcp (K) due to the change of duty cycle for both the luminaires. It can be seen when duty cycle associated with the WWLEDs has been 0% for the S1 luminaire, the maximum CCT value achieved of 6345K then only CWLED array has been glowing. When the WWLED array has been glowing for S2 Luminaire with minimum duty cycle, CCT value has been reducing drastically. Minimum CCT value of 3092K achieved when only WWLED has been glowing and CWLED was in OFF condition which has been set by 0% duty cycle. Variation of light level on the horizontal surface have been measured at a distance of 2.47 meters from the luminaire within the dark laboratory using CL70F (Make: Konika Minolta).

The measurements have been recorded keeping the instrument on a stool on the nadir point to eliminate any measurement error. CCT of the light source can be varied between maximum and minimum values for a soothing night-time environment as per preferences in general. Variation of CCT values in response to variation of illuminance values at the nadir point have been shown in Figure 5-11 for the luminaires. It can be seen from the diagram that presence of two arrays of CWLEDs in S1 luminaire keeps the CCT values at higher level in respect to the S2 luminaire with two arrays of CWLEDs.

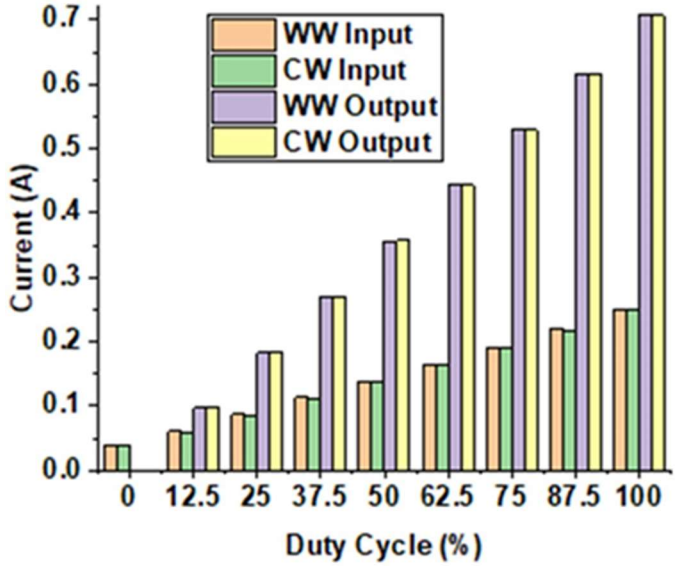

Figure 5-7. Variation of Electrical Current due to variation of Duty cycle

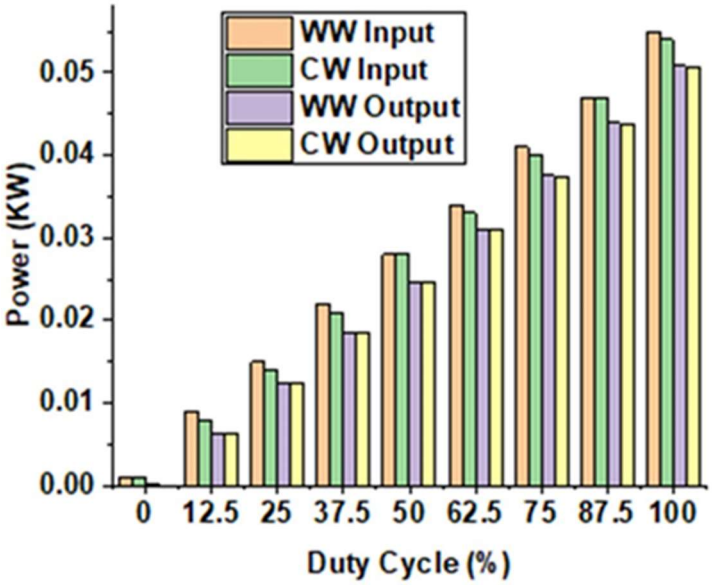

Figure 5-8. Variation of Electrical Power due to variation of Duty cycle

Variation of x y coordinates values on CIE 1931 chromaticity diagram measured by the photometer and their calculated values considering Grassman's color mixing law considering CCT values and Tri stimulus [XYZ] values have been shown in Figure 5-12 for both the luminaires. Equations (14) and (15) have been used to calculate chromaticity coordinates (United States of America Patent No. US 7,024,034 B2, 2006) using the CCT (Tcp) values.

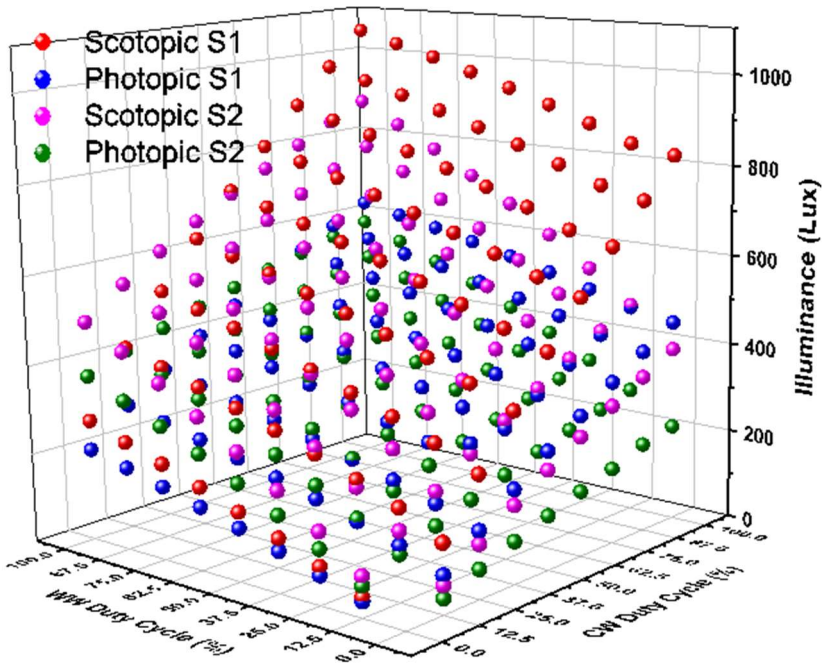

Figure 5-9. Variation of Illuminance level at different duty cycle

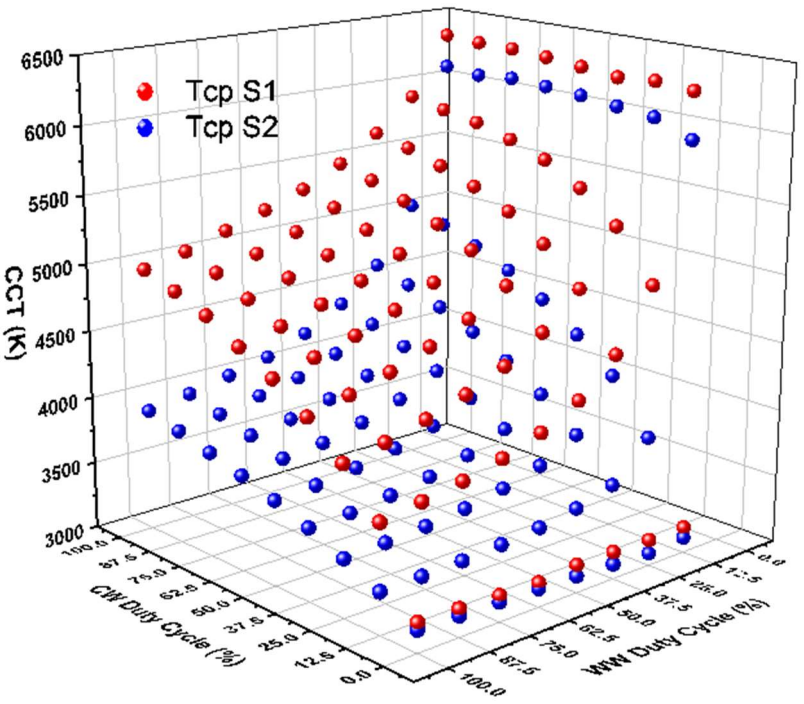

Figure 5-10. Variation of CCT values at different duty cycle

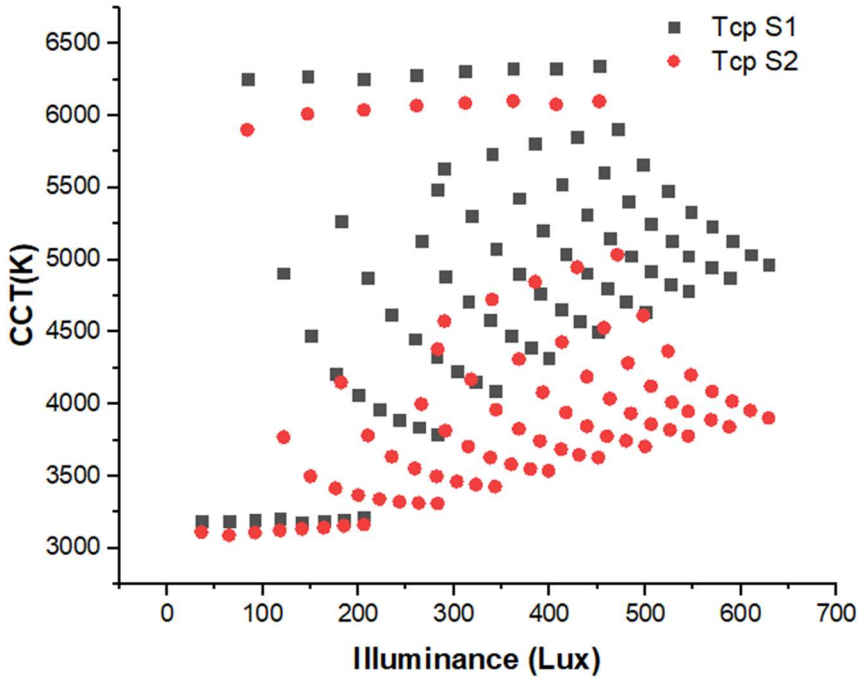

Figure 5-11. Variation of CCT values due to change of illuminance level

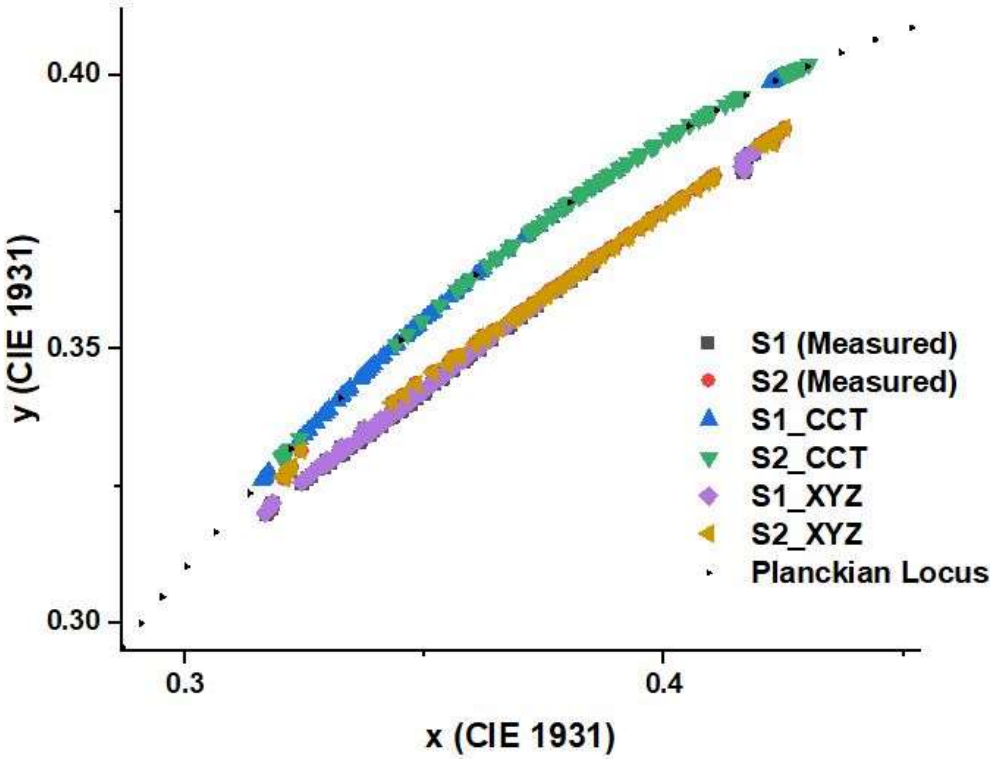

Figure 5-12. Variation of x and y coordinates between measured values and calculated values

For $2222K \leq Tcp \leq 4000K$

$$x = -0.2661239\frac{10^9}{Tcp^3} - 0.2343580\frac{10^6}{Tcp^2} + 0.8776956\frac{10^3}{Tcp} + 0.179910$$

$$y = -0.954947x^3 - 1.37418593x^2 + 2.09137015x - 0.16748867 \quad (14)$$

For $4000K \leq Tcp \leq 25000K$

$$x = 3.0817580\frac{10^9}{Tcp^3} - 2.1070379\frac{10^6}{Tcp^2} + 0.2226347\frac{10^3}{Tcp} + 0.240390$$

$$y = 3.0817580x^3 - 5.87338670x^2 + 3.75112997x - 0.3700148 \quad (15)$$

Figure 5-12 shows the measured x y coordinates for both S1 & S2 the luminaires and calculated values from their tri stimulus values have been similar and do not follow the coordinates of the Planckian Locus. It also shows that the calculated results of the x y coordinates calculated from the CCT values considering equation (14) and (15), follow the coordinates of the Planckian locus.

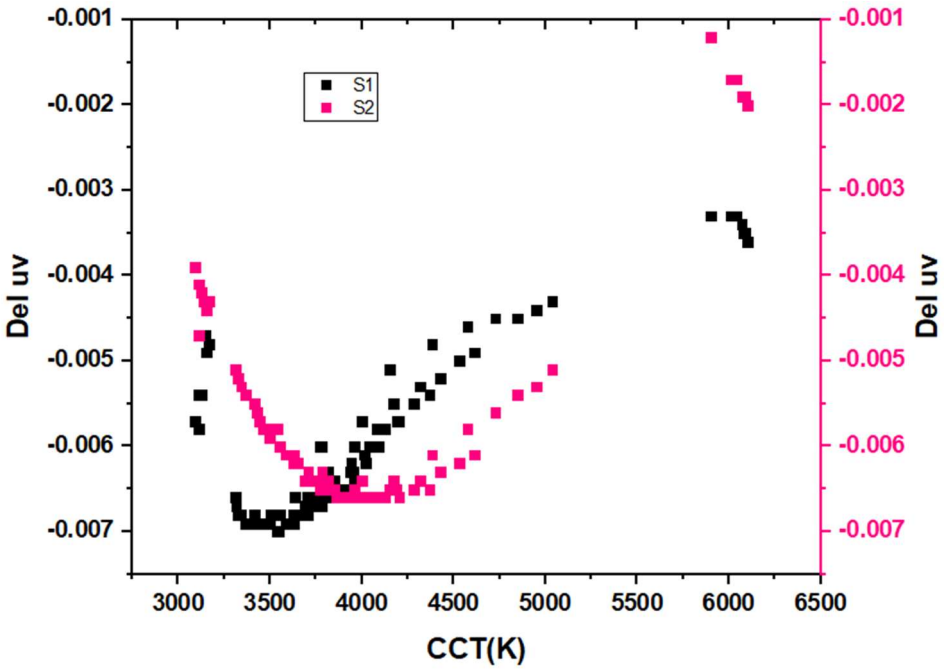

Figure 5-13. Variation of D_uv due to variation in CCT Values

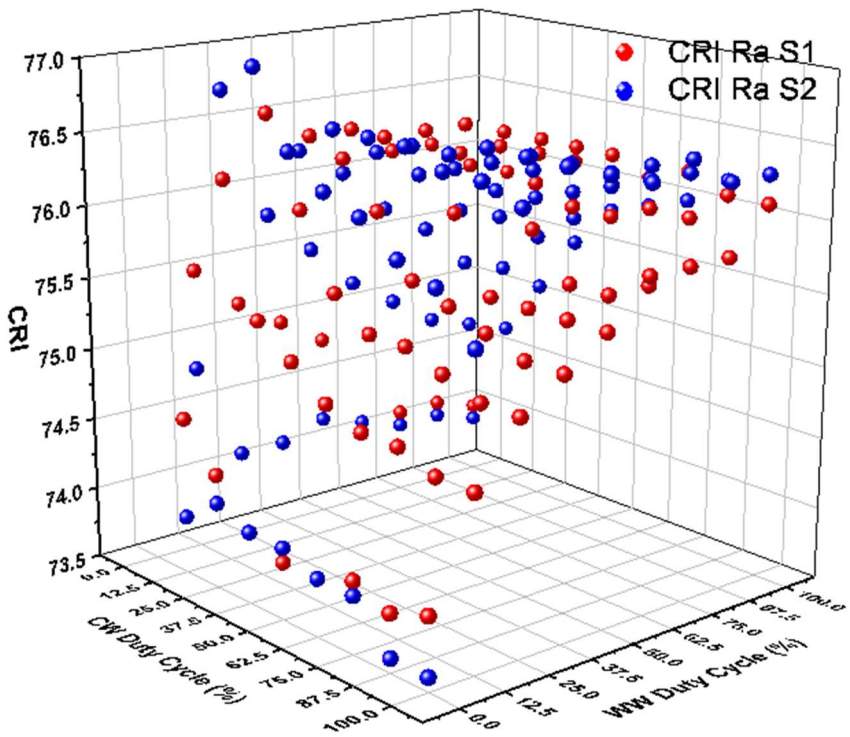

Figure 5-14. Variation of CRI values at different dimming levels

Variation of D_{uv} parameter (chromaticity point's crosswise distance from the blackbody locus) in the u-v chromaticity diagram (Ohno Y. , 2014) has been shown in Figure 5-13. Variation of D_uv due to variation in CCT Values at different CCT values measured from both the light sources due to change of dimming levels. According to studies on white LED lighting preferred chromaticity, chromaticity points slightly below the blackbody locus generally preferred for its better color rendering properties (Dikel, Burns, Veitch, Mancini, & Newsham, 2014) (Ohno & Fein, 2014) (Ohno Y., 2016) (Perz, Baselmans, & Sekulovski, 2016) (Wang & Wei, 2018) (Wei & Houser, 2016). A maximum deviation of -0.007 and -0.0066 can be seen in the graph for luminaires S1 & S2 respectively. Few results show deviation of D_{uv} values have been beyond maximum limits for the white light source (i.e. ±0.006) (Boyce & Stampfli, 2019). It can be inferred that at specific points the light sources have been out of considerable range of white light source. Deviation of D_{uv} values have been very small when only CWLEDs has been glowing for the S2 luminaire with minimum value measured of -0.0012.

Variation of Color Rendering Index (CRI) average value (Ra) also termed as CIE general CRI values due to change in duty cycle has been shown in Figure 5-14. Variation of CRI values at different dimming levels for the luminaires. CIE CRI (Ra) is based on a comparison of a set of eight color samples with defined reference sources (CIE, 1965) (CIE,

1974) (CIE, 1995). Measured values have been improved when both CW & WW LEDs glow together rather than individually for both the luminaires. Maximum value of CIE general CRI of 77 achieved for S2 when WWLED arrays glowing at 12.5% duty cycle and CWLED array glowing at 25% duty cycle. Similarly, maximum CRI value of 76.6 measured for S1 luminaire when WWLED arrays glowing at 25% duty cycle and CWLED array glowing at 12.5% duty cycle.

5.2.3 Measurements of IES Color Fidelity Index (R_f) and Color Gamut Index (R_g)

The most advanced color evaluation parameters are CIE R_f and R_g. The CIE R_f is equivalent to CIE Ra but functionally different. The coordinates of the 99 Color Evaluation Sample (CES) under test light source and the reference illuminant have been put into the same 16 hue-angle bins on the a'-b' plane of the Color Appearance Model-Uniform Color Space (CAM02-UCS) (Moroney, et al., 2002) and the arithmetic means of the a'-b' coordinates for the test light source have been calculated and joined to form polygons (ANSI/IES TM-30-18. IES Method for Evaluating Light Source Color Rendation, 2018) as shown in Figure 5-15 (a) and (b) respectively. Individual CES Fidelity Indices have been provided in Figure 5-22 for each of the 99 CES on a 0-100 scale. These are equivalent to CIE Special CRIs, although there are only 14 of them. The chromatic shift in the vectors of the color vector graph (CVG) in Figure 5-16 has been quantified in a set of 16 local Chroma shift measurements, where each value corresponds to each hue angle bin expressed in graphical form (ANSI/IES TM-30-18. IES Method for Evaluating Light Source Color Rendation, 2018). In the figure a smooth black circle depicts the gamut of the reference illuminant, while a red curve indicates the gamut of the test light source. The average color difference inside a bin of hue angles, denoted by a tiny arrow extending from black to red. The arrow pointing towards the centre indicates a drop in chroma while the arrow pointing away from the centre shows an increase in chroma. The figure also shows the R_f and R_g along with CCT and D_{uv} of the light source under test. Color gamut metrics support the concept that a light source should render surface colors in the way that people like (Boyce & Stampfli, 2019) (Society of Light and Lighting, 2012; Judd, 1967; Feng, Xu, Han, & Zhang, 2017). The variation of CIE R_f for different CCT values have been shown in Figure 5-17(a). The maximum value of R_f achieved for this system has been 76 within the CCT range of 3157K – 4057K and minimum value of 72 has been achieved at the CCT value of 6100K.

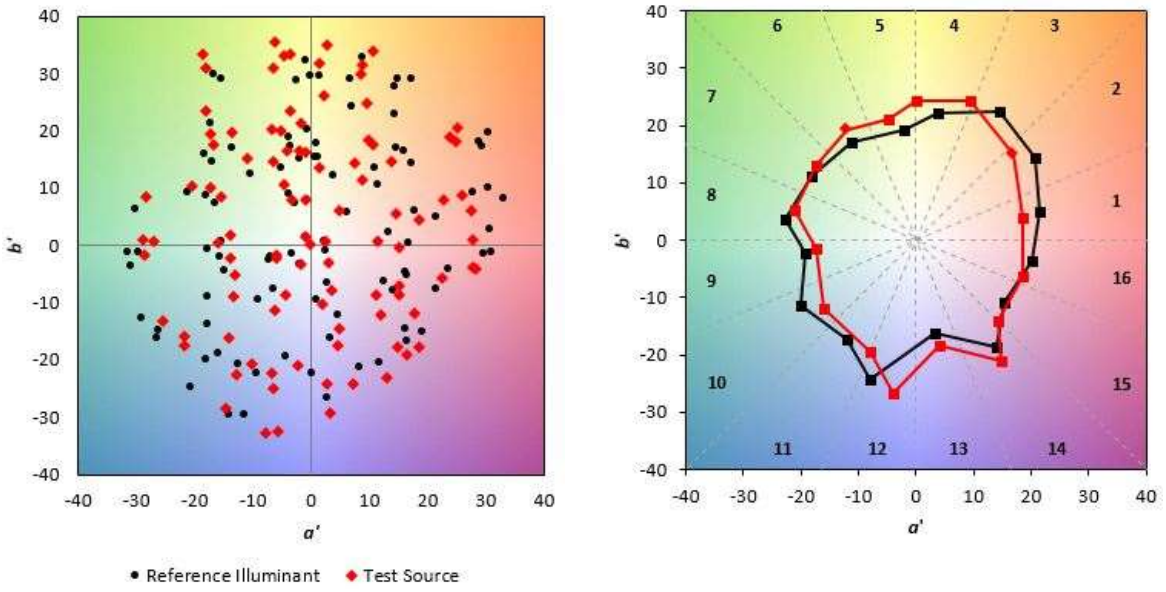

(a) (b)

Figure 5-15. (a) 'The Coordinates of the 99 CES under the test light source and the reference illuminant plotted on the a'-b' plane of CAM02-UCS. (b) The polygons for the test light source and the reference illuminant formed by the average coordinates' *(ANSI/IES TM-30-18. IES Method for Evaluating Light Source Color Rendation, 2018)*

The area encompassed by the average coordinates of the color equivalent samples (CES) for each hue angle bin has been measured by IES Rg. Rg can have a maximum and minimum value of 140 and 60, respectively. A reduction or increase in Rg from 100 will result in a reduction in the color's R_f score. Figure 5-17 (b) shows the Rg value at various CCTs. At CCT 5073, the R_g value peaks at 100 and drops to 96 at CCT ranges of 3157 to 3442 K. Figure 5-18 depicts the variation of R_g values of the system with different R_f values. The figure depicts the different light from the luminaires within triangular area has been within the TM-30-15 library of light sources.

5.2.4 Measurements of Local Chroma Shift and Local Hue Shift per Hue Angle Bin

The CVG's solely tangential change in chromaticity for the color samples in a set of 16 hue angle bin illuminated by the reference illuminant and test light source known as local hue shift. At each hue angle bin, the first one reflects the chroma shift of the test source color from the reference illuminant. Local Chroma shift is the average radial change in chromaticity for the color samples in a given hue angle bin when illuminated by reference illuminant and test light source and therefore represents the chance in chroma. Positive values represent clock wise shift in hue and vice versa. At CCT 4058 K, Figure 5-21 illustrates the local chroma shift per hue angle bin, local hue shift per hue angle bin and IES fidelity Indices for the CIE standard illuminant for 16 hue angle bins respectively for a randomly chosen dimming combination of CW and WW LEDs with a CCT value of 4058 K. As the CCT increases, the chroma and hue shift increase as well. Figure 5-19 and Figure 5-20 shows location of the coordinates of the test light source on 1931 chromaticity diagram and 1976 chromaticity diagram respectively.

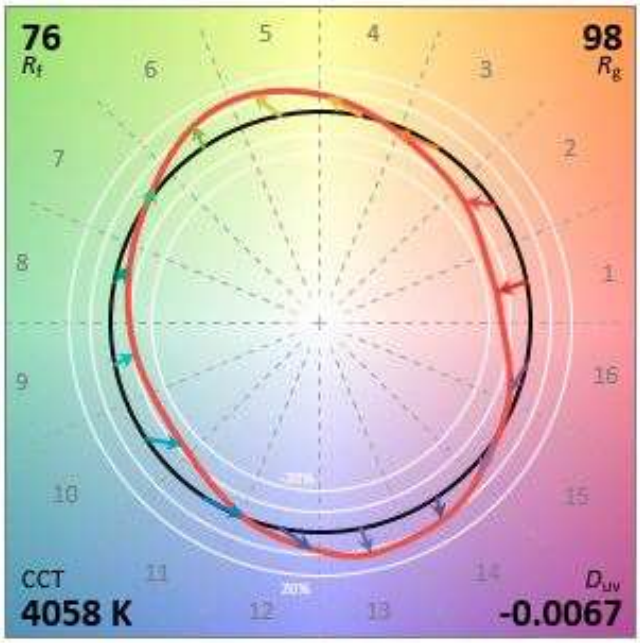

Figure 5-16. The color vector graphic for a test light source (ANSI/IES TM-30-18. IES Method for Evaluating Light Source Color Rendation, 2018)

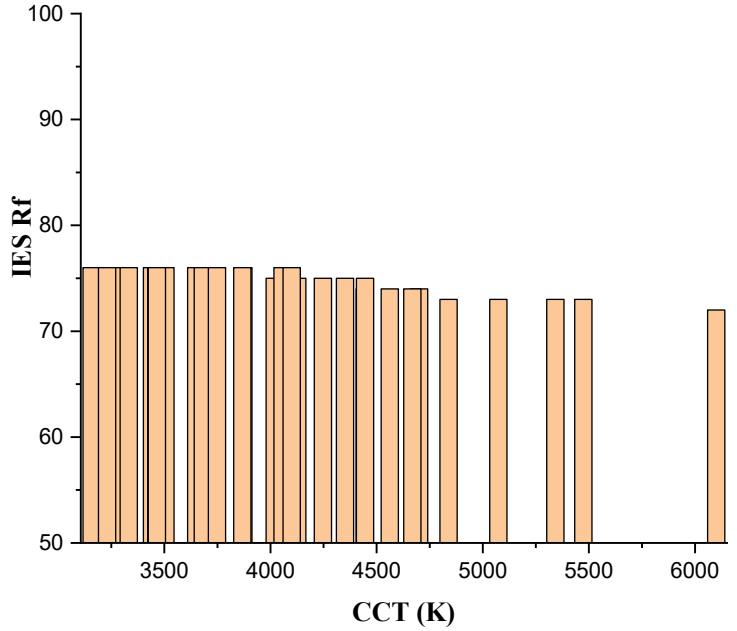

(a)

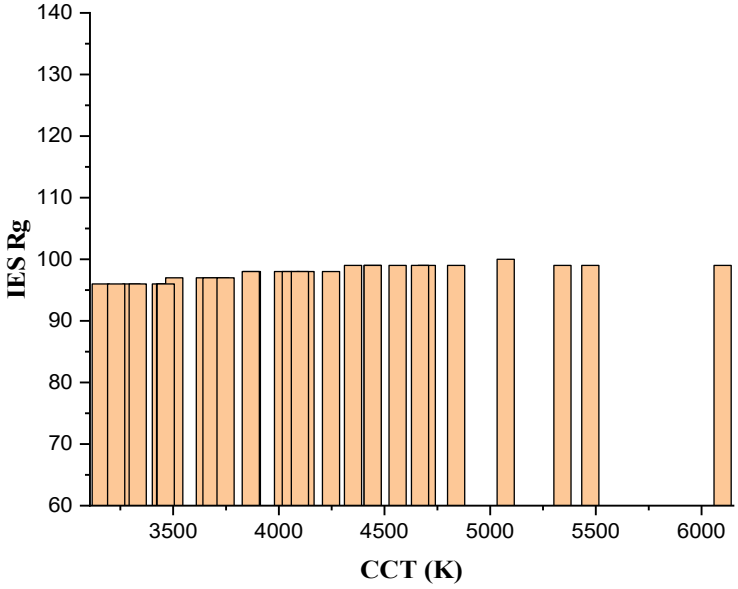

(b)

Figure 5-17. (a) IES Rf values at different CCTs (b) IES Rg values at different CCTs (bottom)

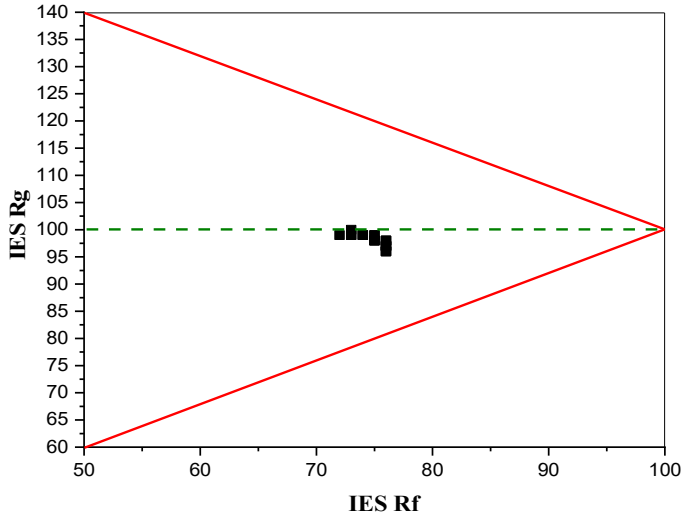

Figure 5-18. IES R_g values at various IES R_f levels.

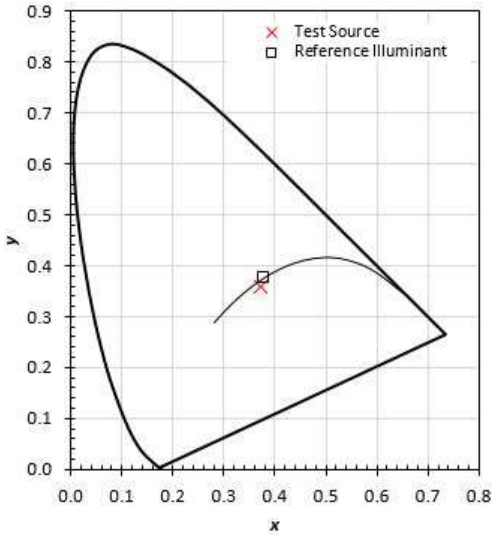

Figure 5-19. location of Test source and Reference illuminant on 1931 Chromaticity diagram

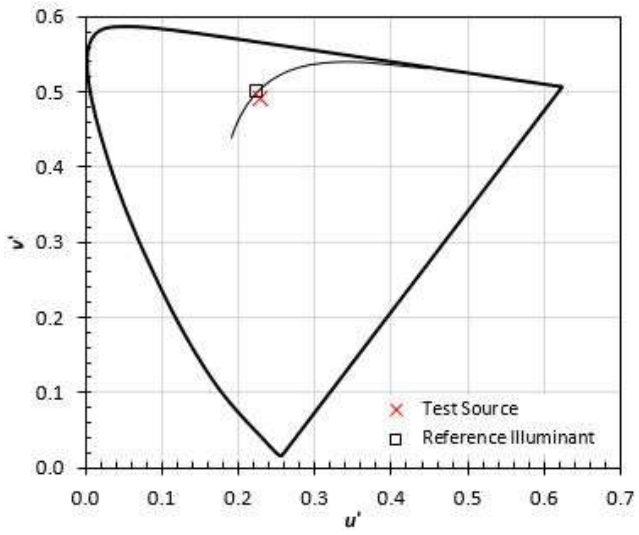

Figure 5-20. location of Test source and Reference illuminant on 1976 Chromaticity diagram

q

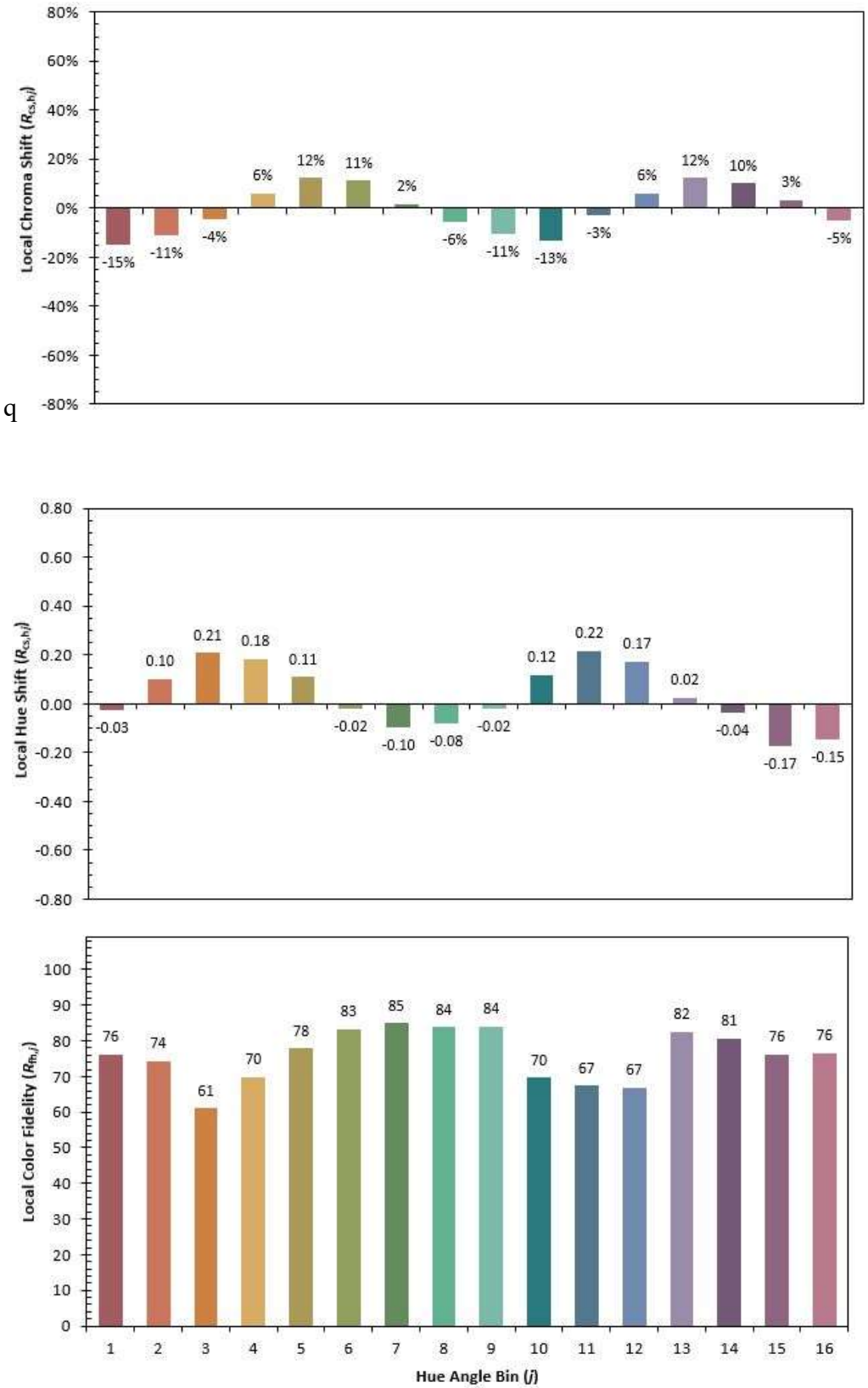

Figure 5-21. 'Local Chroma Shift ($R_{cs,hj}$) (top), Local Hue Shift ($R_{hs,hj}$) (middle) and Local Color Fidelity ($R_{f,hj}$)(bottom) of the light source'

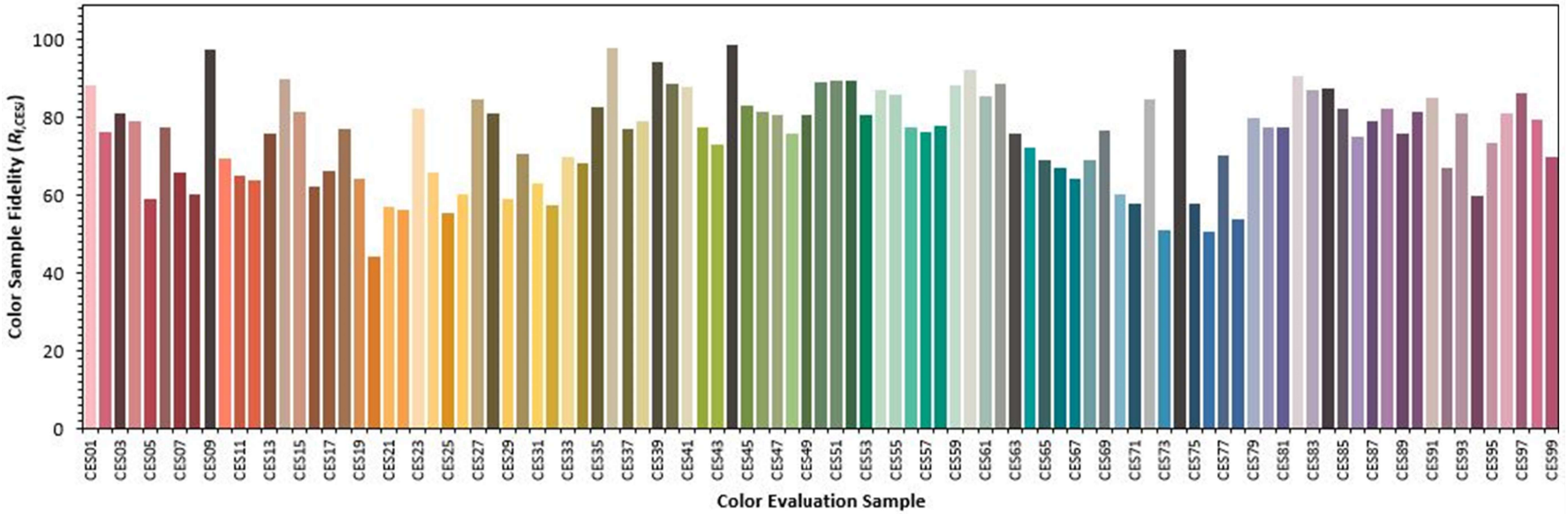

Figure 5-22. 'Distribution of the IES TM-30-18 individual fidelity indices for the 99 CES for the CIE F1 standard illuminant' *(ANSI/IES TM-30-18. IES Method for Evaluating Light Source Color Rendation, 2018)*

5.2.5 Isolux Diagram

The developed LED light source has been installed within a luminaire housing. Illuminance values have been measured on a horizontal surface after mounting the luminaire on a pole at a height of 3 meters. The measurements have been done within a dark room of the Illumination Laboratory of Jadavpur University. Illuminance values have been measured using SOLAR LIGHT illuminance meter on a rectangular grid area of 4 meters x 2.5 meters. Illuminance measurement has been done within a dark room to avoid any kind of stray light error. Maximum values measured of 454 lux and 736 lux for photopic and scotopic illuminance values respectively. The isolux diagram has been shown in Figure 5-23. Each grid point has been shown in the horizontal and vertical axis of 0.5 meters apart. Iso lines show percentage values of the maximum illuminance at the middle of the figure.

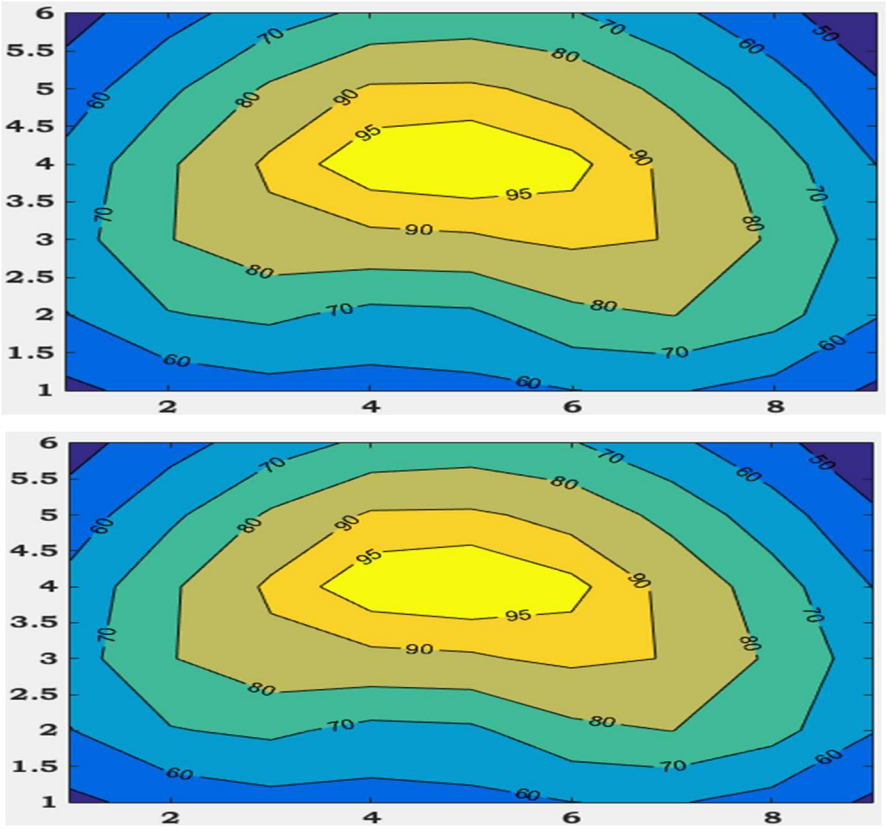

Figure

Figure 5-23. Isolux diagram of Photopic (top) and Scotopic illuminance (bottom) in the percentage of maximum illuminance value from the light source on a horizontal surface

5.2.6 Measurement of Intensity Distribution

The intensity distribution of the developed luminaire has been measured using a C - γ type Goniophotometer (Model: LSG 1700B; Make: Lisun). The intensity distribution data has been shown in Figure 5-24 (a - f). The luminaire can be classified as Type II as per the IES classifications and Very Short type as per Longitudinal Classification. Maximum intensity achieved 5085.57 candelas Figure 5-24 (a). Red contour within the diagrams represents the intensity distribution at the C90^o -C270^o vertical plane i.e., at the front & back side of luminaire and blue contour represents intensity distribution at the C0^o – C180^o vertical plane i.e., at the two sides of the luminaire. Figure 5-24 (a - f) shows intensity distribution of the luminaire at maximum lumen output level, L5, L4, L3, L2, and L1 illuminance selection conditions of the developed S2 type luminaire as per Table 5-4. Where L5 represents photopic illuminance values of 500 (± 3) lux measured at a distance of 2.47 meters within dark laboratory varying the CCT values of S2 type luminaire. Which has been achieved by variation of illumination levels of CW & WW LED arrays within the luminaire. Similarly, L4, L3, L2, L1 represents fixed illuminance values of 400, 300, 200 and 100 lux respectively in similar conditions with variable CCT values. Max Illu represents three sections of the LEDs glowing at maximum illumination level.

5.3 Road Lighting Simulation

The intensity distribution of the developed luminaire was measured using a C - γ type Goniophotometer (Model: LSG 1700B; Make: Lisun) and software compatible digital file (*.ies) for the luminaire has been generated. The digital file (*.ies) was used to simulate multiple street lighting designs using DIALux software. Figure 5-25 shows lighting simulation using DIALux software. The results of the street lighting design have been shown in Table 5-3.

Simulation of road lighting design was done considering standard road of two carriageways, each having 11 meters' width and mounting height of 11 meters with bracket length of 1.5 meters and setback of 0.5 meters. The Lighting design was done in such a way that the Nadir point of the luminaire on the road surface was 1 meter away from the edge of the road surface. The lighting poles have been at opposite sides of the road. The distance between two consecutive poles has been 33 meters.

In case of L1 & L2 type selection of luminaire, the width of the carriageway has been considered as 7 meters and sidewalk of 3 meters.

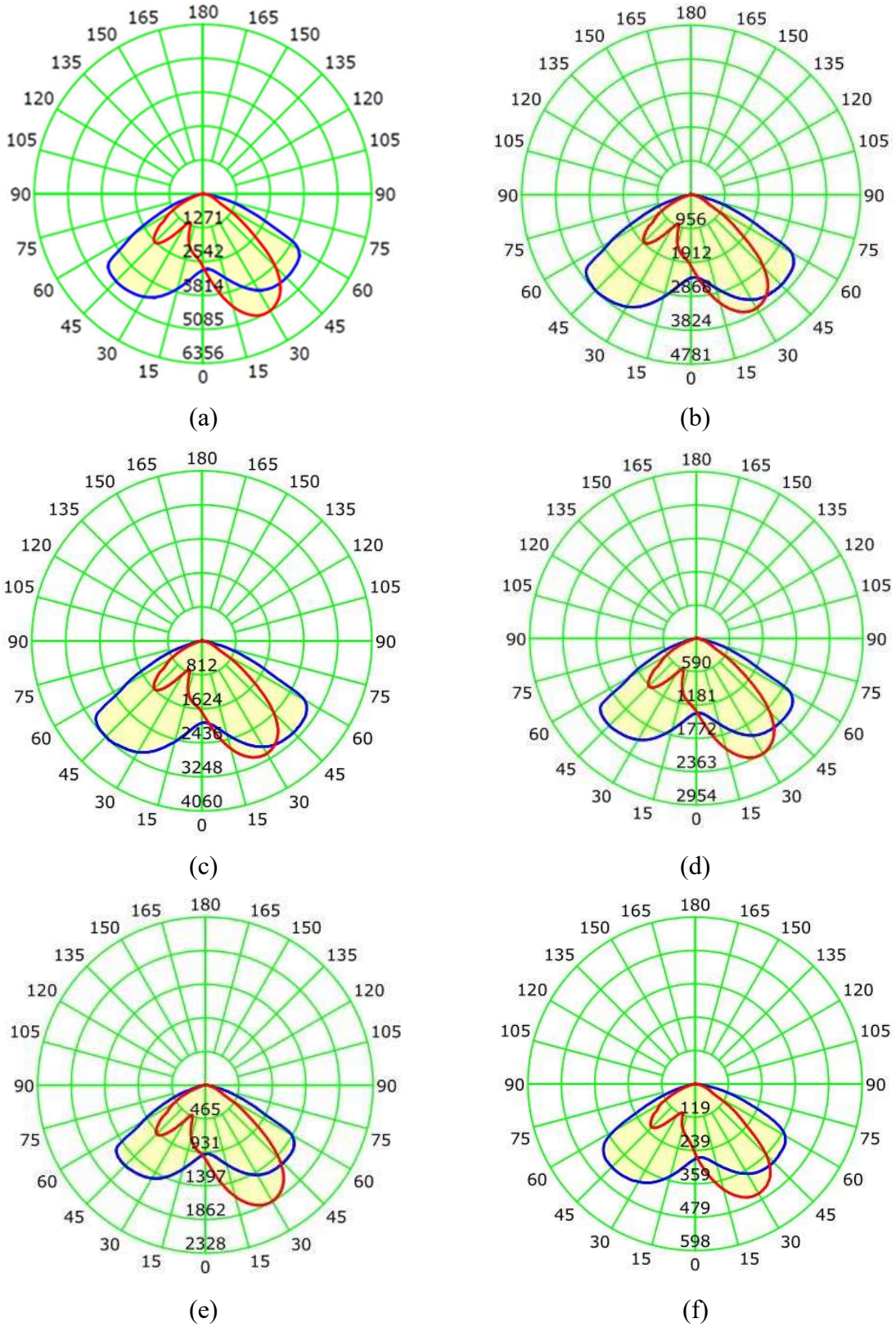

Figure 5-24. Goniophotometric measurements of Intensity Distribution of (a) Max illumination selection, (b) L5, (c) L4, (d) L3, (e) L2, (f) L1 illuminance and CCT selections

Table 5-4 shows the specification of the luminaire at different light level selection and Figure 5-26 shows surface temperature measurement within laboratory environment. Luminaire surface temperature (maximum) measured using Fluke Thermal Imager Ti400 with the surrounding temperature of 29.5º C.

It can be observed that the luminance and illuminance levels have been better when glowing at higher luminous flux. Lighting levels show better results for a bituminous road surface than a concrete surface. Luminaire with light level selection of L1 & L2 failed to match required longitudinal uniformity values on Concrete Road surface.

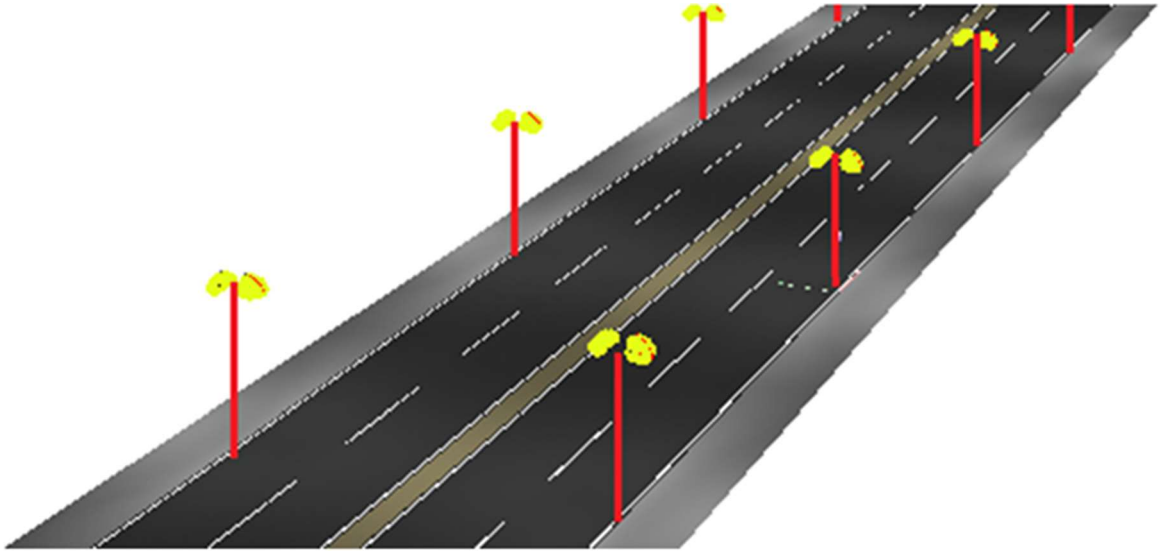

Figure 5-25. Lighting simulation diagram

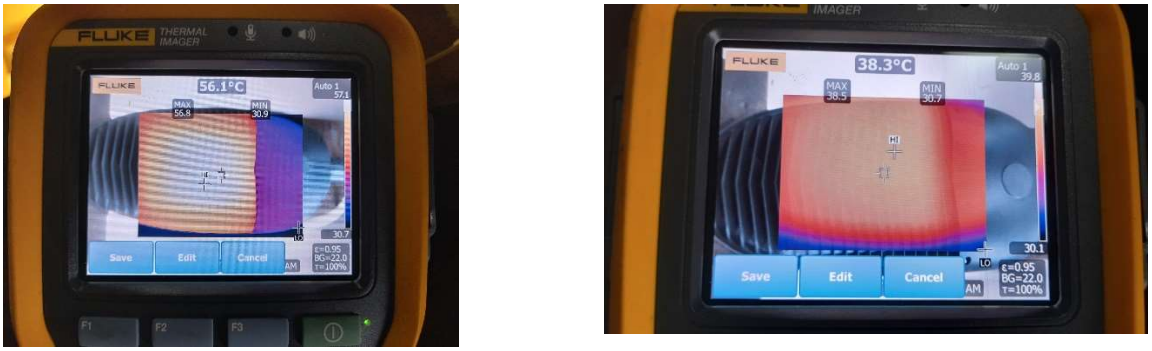

Figure 5-26. Surface Temperature measurement within laboratory environment

Table 5-3. DIALux simulation on Bitumen and Concrete Road Surfaces

Road Surface Type	Luminaire Light Level	Span (m)	Mounting Height (m)	Average Luminance	Overall Uniformity (Luminance)	Longitudinal Uniformity (Luminance)	TI (%)	Surround Ratio	Average Illuminance	Uniformity (Illuminance)	Transverse Uniformity (Illuminance) E_{min}/E_{max}
Bitumen	Max Illu	32	11	2.37	0.6	0.6	4	0.7	55	0.523	0.329
	L5	33	11	2.08	0.59	0.58	4	0.71	40	0.518	0.318
	L4	32	11	1.83	0.59	0.58	4	0.72	38	0.517	0.311
	L3	33	11	1.19	0.56	0.58	4	0.76	27	0.52	0.312
	L2	21	7	3.21	0.55	0.64	6	0.94	62	0.535	0.367
	L1	21	7	1.67	0.55	0.62	5	0.94	33	0.53	0.342
Concrete	Max Illu	34	11	4.9	0.77	0.61	3	0.78	56	0.601	0.402
	L5	34.5	11	3.75	0.76	0.61	3	0.79	43	0.602	0.409
	L4	34	11	3.26	0.75	0.62	3	0.8	37	0.628	0.436
	L3	34	11	2.49	0.74	0.6	2	0.83	29	0.633	0.433
	L2	21	7	4.96	0.7	0.59	4	0.97	56	0.616	0.426
	L1	21	7	3.03	0.69	0.57	3	0.95	35	0.607	0.421

Table 5-4. Luminaire specifications at different Light level selection of the luminaire

Luminaire Light Level selection	Voltage (V)	Current (A)	Power (W)	Power Factor	Surface Temperature (ºC)	Lumen Output (Max)
Max Illu	229.32	0.7547	169.8	0.9808	66.4	35118
L5	229.38	0.5678	125.6	0.9657	58.8	26632
L4	229.36	0.4999	110.2	0.9631	56.8	22434
L3	229.58	0.4096	88.4	0.939	48.3	16554
L2	229.46	0.2872	61.1	61.1	45.4	12674
L1	229.6	0.1824	35.6	0.8504	39.6	6500

5.4 Installation of Luminaires and field measurements

(a)

(b) (c)

Figure 5-27. (a) Luminaires installed and variation of luminous flux and CCT using HHD (b) Pictorial representation of the mounted luminaires (c) Measurement of luminance using CRI Illuminance meter and Luminance meter

Four luminaires have been mounted within JU pathway used for pedestrians near a garden and variation of light output (luminous flux) and CCT has been shown in Figure 5-27(a). Luminaires have been mounted on poles with mounting height of 5.67 meters, pole spacing of 16 meters and road width of 5 meters with concrete surface. Measurement of illuminance and luminance values for L1 type of selection of the luminaires have done. Measurement area on the pathway has been shown in Figure 5-27 (b). CRI Illuminance meter CL70F (make Konica Minolta, Japan) and luminance meter LS 110 (make Konica Minolta, Japan) has been used for measurement within the marked area within middle portion of the four luminaires mounted for considering cumulative effect of all mounted luminaires. Luminance and illuminance values

have been measured at every two meter apart on length wise of the path way and every one meter apart on width wise. Figure 5-27 (c) shows Luminance meter mounted on tripod has been used for measurement. Initial measurement point and the end point on width wise has been considered 0.25m away from the edge of the pathway, and in total 54 measurement points have been considered. Average illuminance of 16.37 lux and maximum illuminance of 32 lux has been measured on horizontal surface. Maximum average luminance of 1.018 cd/m^2 and maximum luminance of 1.59 cd/m2 achieved using Luminance meter.

Table 5-5. Variation of photometric parameters measured due to change in CCT

Serial No.	Color Temperature (K)	Color Rendering Index (Ra)	Dominant Wavelength λ_d (nm)	Average Luminance (cd / m^2)	Maximum Luminance (cd / m^2)
1	3081	73.9	584	0.925	1.37
2	3361	75.1	583	1.018	1.47
3	3724	75.8	583	1.004	1.48
4	3914	75.7	582	1.009	1.49
5	4342	75.6	581	0.981	1.53
6	4661	75.3	581	1.005	1.59

Table 5-5 shows variation of photometric parameters on the pathway along with luminance of the on concrete surface due to variation of color temperature of the luminaire using an HHD. Variation of maximum luminance value of 1.59 cd/m^2 and maximum average luminance of 1.018 cd/m^2 achieved Maximum luminance on concrete surface improves with Cool White LED light.

Annual energy savings potential has been calculated based on the energy consumption as mentioned in the table 5-4.

In case of no dimming of the luminaire, it consumes about 169.8 W. Lumen output of luminaire is comparable to a 400 W luminaire with High Pressure Sodium Vapour (HPSV) lamp tubular type including control gear loss.

In comparison to a HPSV luminaire the developed luminaire without using the dimming features saves about 924 KWh of energy annually considering eleven hours of average glowing time of a single luminaire.

When the developed luminaire glows at full brightness for five hours and then glows in a dimming state of 20% light output (power consumption of 25.1 W), it would save about 316893 Watt-hour i.e. approximately 317 units of energy. If the luminaire operates at L5 state of light output during normal operation in peak traffic conditions and then reduced light output state

during non-peak hours, it would save about 220 units of energy annually. Total four luminaires mounted at the site which would save approximately about 880 units of energy.

Similarly, it would save about 138 KWh and 23 KWh of energy annually if the luminaire operates at L3 and L1 states respectively during peak hours and dim down during non-peak hours for single luminaire.

Variation of Illuminance and CCT as well as other parameters along with duty cycle variations for CW & WW sections of LEDs have been shown in Table 5-6. As the intelligent lighting system has been mounted for illumination of pathway within university, only L1, L2 & L3 selections has been chosen for measurement of photometric parameters. The measurements have been done at the nadir point i.e., directly below luminaire. Variations of Spectral Power Distribution, Color vector graph and related photometric parameters Local chroma, hue shift & color fidelity variations shown in Figure 5-28 for different selection states of luminaires.

Table 5-6. Photometric parameters and duty cycle variations at different state selection of luminaires

Luminaire State Selection	**L1_a**	**L1_b**	**L1_c**	**L2_a**	**L2_b**	**L2_c**	**L3_a**	**L3_b**
CW Duty Cycle %	0	31	26	0	94	79	0	5
WW Duty Cycle %	22	5	6	48	0	6	79	75
CCT [K]	3258	4847	4690	3269	6016	5253	3257	3258
⊿uv	-0.0041	-0.0026	-0.0036	-0.0040	-0.0005	-0.0032	-0.0041	-0.0041
Illuminance [Lux]	23.2	23.2	23.1	42.4	40.6	41.6	61.7	61.5
Lumen	6500	6460	6326	12674	10666	11740	16554	16483
Peak Wavelength [nm]	594	443	443	595	441	442	594	594
CIE1931 x	0.4147	0.3489	0.3533	0.4142	0.3219	0.3381	0.4147	0.4147
CIE1931 y	0.3856	0.3495	0.3508	0.3858	0.3306	0.3397	0.3856	0.3856
CIE1931 z	0.1997	0.3016	0.296	0.2001	0.3476	0.3222	0.1996	0.1997
CIE1976 u'	0.244	0.2148	0.2173	0.2436	0.2036	0.2113	0.244	0.244
CIE1976 v'	0.5105	0.4842	0.4855	0.5105	0.4705	0.4777	0.5105	0.5105
Dominant Wavelength [nm]	584	578	580	583	488	574	584	584
Purity [%]	40.18	9.55	11.24	40.08	4.09	3.35	40.21	40.18
CRI Ra	74.9	76.4	77.4	75.4	73.5	75.6	75	74.9

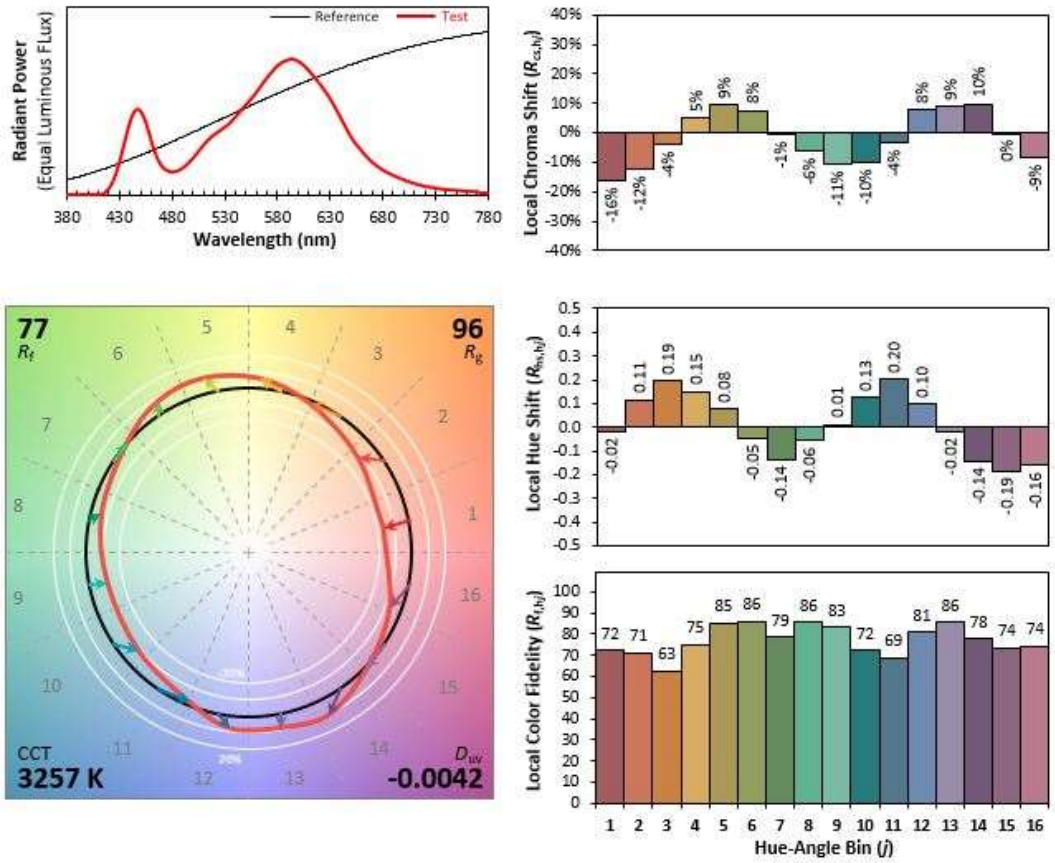
Reference
Test
Radiant Power
(Equal Luminous FLux)
380 430 480 530 580 630 680 730 780
Wavelength (nm)
Local Chroma Shift ($R_{cc,hj}$)
-16% -12% -4% 5% 9% 8% -1% -6% -11% -10% -4% 8% 9% 10% 0% -9%
77
R_f
96
R_g
CCT
3257 K
D_{uv}
-0.0042
Local Hue Shift ($R_{hh,hj}$)
-0.02 0.11 0.19 0.15 0.08 -0.05 -0.14 -0.06 0.01 0.13 0.20 0.10 -0.02 -0.14 -0.19 -0.16
Local Color Fidelity ($R_{f,hj}$)
72 71 63 75 85 86 79 86 83 72 69 81 86 78 74 74
1 2 3 4 5 6 7 8 9 10 11 12 13 14 15 16
Hue-Angle Bin (j)

(a)

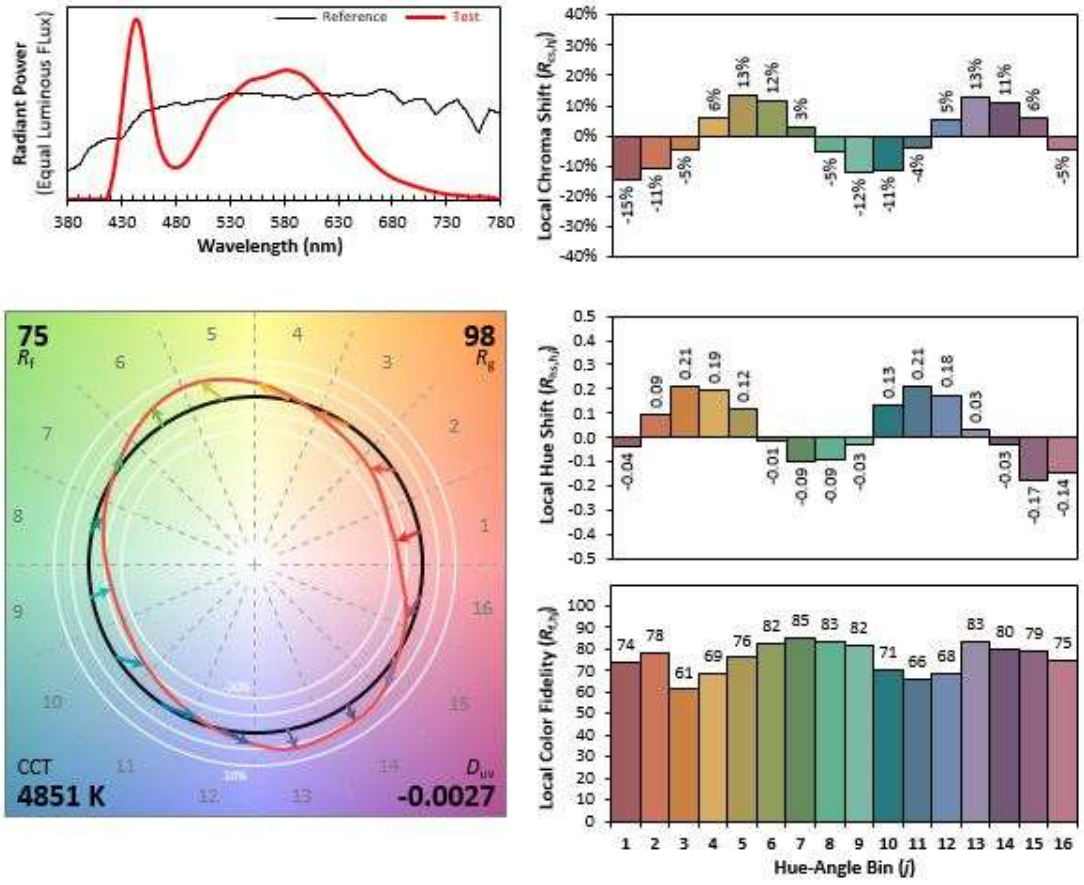
Reference
Test
Radiant Power
(Equal Luminous FLux)
380 430 480 530 580 630 680 730 780
Wavelength (nm)
Local Chroma Shift ($R_{cc,hj}$)
-15% -11% -5% 6% 13% 12% 3% -5% -12% -11% -4% 5% 13% 11% 6% -5%
75
R_f
98
R_g
CCT
4851 K
D_{uv}
-0.0027
Local Hue Shift ($R_{hh,hj}$)
-0.04 0.09 0.21 0.19 0.12 -0.01 -0.09 -0.09 -0.03 0.13 0.21 0.18 0.03 -0.03 -0.17 -0.14
Local Color Fidelity ($R_{f,hj}$)
74 78 61 69 76 82 85 83 82 71 66 68 83 80 79 75
1 2 3 4 5 6 7 8 9 10 11 12 13 14 15 16
Hue-Angle Bin (j)

(b)

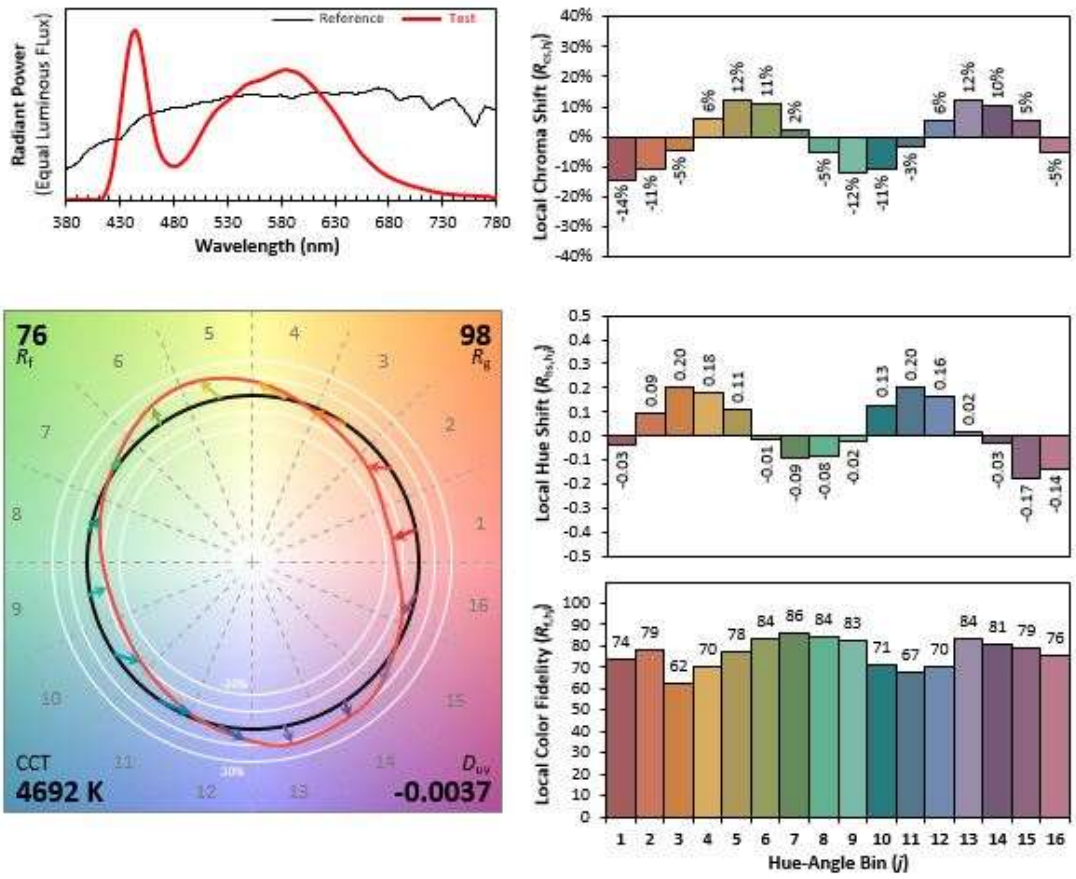
Reference
Test
Radiant Power (Equal Luminous Flux)
Wavelength (nm)
Local Chroma Shift ($R_{cs,h}$)
76 R_f
98 R_g
CCT 4692 K
D_{uv} -0.0037
Local Hue Shift ($R_{hs,h}$)
Local Color Fidelity ($R_{f,h}$)
Hue-Angle Bin (j)

(c)

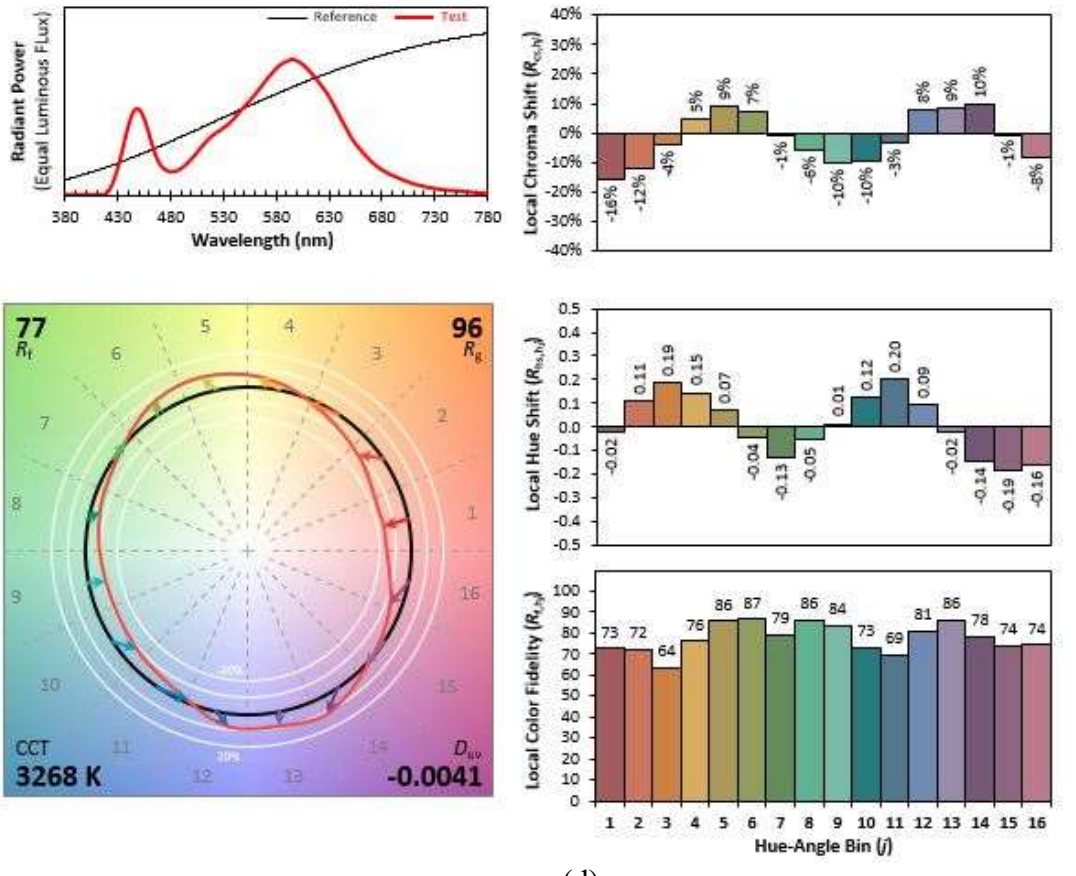
Reference
Test
Radiant Power (Equal Luminous Flux)
Wavelength (nm)
Local Chroma Shift ($R_{cs,h}$)
77 R_f
96 R_g
CCT 3268 K
D_{uv} -0.0041
Local Hue Shift ($R_{hs,h}$)
Local Color Fidelity ($R_{f,h}$)
Hue-Angle Bin (j)

(d)

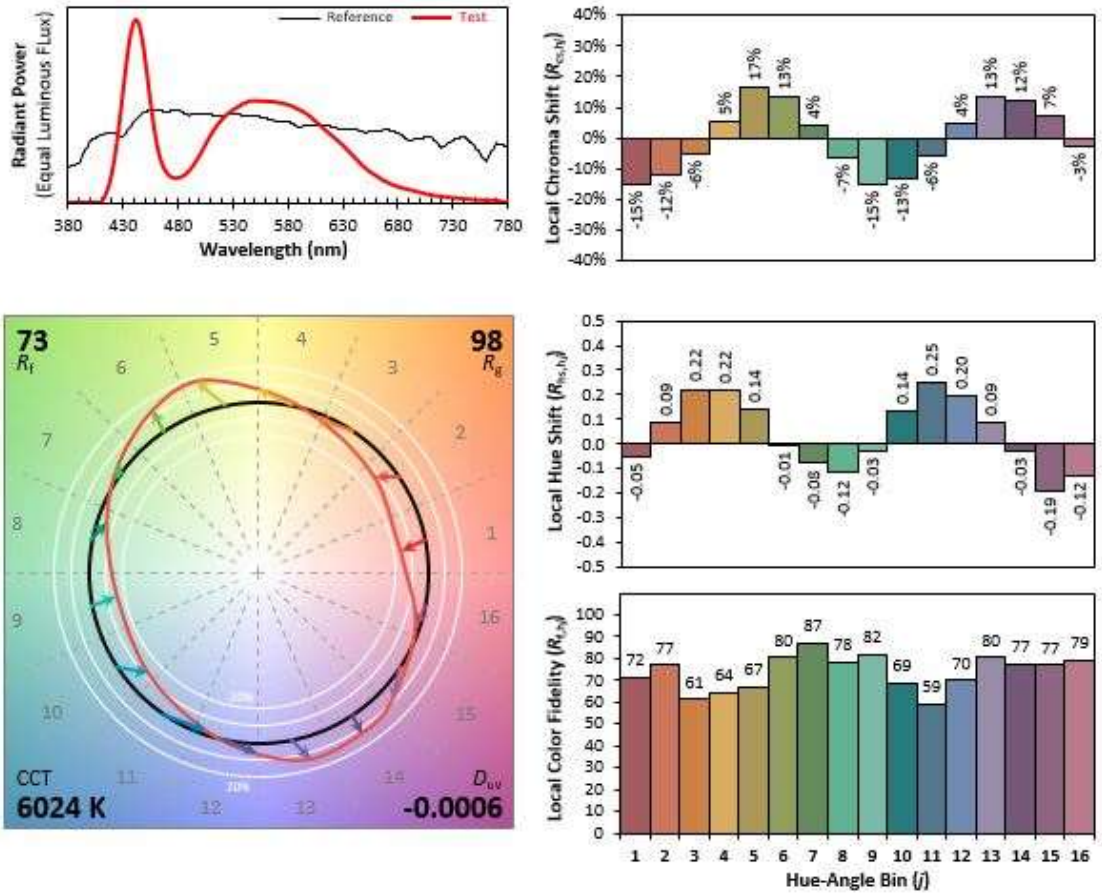
Reference
Test
Radiant Power (Equal Luminous FLux)
Wavelength (nm)
Local Chroma Shift ($R_{cs,hj}$)
73 R_f
98 R_g
CCT 6024 K
D_{uv} -0.0006
Local Hue Shift ($R_{hs,hj}$)
Local Color Fidelity ($R_{f,hj}$)
Hue-Angle Bin (j)

(e)

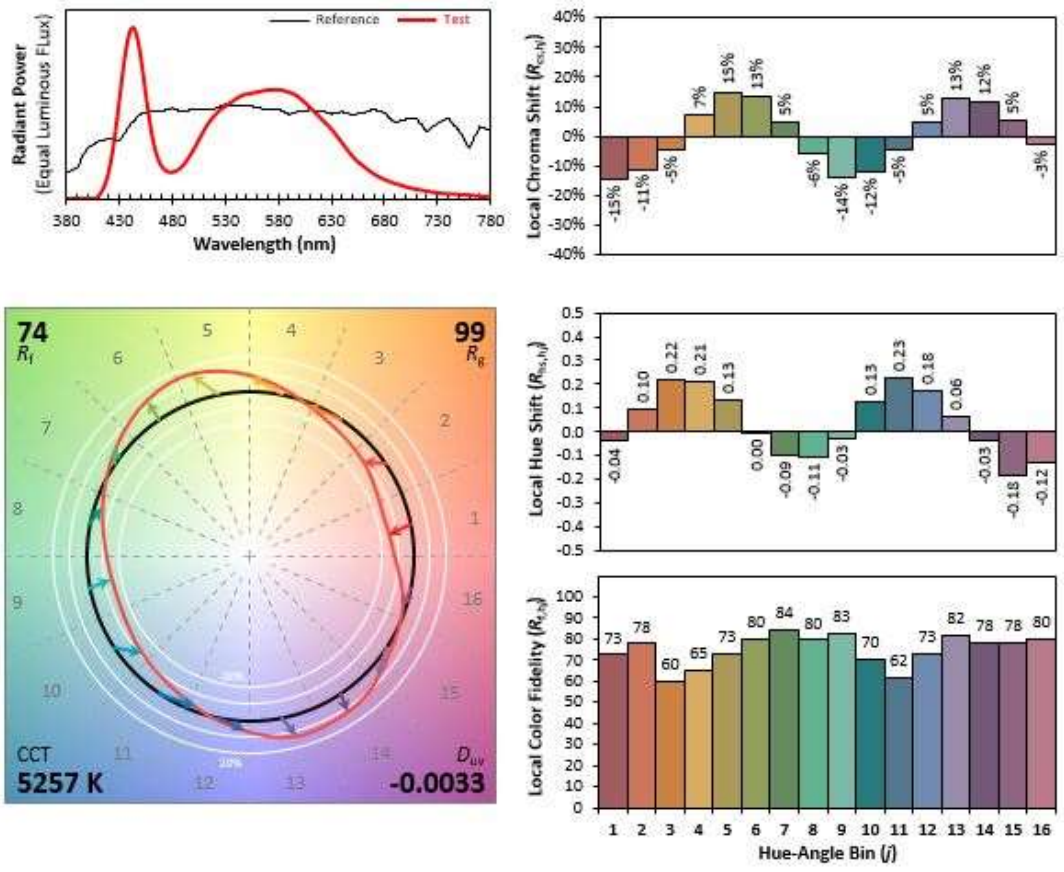
Reference
Test
Radiant Power (Equal Luminous FLux)
Wavelength (nm)
Local Chroma Shift ($R_{cs,hj}$)
74 R_f
99 R_g
CCT 5257 K
D_{uv} -0.0033
Local Hue Shift ($R_{hs,hj}$)
Local Color Fidelity ($R_{f,hj}$)
Hue-Angle Bin (j)

(f)

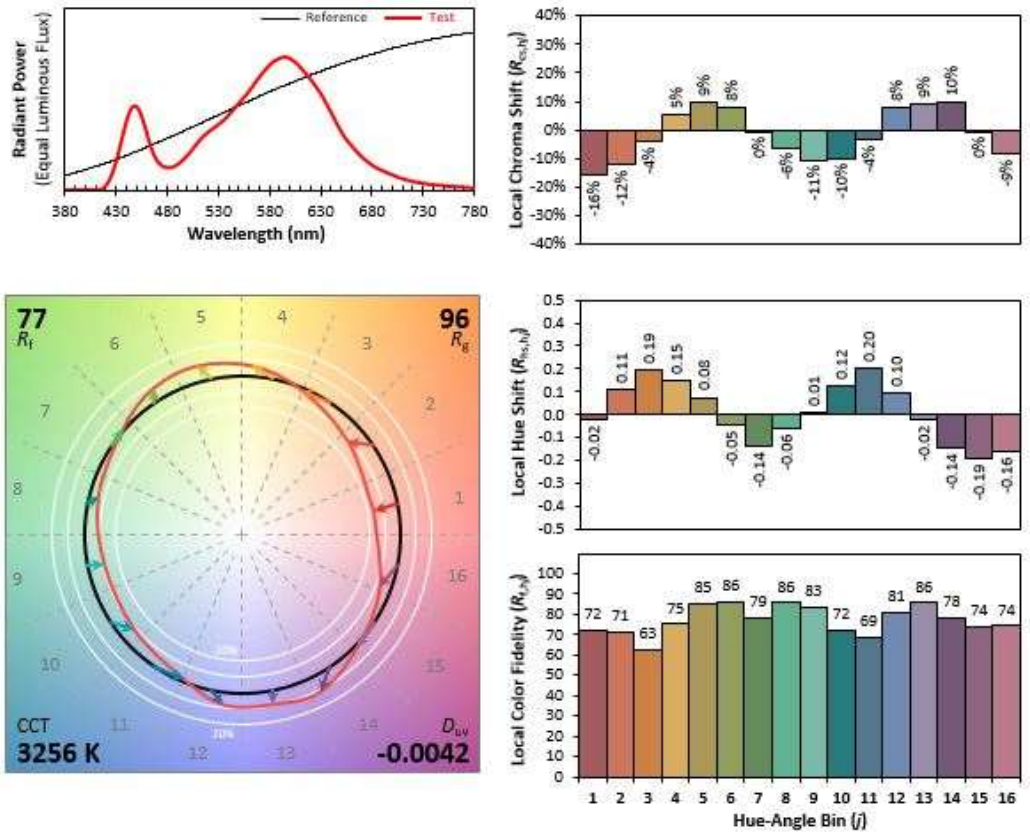

(g)

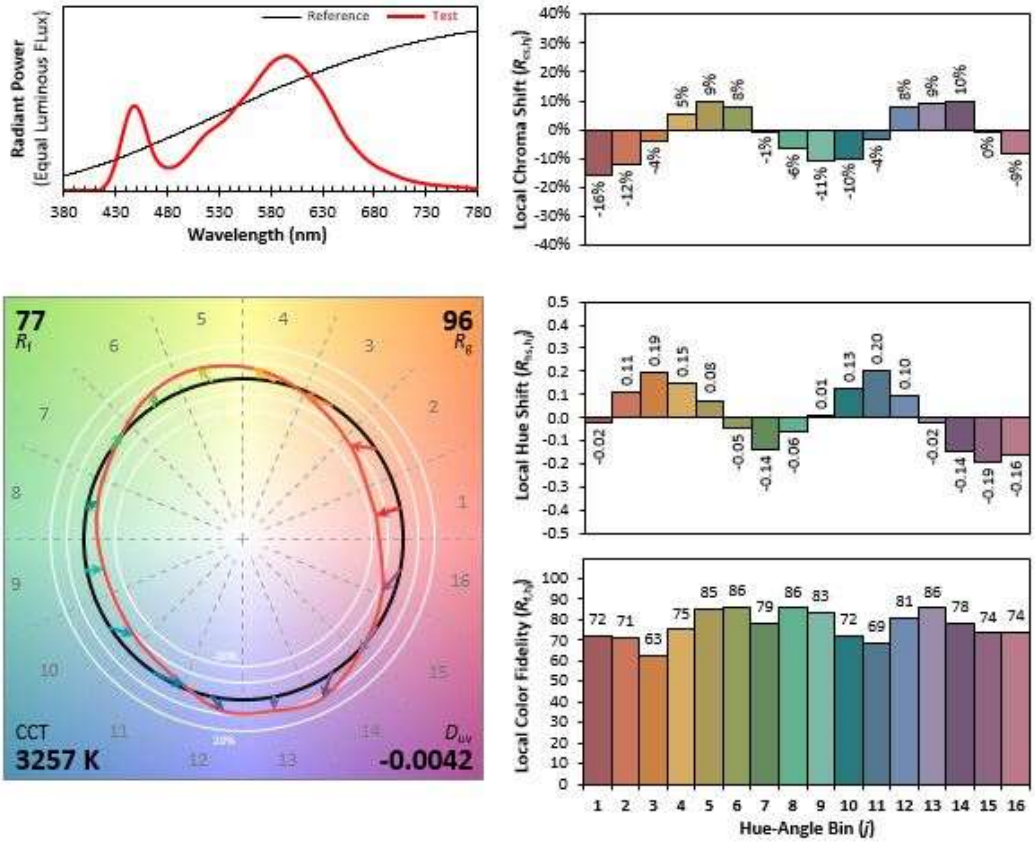

(h)

Figure 5-28. Variations of SPD, R_f, R_g, CCT, D_{uv}, Chroma & Hue shift and Fidelity variations for (a) L1_a, (b) L1_b, (c) L1_c, (d) L2_a, (e) L2_b, (f) L2_c, (g) L3_a & (h) L3_b

5.5 Measurement of physical parameters and Recording

Measurement of physical parameters and recording has been performed by wireless method using an apache-based web server. Figure 5-29 shows physical parameters recording on the storage server. Surrounding temperature (ºC) recording and humidity (%) values can be seen within s2 and s4 columns with time stamp.

←T→				No	s1	s2	s3	s4	s5	s6	Date
☐	Edit	Copy	Delete	2325	0	31.06	1009.25	79.71	2.95	33.52	2022-04-22 10:26:59
☐	Edit	Copy	Delete	2326	0	31	1009.23	79.84	3.19	33.19	2022-04-22 10:28:17
☐	Edit	Copy	Delete	2327	0	30.91	1009.27	80.54	2.76	33.02	2022-04-22 10:29:34
☐	Edit	Copy	Delete	2328	0	30.84	1009.29	80.9	2.8	33.36	2022-04-22 10:30:52
☐	Edit	Copy	Delete	2329	138	30.78	1009.25	80.58	2.97	33.36	2022-04-22 10:32:09
☐	Edit	Copy	Delete	2330	0	30.73	1009.25	80.5	3.11	33.52	2022-04-22 10:33:26
☐	Edit	Copy	Delete	2331	0	30.72	1009.23	80.44	3.26	33.52	2022-04-22 10:34:44
☐	Edit	Copy	Delete	2332	0	30.73	1009.23	80.11	3.4	33.36	2022-04-22 10:36:01
☐	Edit	Copy	Delete	2333	0	30.77	1009.25	79.95	3.54	33.36	2022-04-22 10:37:19

Figure 5-29. Environmental and physical parameters recording

Surrounding temperature (ºC) variation and humidity (%) variation can be seen in Figure 5-30. Variation of temperature and humidity has been recorded within the time period of 10:30 hrs in the morning and 20:30 hrs in evening time. The system was installed beside a garden pathway as can be seen in Figure 5-27(a). Peaks on the diagram represents variation of temperature due to direct sunlight on the temperature sensor that in turn also affect humidity of surrounding the sensor. Maximum temperature has been recorded 41ºC and maximum humidity recorded 82.89 %

Surrounding temperature and humidity when measured for day and night time throughout 24 hours, the pictorial diagram shown in Figure 5-31. The graph shows a smooth variation of temperature and humidity.

Maximum temperature recorded 39.21 ºC and minimum humidity value has been recorded at the same time. Similarly, minimum temperature recorded of 29.36 ºC and at around similar time maximum humidity recorded of 85.99 %. Continuous measurements have been recorded for four days. Both recorded values can be seen on same graph as shown in Figure 5-32. Horizontal axis of the graph represents continuous time scale of recorded span.

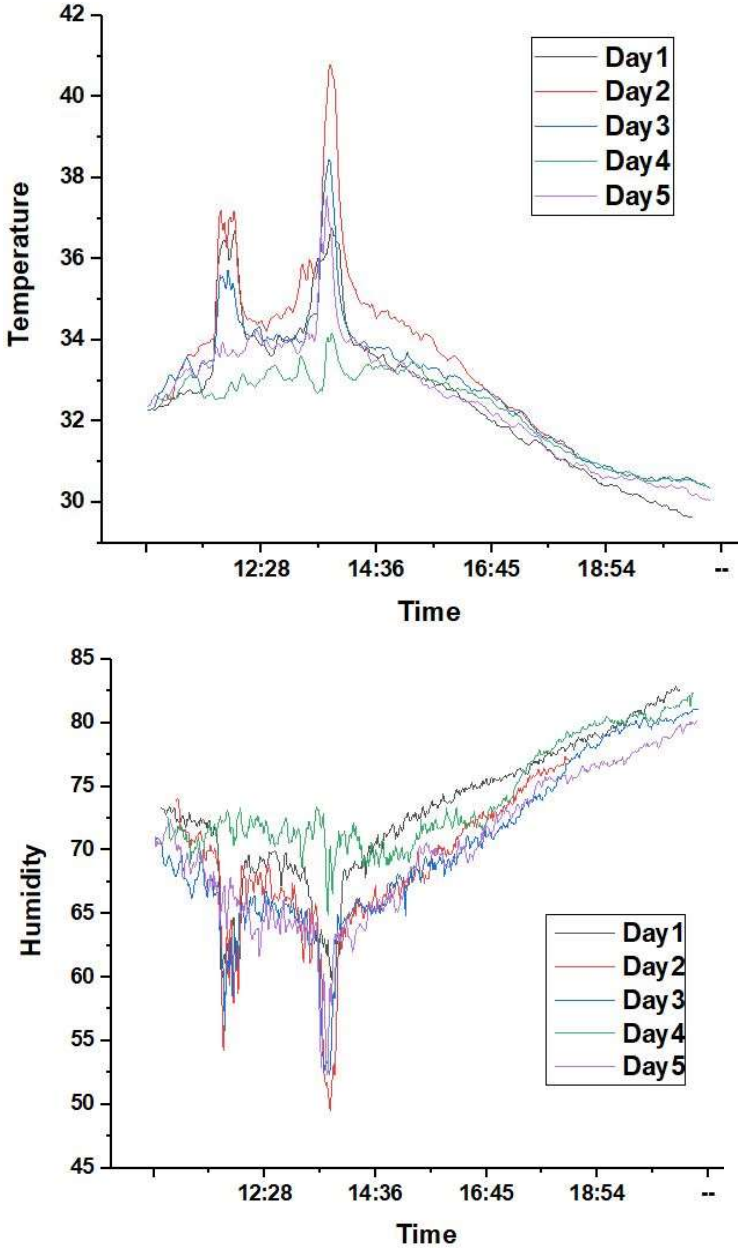

Figure 5-30. Variation of surrounding Temperature (C) and Humidity (%)

5.6 Support Vector Machine (SVM) Learning Based Assessment of Smart Dynamic Controller

Luminaire brightness and color temperature have been controlled by controlling brightness of the individual sections of the luminaire through different duty cycle of the PWM signal as mentioned in section 4.5. While controlling the brightness of the CWLEDs in different steps as C1, C2, C3, C4, C5, C6, C7, & C8 respectively same steps while controlling the WWLEDs as W1, W2, W3, W4, W5, W6, W7, & W8 respectively. By mixing cold white and warm white light sources, a variable CCT can be achieved. CCT is defined based on the chromaticity of the Planckian radiator whose temperature describes the chromaticity coordinates (x,y). Chromaticity coordinates are based on tristimulus values X, Y, Z (Chromaticity). Flux, luminance, and illuminance are proportional to tristimulus values. CCT along with D_{uv} specify the chromaticity of the light sources. Though CCT is a major characteristic of the color appearance, it alone cannot define the multifaceted spectral power distribution. To address this issue, ANSI created the D_{uv} as a parameter that measures the difference in chromaticity between a black body radiator's chromaticity and that of a given light source with an equal CCT. The presented system is useful for Human Centric Lighting where the color of light (CCT) varies based on the mood of persons within the lighted space. The system is also useful for lighting an indoor space that matches the dynamic variation of CCT of the Sunlight. The author experimented with Warm White Light Emitting Diodes (WWLED) and Cool White Light Emitting Diodes (CWLED) by varying their duty cycle. They proposed a supervised machine learning-based model by training a Support Vector Machine (SVM) classifier with the feature values extracted from the experiment to automatically control the brightness of the LEDs.

Experimental setup for two datasets consisting of 72 data points in each of ‘Two Cool White LED sections with one Warm White LED section’ (D1) and ‘One Cool White LED Section with Warm White LED sections’ (D2). The feature set has total of nine features as explained in Table 5-7.

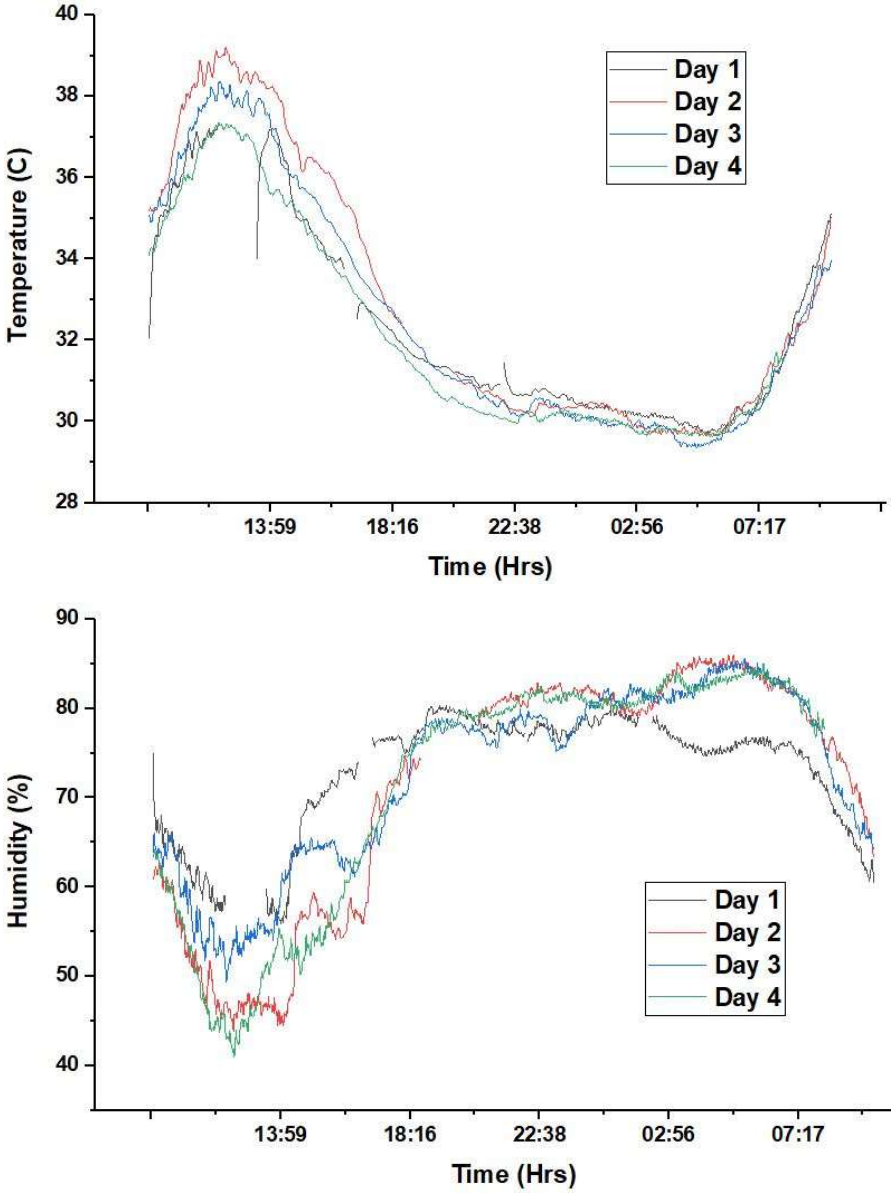

Figure 5-31. Temperature (top) and Humidity (bottom) measured and recorded for 24 hrs.

Table 5-7. Feature set and their descriptions

Feature	Description
CCT	It is the measure of the degree of brightness of yellow or blue color emitted from the light source.
Illuminance	It is the measure of the quantity of light relative to the size of the illuminated surface. SI unit of illuminance is Lux.
Peak Wavelength (λ)	Specific Wavelength out of the total spectrum of the light source where energy density is maximum (varies as CCT value changes).
Dominant Wavelength (λ_d)	The dominant wavelength (DW) of a color indicates its hue. It is also the wavelength of the spectral color whose chromaticity is parallel to the sample point (S) and illuminant point (N),
	Purity or excitation purity is the distance from the illuminant point (N) to the sample point (S), divided by that from the illuminant point (N) to the spectrum locus. Purity percentage, P, is given by the equation $P = {(N - S) * 100}/{(N - DW)}$ It determines the dominant wavelength.
Color Rendering Index (CRI)	It is the measure of the ability of a light source to render the true color of an object.
CIE 1931 XYZ	It was created by the International Commission on Illumination (CIE) in 1931. It is considered the international standard model of human color vision that is used all around us.
CIE 1976 u' v'	The 3D color space of CIE 1931 was not visually uniform. CIE 1976 was introduced to address this issue. Values of u' and v' can be calculated from CIE 1931 XYZ as follows: $u' = \frac{4X}{X+15Y+3Z}$ $v' = \frac{9Y}{X+15Y+3Z}$
D_{uv}	D_{uv} is the closest distance from the Planckian locus.
Tristimulus Values	There are three types of color sensitive cones in human eyes with peaks of spectral sensitivity in short (420 nm – 440 nm), middle (530 nm – 540 nm), and long (560 nm – 580 nm) wavelengths. These wavelengths approximately reflect the three different colors – red, green, and blue respectively.

5.6.1 Classification using Support Vector Machine

Support Vector Machine (SVM) was used for the classification based on brightness levels C1, …, C8 of CWLEDs. For each of the features f_i in the feature set $F = \{f_1, \ldots, f_9\}$ the brightness level of WWLEDs have been increased in steps from W1,….,W8, thus giving rise to a total of 72 features. 50% of data have been used for training and the rest have been given for testing.

The outcome was compared with the result obtained with other machine learning based algorithms such as Multilayer Perceptron (MLP), Random Forest (RF), Naïve Bayes (NB), and Random Tree (RT). SVM has been opted due to the dataset have been high-dimensional and the number of dimensions have been greater than the number of instances.

The one-to-One approach was used for the multiclass classification. With k=8 classes, the classifier uses 28 SVMs. Given a training vector $t_i \in \mathbb{R}^p, i = 1, \ldots, 36$ to classify the data points into 8 classes. The output vector $= \{1,2,3,4,5,6,7,8\}^n$. aim has been to find $\mathbb{w} \in \mathbb{R}^p$ and $m \in \mathbb{R}$ such that the prediction given by $\mathbb{w}^T\varphi(t) + m$ is correct for most instances. It was required to minimize $\| \mathbb{w} \|^2 = \mathbb{w}^T\mathbb{w}$ when incurring a penalty if the instance has been misclassified or within the margin boundary. Ideally, $o_i(\mathbb{w}^T\varphi(t_i) + m) \geq 1$ for all instances. Once the optimization problem has been taken care of, the output of decision function for a given instance t has been,

$$\sum_i o_i \alpha_i K(t_i, t) + m \tag{16}$$

The classification was done by C-SVC with radial basis function (RBF) kernel.

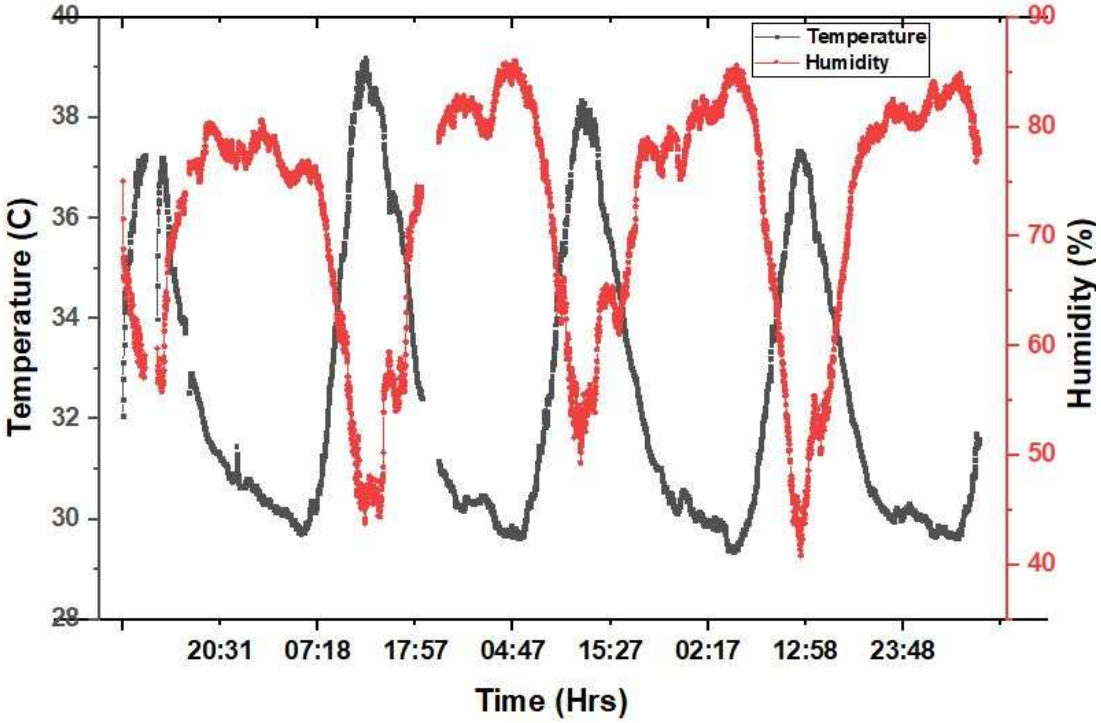

Figure 5-32. Relative values of Temperature and Humidity values

.

Table 5-8. Statistical analysis of the result obtained with SVM

Two Cool White Section with Warm White (D1)						
TP	FP	Precision	Recall	F-Score	ROC	Class
1.0	0	1.0	1.0	1.0	1.0	C1
0.8	0	1.0	0.8	0.889	0.9	C2
1.0	0	1.0	1.0	1.0	1.0	C3
1.0	0	1.0	1.0	1.0	1.0	C4
1.0	0.034	0.0875	1.0	0.933	0.983	C5
1.0	0	1.0	1.0	1.0	1.0	C6
1.0	0	1.0	1.0	1.0	1.0	C7
1.0	0	1.0	1.0	1.0	1.0	C8
One Cool White Section with Warm White (D2)						
1.0	0.033	0.857	1.0	0.923	0.983	C1
1.0	0	1.0	1.0	1.0	1.0	C2
0.83	0	1.0	0.83	0.909	0.917	C3
1.0	0	1.0	1.0	1.0	1.0	C4
1.0	0	1.0	1.0	1.0	1.0	C5
1.0	0	1.0	1.0	1.0	1.0	C6
1.0	0	1.0	1.0	1.0	1.0	C7
1.0	0	1.0	1.0	1.0	1.0	C8

5.6.2 Statistical Analysis

A fundamental part of a predictive modelling problem is the appraisal of a learning method. More than one machine learning algorithm might be suitable for a predictive modelling problem. Model selection involves selecting the best model for the purpose. Two classes of statistical techniques can be used to evaluate the performance:

i. Using statistical parameters such as accuracy, kappa value, true positive (TP), false positive (FP) or type-I error, false negative (FN) or type-II error, true negative (TN), recall or sensitivity, and specificity. Any model that has high TP and TN, and low FP and FN can be considered appropriate for the purpose.
ii. Estimation statistics to quantify the uncertainty of a result using confidence intervals (CI). The author has done a pairwise comparison of the different classifiers.

5.6.3 Results and Discussion

The accuracy obtained with SVM was found to be 99.2% and 97% for Two Cool White Section with Warm White (D1) and One Cool White Section with Warm White (D2) respectively. The statistical analysis of both the data sets yielded the result given in Table 5-8 and the confusion matrix has been given in Table 5-9. The accuracy obtained with MLP, RF, Random Tree, and Naïve Bayes have been 91.8%, 94.5%, 93.8%, and 94.4% respectively for D1. For D2 the

accuracy has been 87.5%, 86%, 89%, and 86% respectively for MLP, RF, Random Tree, and Naïve Bayes

Statistical analysis of the performance of different classifiers has been given in Table 5-10. The comparison of performance has been depicted diagrammatically for both sets of data in Figure 5-33 (a) – (b). Statistical parameters such as sensitivity, specificity, TP, FP, TN, FN for SVM of both the data sets have been given in Table 5-11.

Table 5-9. Confusion matrix of the result obtained with SVM

Two Cool White Section with Warm White (D1)								
C1	C2	C3	C4	C5	C6	C7	C8	
6	0	0	0	0	0	0	0	C1
0	4	0	0	1	0	0	0	C2
0	0	5	0	0	0	0	0	C3
0	0	0	3	0	0	0	0	C4
0	0	0	0	7	0	0	0	C5
0	0	0	0	0	2	0	0	C6
0	0	0	0	0	0	4	0	C7
0	0	0	0	0	0	0	4	C8
One Cool White Section with Warm White (D2)								
6	0	0	0	0	0	0	0	C1
0	3	0	0	0	0	0	0	C2
1	0	5	0	0	0	0	0	C3
0	0	0	3	0	0	0	0	C4
0	0	0	0	6	0	0	0	C5
0	0	0	0	0	4	0	0	C6
0	0	0	0	0	0	4	0	C7
0	0	0	0	0	0	0	4	C8

Accuracy of classification using SVM has been the highest for both sets of data. Residuals provide the measurement of the distance of the data points from the line of regression. Root Mean Square Error [RMSE] is the standard deviation of the residuals. Table 5-10 and Figure 5-33 shows that RMSE for both D1 and D2 have been the lowest for SVM indicating fewer outliers (RMSE). Kappa (κ) provides an assessment of the extent to which the collected data are an accurate measure of the features used. $\kappa \geq 0.8$ represents good agreement. In our experiment, $\kappa \geq 0.95$ for both sets of data, indicating an excellent inter-rater agreement (Kappa). The 8 × 8 confusion matrix in Table 5-9 has been used for the evaluation of the performance of the classification model. This matrix compares the actual target values with those predicted by the SVM. The percentage of misclassification was only 1.5% for both D1 and D2.

TP and TN have been the predicted value that matches the actual value. FP and FN indicate that the predicted class was falsely predicted. Low values of Type-I and Type-II errors and high values TP and TN from Table 5-11 indicate the robustness of the proposed method. Sensitivity is the ability of the test to detect TPs, whereas, specificity is the ability of the system to detect TNs (Parikh, Mathai, Parikh, & Thomas, 2008). The two values have been high (greater than 0.9) for both D1 and D2, i.e. the proposed SVM-based model adequately covers all the TPs and TNs respectively.

Table 5-10. Statistical analysis of the performance of different classifiers

Two Cool White Section with Warm White (D1)					
	SVM	**MLP**	**RF**	**NB**	**RT**
Accuracy	0.992	0.918	0.945	0.944	0.938
kappa	0.968	0.904	0.936	0.936	0.936
MAE	0.007	0.029	0.034	0.014	0.014
RMSE	0.083	0.127	0.119	0.118	0.118
Wt. avg. TP	0.972	0.917	0.944	0.944	0.938
Wt. avg. FP	0.007	0.006	0.003	0.008	0.006
Wt. avg. Precision	0.976	0.951	0.972	0.954	0.954
Wt. avg. Recall	0.972	0.917	0.944	0.944	0.938
Wt. avg. F-Score	0.972	0.922	0.951	0.946	0.946
Wt. avg. ROC	0.983	0.987	0.988	0.981	0.969
One Cool White Section with Warm White (D2)					
Accuracy	0.97	0.875	0.86	0.86	0.89
kappa	0.968	0.857	0.841	0.841	0.873
MAE	0.007	0.035	0.031	0.035	0.028
RMSE	0.083	0.164	0.149	0.186	0.168
Wt. avg. TP	0.970	0.875	0.861	0.861	0.890
Wt. avg. FP	0.006	0.017	0.019	0.022	0.016
Wt. avg. Precision	0.976	0.884	0.866	0.873	0.890
Wt. avg. Recall	0.970	0.875	0.861	0.861	0.889
Wt. avg. F-Score	0.970	0.875	0.861	0.865	0.888
Wt. avg. ROC	0.983	0.955	0.994	0.781	0.936

Table 5-11. Statistical parameters of SVM for D1 and D2

Data Set	TP	FP	TN	FN	Sensitivity	Specificity
D1	0.992	0.007	0.318	0.028	0.972	0.968
D2	0.97	0.006	0.2	0.03	0.97	0.971

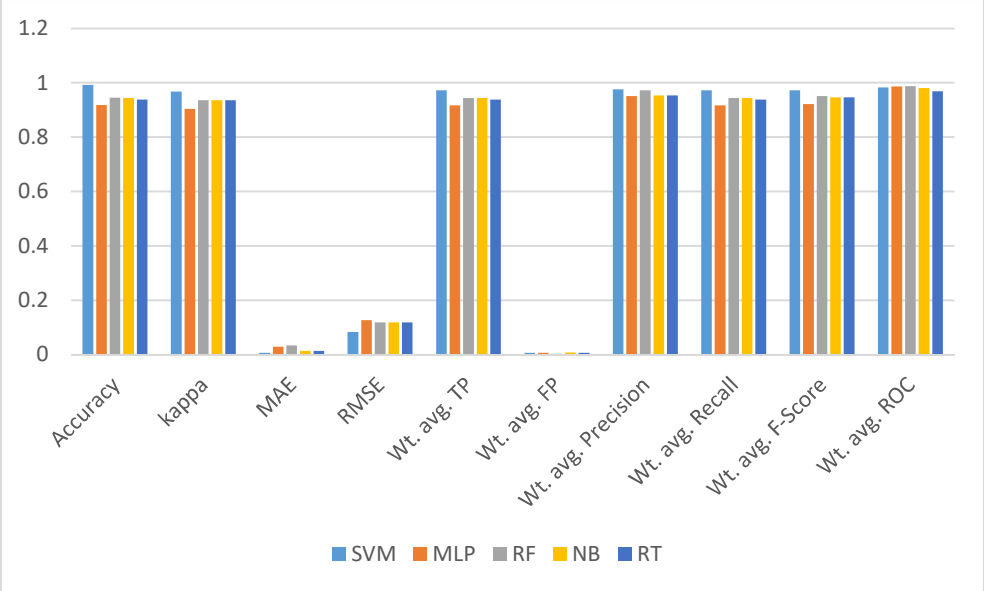

(a)

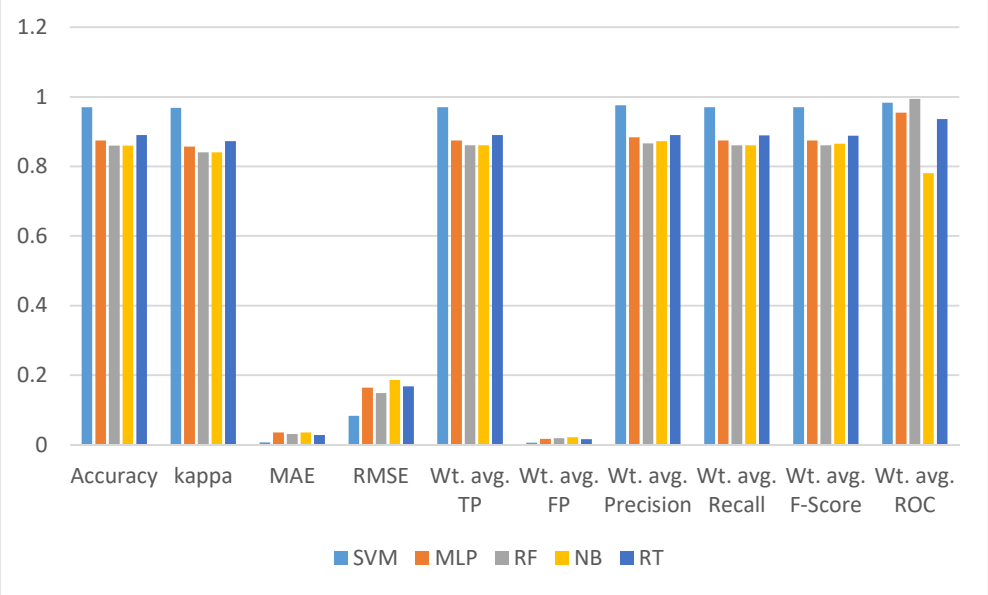

(b)

Figure 5-33. Performance comparison of the classifiers

Chapter 6: Conclusion and Future scopes

Since the very early times, when light sources have been first discovered, non-electrical lighting such as oil, gas, sodium vapour, mercury vapour, and eventually LED has been used to illuminate roads. An empirical mathematical model based on multiple linear regression to approximate the average illuminance level, uniformity of illumination, and illuminance diversity, important pieces of information for classifying roads and installing new lighting poles or revamping existing road lighting systems, has been proposed based on photometric simulation of road lighting using software simulation. Research has been carried out through the use of a simulation process, during which the effect of the luminaires has been altered due to a change in the wattage of LED-based luminaires in place of conventional luminaires. This investigation took into account changes in photometric parameters such as average, maximum, and minimum illuminances, uniformity, etc., with conventional luminaire fittings being replaced one to one with LED luminaires while maintaining the same road width, pole span, pole height, overhang, tilt.

Lighting system has been designed and developed that can control the illuminance level on the road surface, as well as cool white or warm white light appearances i.e., corelated color temperature (CCT) values can be varied using a hand held device using different wireless communication protocol during surrounding dark condition for a stipulated duration of few hours and then the light output of the lighting system will dim down for rest of the night time except in presence of any person nearby for fixed duration of three minutes. The lighting system monitors energy consumption of the luminaires along with surrounding environmental parameters like Temperature, Humidity, air quality etc. and the system has provision to monitor other environmental and physical parameters when needed.

Zigbee communication based intelligent lighting system prototype in section 4.1 has been design and developed. The system uses Zigbee as communication protocol to transmit data between two xbee modules that has been utilized to make the system intelligent and make the whole system self-operative. The system has the limitation of poor communication distance; it can be improved by other advanced version of xbee module. It also enables supervisory control of the system from local control station. Raspberry Pi module with specific IP address has been connected with the system to transmit & receive information using internet network. In that

scenario encryption & decryption methodologies become very important to make the system secure enough and fault free in future, not allowing unauthorized access.

Mobile communication-based lighting system in section 4.2 approaches to industrial automation and security system design which is almost standardized now a day. The developed system, may save lives of many people by giving early warning during emergency conditions.

This combined smoke detector system with emergency lighting and communication system may be used outside of official building or heritage building etc. At night, when the density of people of any area would be very low, if any fire hazard related emergency occurs outside, the fire may spread rapidly and may affect the surroundings and the buildings nearby if any and damage various important documents, instruments or artefacts. This developed smoke detector system with emergency lighting and communication system may protect these hazardous situations.

This combined smoke detector system may effective in wildfire. Wildfire spreads very fast and come to the local premises. This may cause extensive damage to property, human life, wild life etc. This developed smoke detector with SMS alarm system may save extensive damage of property, human life, wildlife, forest etc. from the wildfire.

Lighting control system in section 4.3 using different communication protocol and android application implements ways of achieving automatic street light system using Bluetooth, LoRa wireless and IOT communication. The developed system has solar panel which has been used to charge the lithium battery and PIR sensor has been used to detect the road user and smd LEDs have been used to illuminate path way. To interface with mobile app Bluetooth and WiFi module have been used. In addition, communication through LoRa also worked out. While Bluetooth interface, Atmega328 microcontroller has been used. When at WiFi interface (IOT) nodemcu esp8266 has been used. When the presence detection sensor detects movement of road users, luminaires will switch ON.

In case of Bluetooth, the proposed system can be controlled through mobile app with Bluetooth inbuilt android mobile, where the short distance communications. It can be used for indoor, urban streetlights and commercial light shops. Here Bluetooth HC-05 has been used for luminaire side, so the maximum 100m distance communication has been established. However, by using long distance Bluetooth like HC-12 communication distance can be increased with the same protocol.

Considering advantages of Bluetooth device, which is Easy to use. There is no need of LOS (Line of sight) required for data transfer. The Less power consumption makes its usage

very practical and 2.4 GHz radio frequency ensures worldwide operability. The data rate is high i.e. around 3Mbps.

In case of LoRa, another LoRa module can control the proposed system. A pair of WIR-1286 module have been used; one at luminaire side and another at controller side. Master-slave communication protocol (single directional), without status monitoring system has been established. Developed prototype controller with LoRa communication protocol has been very effective for monitoring and control of lighting system within the area application. The system also used HHD for controlling and status monitoring of the lighting system but HHD like smart phones does not have any interface for LoRa adaptive system. To resolve the issue another controller with Bluetooth communication protocol has-been used to interface between developed LoRa based controller and HHD.

Since WIR-1286 module is a low-power and high range wireless communication solution that is ideal for Smart Grid, home automation, smart lighting, and industrial lighting. This module operates at 868MHz band and has 5 channel options. It can offer up to 2 kilometres over the air range and even more if modules configured as repeaters have been used.

According to the studies of Ismail Butun (Butun, Pereira, & Gidlund, 2019) security risk analysis, LoRaWAN v1.0 appeared to have a couple of relevant security threats (especially vulnerabilities against end-device physical capture, rogue gateway and replay attacks). Other than the LoRaWAN v1.1 has proven to be more secure and reliable, compared to its earlier version (v1.0). Therefore, with the addition of these new features of roaming and mobility support (the existing ones have been long range, wide availability of low-cost devices, high community support, easily implementable devices), it may be predicted that LoRaWAN to be more and more attractive for IoT applications.

Compared with Bluetooth LoRa has low data rate, (upto 27 kbps). In addition, it is not ideal candidate to be used for real time applications requiring lower latency and bounded jitter requirements.

In case of WiFi, the proposed system can be controlled and monitor by using android based mobile app. It can control and monitor group of lighting systems from urban base station. The lighting system can be monitor through firebase project internet site.

In comparison the Zigbee based controller system achieved a communication distance of 5.8 metres. In the case of the Bluetooth based controller, the lighting system has been controlled from a distance of 20 metres. Using an advanced version of Bluetooth can increase the communication distance of 100 metres. In the case of the LoRa based developed controller,

communication distance achievable up to 1000 metres. That is suitable for remote areas without the internet. GSM communication based lighting systems have been very much effective for large distances with or without any barrier. A recurring cost is involved to keep the communication network active. Whereas the communication distance for the WiFi based controller when used from a fixed router is limited up to 300 metre in outdoor environment.

The lighting system in section 4.4 with WiFi communication has been designed and developed to perform intelligently. The system measures and records physical parameters wirelessly. The intelligent system has been developed with dusk and dawn sensor within it to detect surrounding light level and accordingly the system switches ON and OFF. The system measures and records physical parameters like Surrounding temperature, humidity etc. along with electrical parameter wirelessly.

The lighting system has been developed with variable color temperature lighting output. Performance parameters of the luminaires has been experimented with different photometric and colorimetric analysis. The developed luminaire has been used to generate multiple digital documents (*.ies files) compatible for software-based simulation purposes. Software simulation of the lighting system based on the digital version of the luminaires have been done. Best results of the simulations have been presented.

The developed lighting systems have been mounted on poles and installed near a garden on a pathway within Jadavpur University campus. Performance parameters of the lighting systems have been measured at different set points & controlled wirelessly using WiFi protocol. The developed systems have been used to monitor and record physical parameters like surrounding humidity and temperature etc.

Performance of the system has been evaluated in section 5.7 by machine learning based support vector machines technique. A smart dynamic lighting system aims to illuminate the environment according to the context. SVM based model exhibited a high accuracy for both sets of data. Thus, the controlling duty cycle of the brightness used for both WWLED and CWLED have been sufficient for the successful implementation of the proposed system.

In comparison to the literature the thesis discussed procedure and well developed look up table while retrofitting operation and changing the conventional luminaires to advanced LED based luminaires on existing lighting pole arrangements that may be followed by different urban local bodies, municipalities, road transport authorities. The intelligent system has been designed, developed and remote monitoring and control has been tested using different

communication protocols over different prototypes. Contrary to the discussed literatures and conventional lighting systems the developed system has been designed for dynamic illumination on road surface along with variable CCT of light i.e. changing colour of light from the luminaire both may be programmed and changed based on requirements. Performance parameters of the dynamic CCT of light from the luminaire has been analysed. The system has been developed to measure and record the environmental parameters remotely with provision for multiple sensors mounting and recording.

Digital model of the developed system has been generated for software based analysis of the luminaire considering different aspects of road lighting pole mounting and luminaire mounting arrangements on different road types. The developed luminaires have also been mounted on road ways to verify the performance parameters through real time experimental measurements.

In comparison to the experimental system developed by He et.al, the developed system can be used for in situ verification of performance varying the CCT level and there by S/P ratio variation. The developed system is suitable for analysing drivers' or pedestrians' on-axis and off-axis obstacle detection performance and accordingly providing the right lighting environment on the road surface. The developed system is also suitable as a replacement for the experimental system of Goswami et. al, (Goswami, Roy, Naskar, & Chakraborty, 2022) for in situ measurement of visibility level and small target visibility under varying CCT level of light output from luminaire.

In comparison to the commercial lighting systems mentioned in the literature section like InteliLight, Aaeon Intelligent Lighting system, Kanglight etc., the developed system provides flexibility over the control of the colour of light emitting from the luminaire for choosing the proper visibility level and ability to observe small objects by varying the scotopic and photopic illumination level ratio. The developed luminaire is cost effective and easily customisable in comparison to the commercially available systems.

6.1 Recommendation for future work

In future the lighting system will be used to find out the small target visibility on outdoor application and measurement of performance indices during night time activities for pedestrians and drivers.

The lighting system will also be used to measure response time detection during night time activities of the users under different lighting conditions i.e. at different lighting levels and variation of color temperature variations.

In future the lighting system will also be equipped with other sensors to measure and record physical parameters.

Urban Local bodies, Municipalities, energy saving companies (ESCO) may follow the outcomes instead of following thumb rules for upgradations from conventional systems. They will get a guidance for right installations by going through the outcome of the current study.

References

Aaeon. (2020, 07 23). Retrieved 01 05, 2022, from https://www.aaeon.com/: https://www.aaeon.com/en/ai/aaeon-intelligent-street-lighting

Akashi Y. Rea M.S. Bullough, J. (2007). Driver decision making in response to peripheral moving targets under mesopic light levels. *Lighting Res. Technol., 39,*, 53-67.

Akashi Y., R. M. (2007). Driver decision making in response to peripheral moving targets under mesopic light levels. *Lighting Research and Technology, 39*(1), 53-67.

Akashi, Y., & Rea, M. (2002). Peripheral Detection While Driving under a Mesopic Light Level. *Journal of Illumination Engineering Society, 31*(1), 85-94.

Akin, D., Sisiopiku, V. P., & Skabardonis, A. (2011). Impacts of Weather on Traffic Flow Characteristics of Urban Freeways in Istanbul. *Procedia Social and Behavioral Science, 16*, 89-99.

Al Irsyad, M. I., & Nepal, R. (2016). Al Irsyad, M. I., & Nepal, R. (2016). A survey based approach to estimating the benefits of energy efficiency improvements in street lighting systems in Indonesia. *Renewable and Sustainable Energy Reviews, 58*, 1569-1577.

Albu, H. C., Halonen, L., Tetri, E., Pop, F., & Beu, D. (2013). Luminous and power quality analysis of office building light sources. *Lighting Res. Technol., 45*(6), 740-751.

Anguraj, D. K., Balasubramaniyan, S., Kumar, E. S., Rani, J. V., & Ashwin, M. (2021). Internet of things (IoT)-based unmanned intelligent street light using renewable energy. *Int. J. Intell. Unmanned Syst., 10*(1), 34-47.

(2018). *ANSI/IES TM-30-18. IES Method for Evaluating Light Source Color Rendation.* New York, IESNA: Illuminating Engineering Society of North America.

ANSI/IESNA RP-8-00. (2000). *American National Standard Practice for Roadway Lighting*.

Ayaz, R., & Ozcanli, A. K. (2021). Life cycle cost analysis on M1 and M2 road class luminaires installed in Turkey. *Light & Engineering, 27(1)*.

Bachanek, K. H., Tundys, B., Wiśniewski, T., Puzio, E., & Maroušková, A. (2021). Intelligent Street Lighting in a Smart City Concepts—A Direction to Energy Saving in Cities: An Overview and Case Study. *Energies, 14*(11), 1-19.

Bamisile, O. O., Dagbasi, M., & Abbasoglu, S. (2016). Economic feasibility of replacing sodium vapor and high pressure mercury vapor bulbs with LEDs for street lighting. *Energy Policy Res.*, 27-31.

Barve, V. (2017). Smart Lighting for Smart Cities. *2017 IEEE Region 10 Symposium (TENSYMP)* (pp. 1-5). Kochi, India: IEEE.

Beckwith, D., Zhang, X., Smalley, E., Chan, L., & Yand, M. (2011). LED streetlight application assessment project: pilot study in Seattle. *Washington. Transp. Res. Rec, 2250*(1), 65–75.

Bellido-Outeiriño, F. J.-L.-M.-A.-G.-L. (2016). Streetlight control system based on wireless communication over DALI protocol. *Sensors, 16*(5), 1-23.

Bhattacharya, S. M. (2022). Estimation of daylight availability in Kolkata and approximation of indoor daylight levels for different daylighting methods. *International Journal of Sustainable Energy, 41*(1), 29-57.

Bingöl, E. K. (2019). LoRa-based Smart Streetlighting system for Smart Cities. *2019 7th international Istanbul Smart Grids and Cities Congress and Fair (ICSG)* (pp. 66-70). Istanbul, Turkey: ICSG.

Birol, F. (2020). *https://www.iea.org/reports/world-energy-outlook-2020*. Retrieved 02 19, 2022, from https://www.iea.org/: https://www.iea.org/

Biswas, R., Chakraborty, S., & Nath, P. (2018). Laboratory based EEG study to investigate the influence of light sources on brain processing for detection of object designed with metal halide and high-pressure sodium lamp. *Journal of Science and Technology in Lighting*, 30-39.

Blanco A.M., S. R. (2013). ower quality disturbances caused by modern lighting equipment (CFL and LED). *IEEE Grenoble Conf. IEEE*.

Boyce, P. R. (2014). *Human Factors in Lighting,.* CRC Press, Tailor & Francis Group.

Boyce, P. R., & Bruno, L. D. (1999). An evaluation of high pressure sodium and metal halide light sources for parking lot lighting. *Journal of Illuminating Engineering Society, 29*, 16-32.

Boyce, P. R., & Stampfli, J. R. (2019). New colour metrics and their use. *Lighting Research and Technology, 51*(5), 657- 681.

Brons, J. A., Bullough, J. D., & Frering, D. C. (2021). Rational Basis for Light Emitting Diode Street Lighting Retrofit Luminaire Selection. *Journal of the Transportation Research Board, 2675*(9), 634-638.

Bullough, J. D., Radetsky, L. C., Besenecker, U. C., & Rea, M. S. (2014). Bullough, J. D., Radetsky, L. C., Besenecker, U. C., & Rea, M. S. . *Leukos, 10(1)*, 3-9.

Butun, I., Pereira, N., & Gidlund, M. (2019). Security Risk Analysis of LoRaWAN and Future Directions. *Future Internet 11(1), 3*.

Castro, M., Jara, A. J., & Skarmeta, A. F. (2013). Smart lighting solutions for smart cities. *Proceedings of the 27th IEEE International Conference on Advanced Information Networking and ApplicationsWorkshops (WAINA)* (pp. 1374–1379). Barcelona, Spain: IEEE.

Chakraborty S., B. P. (2018). Road classification based energy efficient design and its validation for Indian roads. *Light & Engineering*, 110-121.

Chakraborty S., R. D. (2021). An EEG based comparative study on driver's performance under the influence of metal halide and high pressure sodium lighting,. *Optik, 245*. doi:https://doi.org/10.1016/j.ijleo.2021.167676.

Chakraborty, S., & Mazumdar, S. (2022). Laboratory experiment based studies on effect of peripheral source on on-axis visual performance. *Light & Engineering 30(2)*, 4-14.

Chase, M. (n.d.). *The Disadvantages of Smoke Alarms.* Retrieved from www.hunker.com/13419400/the-disadvantages-of-smoke-alarm: www.hunker.com/13419400/the-disadvantages-of-smoke-alarm

Chen, H. T. (2014). Color variation reduction of GaNbased whitelight emitting diodes via peak-wavelength stabilization. *IEEE Trans. Power Electron., 29*(7), 3709-3719.

Chenani, S. B., Rasanen, R. S., & Tetri, E. (2018). Advancement in road lighting. *Light & Engineering, 26*(2), 99–109.

Cheng, C. A., Chang, C. H., Chung, T. Y., & Yang, F. L. (2015). Design and Implementation of a Single Stage Driver for Supplying an LED Street-Lighting Module With Power Factor Corrections. *IEEE Transactions on Power Electronics, 30*(2), 956-966.

CIE. (1965). *CIE Publication E-1.3.2: Method of measuring and specifying colour.* Vienna: CIE Publication.

CIE. (1974). *CIE Publication 13.2: Method of measuring and specifying colour rendering properties of light sources.* Vienna: CIE.

CIE. (1995). *CIE Publication 13.3 Method of measuring and specifying colour rendering of light sources, 3rd edn.* Vienna: CIE.

Ciriminna, R., Meneguzzo, F., Albanese, L., & Pagliaro, M. (2017). Solar street lighting: a key technology en route to sustainability. *Wiley Interdiscip. Rev. Energy Environ., 6*(2).

Clowers, B. (2014, 07 31). *https://www.davisvanguard.org/2014/07/street-lights-what-are-the-issues/*. Retrieved 02 17, 2022, from https://www.davisvanguard.org/: https://www.davisvanguard.org/

Czyzewski D., F. I. (2020). The influence of photometric Intensity curve measurements quality on road lighting design parameters. *Energies*, 3301.

D.O.No. N - 11025/89/2011-UCD. (2013, March 15th). *The Ministry of Urban Development, Nirman Bhavan*. New Delhi.

Daely, P. T., Reda, H. T., Satrya, G. B., Kim, J. W., & Shin, S. Y. (2017). Design of Smart LED Streetlight system for Smart City with web-based management system. *IEEE Sens J, 17*(18), 6100–6110.

Davidovic, M., & Kostic, M. (2022). Comparison of energy efficiency and costs related to conventional and LED road lighting installations. *Energy*, 124299.

De Almeida, A., Santos, B., Paolo, B. M., & Quicheron. (2014). Solid state lighting review–potential and challenges in Europe. *Renew. Sustain. Energy Rev.*, 30-48.

Dikel, E. E., Burns, G. J., Veitch, J. A., Mancini, S., & Newsham, G. R. (2014). Preferred chromaticity of color-tunable LED lighting. *LEUKOS, 10*(2), 101-115.

Dizon, E., & Pranggono, B. (2021). Smart streetlights in Smart City: a case study of Sheffield. . *Dizon, E., & Pranggono, B. (2021). Smart streetlights in Smart City: a case Journal of Ambient Intelligence and Humanized Computing*, 1-16.

Djuretic, A., & Kostic, M. (2018). Actual energy savings when replacing high-pressure sodium with LED luminaires in street lighting. *Energy*, 367-378.

DOE (U.S. Department of Energy). (2016). *Solid-state lighting program 'R&D plan* .

Domenichini, L., La Torre, F., Vangi, D., Virga, A., & Branzi, V. (2017). Influence of the lighting system on the driver's behavior in road tunnels: A driving simulator study. *Journal of Transportation Safety & Security, 9(2)*, 216-238.

Dyble, M., Narendran, N., Bierman, A., & Klein, T. (2005). Impact of dimming white LEDs:Chromaticity shift due to different dimming methods. *5th International Conference on Solid State Lighting, Proceeding of SPIE*, (p. 291).

Eichelberger, C. (2010). LEDs come to the forefront of general lighting applications. *Inf. Disp., 26*(1), 16-20.

Elejoste, P., Angulo, I., Perallos, A., Chertudi, A., Zuazola, I. J., Moreno, A., & Villadangos, J. (2013). An easy to deploy street light control system based on wireless communication and led technology. *Sensors, 13*(5), 6492–6523.

El-Faouri, F. S., Sharaiha, M., Bargouth, D., & Faza, A. (2016). A smart street lighting system using solar energy. *2016 IEEE PES Innovative Smart Grid Technologies Conference Europe (ISGT-Europe)* (pp. 1-6). Ljubljana, Slovenia: IEEE.

Eloholma, M., Halonen, L., & Ketomuki, J. (1999). The effects of light spectrum on visual performance at mesopic light levels. (5.–5. Commission Internationale de l′ a ́clairage, Ed.) *Proceedings of the CIE Symposium: 75 Years of CIE Photometry.*

Feng, X. F., Xu, W., Han, Q. Y., & Zhang, S. D. (2017). Colour-enhencedlight emitting diode light with high gamut area for retail lighting. *Lighting Research and Technology, 49*, 329-342.

Fernandes, R. F., Fonseca, C. C., Brandão, D., Ferrari, P., Flammini, A., & Vezzoli, A. (2014). Flexible Wireless Sensor Network for smart lighting applications. *2014 IEEE International Instrumentation and Measurement Technology Conference (I2MTC)* (pp. 434-439). Montevideo: IEEE.

Fotios, S., Cheal, C., & Boyce, P. R. (2005, January). Light source spectrum, brightness perception and visual performance in pedestrian environments: a review. *Lighting Research and Technology, 37*(4), 271-294.

Gacio, D., Alonso, J., Garcia, J., Campa, L., Crespo, M., & Rico-Secades, M. (2010). High frequency PWM technique for high power factor converters in LED lighting. *Twenty fifth Annual IEEE Applied Power Electronics Conference and Exposition (APEC)*, (p. 743).

Gagliardi, G., Lupia, M., Cario, G., Tedesco, F., Cicchello Gaccio, F., Lo Scudo, F., & Casavola, A. (2020). Advanced Adaptive Street Lighting Systems for Smart Cities. *MDPI, 3*(4), 1495-1512.

Ganguly, P., Gupta, V., & Satvaya, P. (2019). Performance Study and Stability Analysis of an LED Driver. In P. Ganguly, V. Gupta, P. Satvaya, T. K. Basu, S. K. GOswami, & N. Sanyal (Eds.), *Lecture Notes in Electrical Engineering book series, LNEE* (Vol. 591, pp. 147-158). Singapore: Springer.

Gas Leakage Detector using Arduino and GSM Module with SMS Alert and Sound Alarm,. (n.d.). Retrieved from http://www.circuitstoday.com/gas-leakage-detector-using-arduino-with-sms-alert

Gilman, J. M., Miller, M. E., & Grimaila, M. R. (2013). A simplified control system for a daylightmatched LED lamp. *Lighting Research and Technology, 45*(5), 614–629.

Gorgulu, S., & Kocabey, S. (2020). An energy saving potential analysis of lighting retrofit scenarios in outdoor lighting systems: A case study for a university campus. *Journal of Cleaner Production, 260*, 121060.

Goswami, A. D., Roy, J., Naskar, A., & Chakraborty, S. (2022). A laboratory based study on the effect of CCT change of LED light sources on reaction time and visibility level for object recognition. *Optik, Volume 264,*, 169353.

Güler, Ö., & Onaygil, S. (2003). The effect of luminance uniformity on visibility level in road lighting. *Light. Res. Technol.*, 199-213.

Guo, S., Gu, H., Wu, L., & Jiang, S. (2011). Energy-saving tunnel illumination system based on LED's intelligent control. *Journal of Physics: Conference Series (Vol. 276, No. 1)*, 012164.

He Y., R. M. (1997). Evaluating light source efficacy under mesopic conditions using reaction times. *J. Illum. Eng. Soc., 26,*, 125-138.

Houser, K. W., Wei, M., David, A., & Krames, M. R. (2014). Whiteness perception under LED illumination. *Leukos, 10*(3), 165–180.

India's clean Revolution. (2011, March). Retrieved from The Climate Change,: http://www.theclimategroup.org/ assets/files/Indias-Clean-Revolution-Report-March-2011.pdf

InteliLIGHT. (2021, 06 30). *https://intelilight.eu/intelligent-street-lighting-control/*. Retrieved 01 07, 2022, from https://intelilight.eu/: https://intelilight.eu/

Interact. (2022, 01 26). *https://www.interact-lighting.com/global/what-is-possible/interact-city/lighting-asset-management*. Retrieved 01 27, 2022, from https://www.interact-lighting.com/: https://www.interact-lighting.com/

Interact City. (2019). *A powerful street lighting transformation fully financed from energy savings.* 04: 09.

Islam, M. S., Chowdhury, N. A., Sakil, A. K., Khandakar, A., Iqbal, A., & Abu-Rub, H. (2015). Power quality effect of using incandescent, fluorescent, CFL and LED lamps on utility grid. *First Workshop on Smart Grid and Renew. Energy (SGRE) IEEE*.

Jagadeesh, Y. M., Akilesh, S., & Karthik, S. (2015). Intelligent Street Lights. *ScienceDirect, 21*, 547-551.

Janoff, M., & Havard, J. (1997). The effect of lamp color on the detection and recognition of small targets. *Proceedings of the Illuminating Engineering Society Annual Conference.* (pp. 465-497). Illuminating Engineering Society of North America,.

Jiang, Y., Li, S., Guan, B., & Zhao, G. (2015). Cost effectiveness of new roadway lighting systems. *Journal of traffic and transportation engineering (English edition), 2(3)*, 158-166.

Johnson, A., Phadke, A., & Stephane, R. C. (2014). *Energy Savings Potential for Street Lighting in India.* New Delhi: Environmental Energy Technologies Division.

Judd, D. (1967). *A flattery index for artificial illuminants.* Illumination Engineering.

Jung, H. M., Kim, J. H., Lee, B. K., & Yoo, D. W. (2010). A new PWM dimmer using two active switches for AC LED lamp. *International Power Electronics Conference-ECCE ASIA* (pp. 1547-1551). IEEE.

Kaleem, Z., Ahmad, I., & Lee, C. (2014). Smart, energy efcient LED Street light control system using ZigBee network. *12th international conference on frontiers of information technology* (pp. 361-365). Islamabad, Pakistan: CIIT.

Kanglight. (2022, 01 13). *https://kanglight.com/ushering-in-a-new-era-of-led-street-light/*. Retrieved 01 25, 2022, from https://kanglight.com/: https://kanglight.com/

Karmakar, N. C., Aruna, M., Rao, Y. V., & Yaragatti, U. K. (2006). Design of haul road lighting system. Part 1: design based on optimal energy consideration. *Int. J. Min. Reclam. Env.*, 165-174.

Kim, D., & Park, S. (2017). Improving community street lighting using CPTED: a case study of three communities in Korea. *Sustain. Cities Soc., 28*, 233–241.

Kim, J. H., Jung, J. H., Ryu, M. H., & Baek, J. W. (2011). A simple dimmer using a MOSFET for AC driven lamp. *IECON 2011-37th Annual Conference of the IEEE Industrial Electronics Society* (pp. 2872-2876)). IEEE.

Kim, Y.-S., Cho, B.-H., Kang, B.-S., & Doo-II, H. (2006). *United States of America Patent No. US 7,024,034 B2.*

Kostic, A., Kremic, M., Djokic, L., & Kostic, M. (2013). Light emitting diodes in street and roadway lighting-a case study involving mesopic effects. *Light. Res. Technol.*, 217-229.

Lau, S. P., Merrett, G. V., Weddell, A. S., & White, N. M. (2015). A traffic-aware street lighting scheme for Smart Cities using autonomous networked worked sensors. *Comput Electr Eng, 45*, 192–207.

Lavric, L., & Popa, V. (2015). “Performance evaluation of large-scale wireless sensor networks communication protocols that can be integrated in a smart city. *International Journal of Advanced Research in Electrical, Electronics and Instrumentation Engineering, 4*(5), 113-118.

Leccese, F. (2012). Remote-control system of high effciency and intelligent street lighting using a ZigBee network of devices and sen. *IEEE Trans Power Deliv, 28*, 21-28.

Leccese, F., Cagnetti, M., & Trinca, D. (2014). A smart city application: a fully controlled street lighting isle based on Raspberry-Pi card, a ZigBee sensor network and WiMAX. *Sensors, 14*, 24408–24424.

Lewis, A. (1999). Visual Performance as a Function of Spectral Power Distribution of Light Sources at Luminances Used for General Outdoor Lighting. *Journal of the illuminating Engineering Society, 28*, 37-42.

Lewis, S. (2019, 12 10). *https://internetofthingsagenda.techtarget.com/definition/smart-streetlight*. Retrieved 02 16, 2022, from https://internetofthingsagenda.techtarget.com/.

Maiti, P. K. (2015). Development of Dynamic Light Controller for Variable CCT White LED Light Source. *LEUKOS, 11*(4), 209-222.

Maiti, P. K., & Roy, B. (2018). Evaluation of a light controller for a LED-based dynamic light source. *Lighting Res. Technol., 50*, 571–582.

Maiti, P., & Roy, B. (2017). Development and Performance Assessment of White LED Dimmer. *J. Inst. Eng. India Ser., 98*(5), 461-466.

Marı´a Morillas, R., & Ramo´n de Andre´s, J. (2019). Renewing street lighting with LED technology: a single case study in Casarabonela. *Light & Engineering, 27*(6), 16–26.

Mathur, A. (2010). *Energy Efficient Street Lighting.* New Delhi: USAID ECO-III Project.

Mills, E. (2002). Global lighting energy savings potential. *Light Eng., 10*(4), 5–10.

Ministry of Power, Govt. of India. (2018). Retrieved from http://www.cea.nic.in/reports/monthly/installedcapacity/2018/installedcapacity-01.pdf

Mirvakili, A. &. (2012, July). High efficiency LED driver design for concurrent data transmission and PWM dimming control for indoor visible light communication. *IEEE Photonics Society Summer Topical Meeting Series*, pp. 132-133.

Mirzaei, M. J. (2015). An asset-management model for use in the evaluation and regulation of public-lighting systems. *Utilities Policy, 32*, 19-28.

Mohandas, P., Dhanara, J. A., & Gao, X. Z. (2019). Artifcial Neural Network based Smart and Energy Efcient Street Lighting system: a case study for residential area in Hosur. *Sustainable Cities and Society, 48*, 1-13.

Moreno, I., Avendaño-Alejo, M., Saucedo-A, T., & Bugarin, A. (2014). Modeling LED street lighting. *Applied optics, 53(20),, 53*(20), 4420–4430.

Moroney, N., Fairchild, M. D., Hunt, R. W., Li, C., Luo, M. R., & Newman, T. (2002). The CIECAM02 Color Appearance Model. *IS&T/SID Tenth Color Imaging Conference.* Scottsdale, Arizona: The Society for Imaging Science and Technology. ISBN 0-89208-241-0.

Muhaisen, N., Khan, S., Habaebi, M. H., Ahmed, N. A., & Ahmed, M. M. (2021). Feasibility analysis of implementing PV street lighting system in an arid region. *Int. J. Sustain. Energy, 41*(4), 1-22.

Mukherjee, S., Satvaya, P., & Mazumdar, S. (2019). Development of a micocontroller based emergency lighting system with smoke detection and mobile communication facilities. *Light & Engineering, 27*(1), 46-50.

Müllner, R., & Riener, A. (2011). An energy efficient pedestrian aware Smart Street Lighting system. *Int J Pervas Computer Communication, 7*(2), 147–161.

Najim , S. A., Al-Omari , Z. A., & Said , S. M. (2008). On the application of artificial neural network in analyzing and studying daily loads of Jordan power system plant. *Computer Science and Information Systems, 5*(1), 127-136.

Nhede, N. (2019, 10 07). *https://www.smart-energy.com/industry-sectors/energy-grid-management/smart-streetlights-india-celebrates-1-million-units-milestone/.* Retrieved 01 25, 2022, from https://www.smart-energy.com: https://www.smart-energy.com/

Novak, T., Pollhammer, K., Zeilinger, H., & Schaat, S. (2014). Intelligent streetlight management in a smart city. *2014 IEEE Emerging Technology and Factory Automation (ETFA)* (pp. 1-8). Barcelona, Spain: IEEE.

Ohno Y., O. S. (2016). Vision experiment II on white light chromaticity for lighting. *CIE Publication x042:2016: Lighting quality & energy efficiency* (pp. 175–184). Melbourne, Australia: CIE.

Ohno, Y. (2014). Practical use and calculation of CCT and Duv. *LEUKOS, 10*(1), 47-55.

Ohno, Y., & Fein, M. (2014). Vision experiment on acceptable and preferred white light chromaticity for lighting. *Proceedings of CIE 2014: Lighting quality and energy efficiency* (pp. 1-8). Kuala Lumpur, Malaysia: CIE.

Onaygil, S., Guler, O., & Erkin, E. (2012). Cost analyses of LED luminaires in road lighting. *Light Eng., 20*(2), 39–45.

Oundhakar, S. A. (2019, 05 01). *https://www.electricalindia.in/switch-to-smart-street-lighting/*. Retrieved 02 07, 2022, from https://www.electricalindia.in/: https://www.electricalindia.in/

Panchuk, A. (2009, 12). *https://www.smart-energy.com/industry-sectors/smart-meters/street-lighting-problems-and-solutions/*. Retrieved 02 17, 2022, from https://www.smart-energy.com/: https://www.smart-energy.com/

Parikh, R., Mathai, A., Parikh, S. G., & Thomas, R. (2008). Understanding and using sensitivity, specificity and predictive values. *Indian Journal of Opthalmology, 56(1)*, 45-50.

Pasolini, G., Buratti, C., Feltrin, L., Zabini, F., De Castro, C., Verdone, R., & Andrisano, O. (2018). Smart City Pilot Projects Using LoRa and IEEE802.15.4 Technologies. *Sensors, 18*(4), 1-17.

Pen˜a-Garcı´a, A., Go´mez-Lorente, D., Espı´n, A., & Rabaza, O. (2016). New rules of thumb maximizing energy efficiency in street lighting with discharge lamps: the general equations for lighting design. *Eng. Optim.*, 1080–1089.

Perz, M., Baselmans, D., & Sekulovski, D. (2016). Perception of illumination whiteness. *Proceedings of the 4th CIE expert symposium on colour and visual appearance.* Prague: CIE Publication x043.

Phannil, N., Jettanasen, C., & Ngaopitakkul, A. (2018). Harminics and reduction of energy consumption in lighting systems by using LED lamps. *Energies*, 3169.

Pinho, P., Hytönen, T., Rantanen, M., Elomaa, P., & Halonen, L. (2013). Dynamic control of supplemental lighting intensity in a greenhouse environment. *Lighting Research and Technology, 45*(3), 295–304.

Pitchipoo P., S. R. (January, 2014). Analysis of Prime Reasons for Night Time Accidents in Public Transport Corporations. *Advances in Industrial Engineering Applications*, (pp. 6-8).

Pracki, P. (2011). A proposal to classify road lighting efficiency. *Light. Res. Technil.*, 271-280.

Protzman, J. B., & Houser, K. W. (2006). LEDs for General Illumination: The State of the Science. *Leukos, 3*(2), 121-142.

Rabaza, O., Gómez-Lorente, D., Pérez-Ocón, F., & Peña-García, A. (2016). A simple and accurate model for the design of public lighting with energy efficiency functions based on regression analysis. *Energy*, 831-842.

Rajput, K. Y., Khatav, G., Pujari, M., & Yadav, P. (2013). Intelligent street lighting system using gsm. *International Journal of Engineering Science Invention, 2*(3), 60-69.

Raul, D., & Ghosh, K. (2019). Performance of chip-on-board and surface-mounted high-power LED luminaires at different relative humidities and temperatures. *Light. Res. Technol., 51*(8), 1249–1262.

Rea, M. S. (Ed.). (2000). *The IESNA Lighting Handbook.* New York: Illuminating Engineering Society.

Rea, M. S., Bullough, J. D., & Akashi, Y. (2009). Several views of metal halide and high-pressure sodium lighting for outdoor applications. *Lighting Research and Technology, 41*(4).

Report No: AUS7490. (2015). *India: Energy-Efficient Street Lighting—Implementation and Financing Solutions.* New Delhi: The World Bank. Retrieved 02 27, 2022

Roy, S., Satvaya, P., Bhattacharya, S., Majumder, S., Majumder, S., & Sardar, I. H. (2022). An exposition of a road lighting model to facilitate simple estimation of road surface

illuminance parameters for conventional system specifications and recommendations for retrofitting of luminaires. *J Opt*, 1-12.

Sahana, S., Paul, A., & Roy, B. (2019). Adaptation luminance variation under lamps of different spectral compositions with variable surrounding luminance effects. *J. Opt.*, 527–538.

Satrya, G. B., Reda, H. T., Woo, K. J., Daely, P. T., Shin, S. Y., & Chae, S. (2017). IoT and public weather data based monitoring & control software development for variable color temperature LED street lights. *Int. J. Adv. Sci. Eng. Inf. Technol., 7*(2), 366–372.

Satvaya P., M. S. (2014). Studies on road lighting luminaires with advanced features. *Light & Engineering, 22*(2), 59-64.

Satvaya, P., Mondal, I., Sur, A., & Mazumdar, S. (2018). Design and development of an intelligent street lighting system using Zigbee protocol for communication. *Proceedings of the 8th Lux Pacifica* (pp. 100-106). Tokyo, Japan: LuxPacifica.

Schubert, E. F. (2003). *Light-emitting diodes* (First ed.). New York: Cambridge University Press.

Sedziwy, A. (2016). A new approach to street lighting design. *LEUKOS, 12*(3), 151–162.

Shahzad, G., Yang, H., Ahmad, A. W., & Lee, C. (2016). Energy Efficient Intelligent Street Lighting System Using Traffic Adaptive Control. *n IEEE Sensors Journal, 16*(13), 5397-5405.

Signify. (2020, 06 12). *https://www.climatechangenews.com/2020/06/12/smart-street-lighting-will-help-future-proof-cities/*. Retrieved 01 04, 2022, from https://www.climatechangenews.com/: https://www.climatechangenews.com/

Sikder, A. K., Acar, A., Aksu, H., Uluagac, A. S., Akkaya, K., & Conti, M. (2018). IoT-enabled Smart Lighting Systems for Smart Cities. *2018 IEEE 8th Annual Computing and Communication Workshop and Conference (CCWC)* (pp. 639-645). Las Vegas, USA: IEEE.

SLAT. (2017, 01 11). *https://www.ledinside.com/news/2017/1/singapore_aims_to_convert_all_roads_to_smart_led_streetlighting_systems_by_2022.* Retrieved 02 01, 2022, from https://blogs.constellation.com/: https://blogs.constellation.com/

(2012). *Society of Light and Lighting.* london: SSL Code for lighting.

Son, Y. S., Pulkkinen, T., Moon, K. D., & Kim, C. (2010). Home energy management system based on power line communication. *IEEE Transactions on Consumer Electronics, 56*(3), 1380–1386.

Tähkämö, L., & Halonen, L. (2015). Life cycle assessment of road lighting luminaires – Comparison of light-emitting diode and high-pressure sodium technologies. *Journal of Cleaner Production, 93*, 234-242.

Tata Communications. (2018, 04 21). *https://www.tatacommunications.com/wp-content/uploads/2018/12/JUSCO-IoT-Smart-Lighting-Case-study.pdf.* Retrieved 01

27, 2022, from https://www.tatacommunications.com/: https://www.tatacommunications.com/

Telensa. (2020). *The City of Edinburgh Council: case study.* Edinbugh: The City of Edinburgh. Retrieved 01 27, 2022, from https://cdn2.hubspot.net/hubfs/5499288/Edinburgh-case-study-170120-FINAL-1.pdf

The Climate Group. (2015). *https://cdkn.org/sites/default/files/files/Up-LED-street-lighting-in-India-1.pdf*. Retrieved 02 07, 2022, from https://cdkn.org/: https://cdkn.org/

The Climate Group. (2019). *Annual Report and Accounts 2018/19.* London: The Climate Group.

Todorovic, B., & Samardzˇija, D. (2017). Road lighting energy-saving system based on wireless sensor network. *Energy Effic.*, 239-247.

Transport Research Wing, Ministry of Road Transport and Highways, Govt. of India. Road Accidents in India. (2019).

TviLight. (2021). *Jaipur becomes a Smarter & Safer City.* Jaipur: Tvilight. Retrieved 01 27, 2022

U.S Dept. of Energy. (2016). *Outdoor Lighting Challenges and Solution Pathways.* New York: Better Building Solutions. Retrieved 02 27, 2022

Unlu, D. (2022). The optical design of a LED-reflector module for road illumination. *Light & Engineering, 30(3)*, 43-52.

Veena, P. C., Tharakan, P., Haridas, H., Ramya, K., Joju, R., & Jyothis, T. S. (2016). Smart street light system based on image processing. *2016 International Conference on Circuit, Power and Computing Technologies (ICCPCT)* (pp. 1-5). Nagercoil: IEEE.

Wang, Y., & Wei, M. (2018). Preference among light sources with different Duv but similar colour rendition: a pilot study. *Lighting Res Technol, 50*(7), 1013–1023.

Wei, M., & Houser, K. W. (2016). What is the cause of apparent preference for sources with chromaticity below the blackbody locus? *LEUKOS, 12*(1-2), 95–99.

Whitepaper Intelligent street lighting. (2009). Retrieved from www.authenticshoes-cheap.com/pdfbook automatic-street-light-control-system-project/ JN-WP-7001 Intelligent street lighting.pdf

Yoomak, S., Jettanasen, C., Ngaopitakkul, A., Bunjongjit, S., & Leelajindakrairerk, M. (2018). Comparative study of lighting quality and power quality for LED and HPS luminaires in a roadway lighting system. *Energy Build.*, 542-557.

Zissis, G. (2016). Energy Consumption and Environmental and Economic Impact of Lighting: The Current Situation. In R. Karlicek, C. C. Sun, G. Zissis, & R. Ma (Eds.), *Handbook of Advanced Lighting Technology* (pp. 1-13). Cham, Switzerland: Springer.

Zukauskas, A., Shur, M., & Gaska, R. (2002). Introduction to solid-state lighting,. *1st edn*, p. 207.


Parthasarathi Satvarya.